An Open Access Journal Available Online

Covenant Journal of Engineering Technology (CJET)

Vol. 3 No. 1, June 2019

**Publication of the College of Engineering,
Covenant University, Canaanland.**

Articles

An Open Access Journal Available Online

Evaluation of Frictional Heat and Oil Cooling Rate in Mechanical Contact Due to Debris Formation

Achebe C. H[1]., Nwagu I. A[1], Chukwuneke J. L[1*] & Sinebe J. E[2]

1Department of Mechanical Engineering, Nnamdi Azikiwe University, Awka, Nigeria
2Department of Mechanical Engineering, Delta State University, Abraka, Nigeria
*jl.chukwuneke@unizik.edu.ng

Abstract- This paper evaluated experimentally, the amount of frictional heat generated in a Mitsubishi main journal bearing and the cooling performance of the lubricating oils A, B and C. The test rig used in this experiment is a mechanical apparatus that consists of mechanical drive, metal support, bevel gear, a rotating shaft and a bearing attached at its lower end. When the shaft was rotated by the mechanical drive of power 0.75kw and speed 1440rpm, the frictional force in journal bearing helped to convert the mechanical energy of the drive into frictional heat. The amount of heat absorbed from the surface of the journal bearing by the oil cooled the surface. The cooling rate of the oil was obtained at each time interval. The vibrating movement of the molecules helped to transfer the frictional heat to the lubricant and the calorimeter. This effect caused the temperature of the system to rise. The frictional heat generated at the contact increased linearly with the change in temperature in the mechanical contact which was absorbed differently in the three lubes, depending on their heat capacity and molecular movement. When there was no debris in the contact, the temperature changed within the range of 1.2-1.80C at interval of 3minutes in oil B, 10C in oil C and 0.8-1.20C in oil A. When there was sand debris in the contact, the temperature changed within the range of 2-2.50C at interval of 3minutes in oil B, 1.5-20C in oil C and 20C in oil A. Oil B has the best cooling performance based on the three local lubes used and was equally the most expensive. Mechanical failures like galling, fatigue and surface indentation occurred when the vibrational force (energy) of the molecules were greater than the binding force or energy of the atomic lattice of the bearing.
Keywords: Cooling rate, Debris, Frictional heat, Journal bearing, Lubricant, Mechanical contact, Temperature

1. Introduction
Friction has a stick-slip effect at the interaction of two surfaces moving relative to each other. If two metal surfaces are moved relative to each other, one or both surfaces will

URL: *http://journals.covenantuniversity.edu.ng/index.php/cjet*

gradually be eroded. The process of erosion depends on the nature of the surfaces but, in general, tiny fragments (debris) are torn out of the surfaces as the welded junctions shear at the areas of contact. The use of a lubricant such as oil or grease between the surfaces reduces the frictional force but does not entirely eliminate it. So, it seems that friction is undesirable, wasteful of energy (frictional heat) and costly in terms of the wear it creates and the power expended in machines to overcome it. Microscopic particles are the most harmful form of contamination in lubricants. They can irreversibly damage gear and bearing surfaces, shorten the service life of the equipment, and cause unexpected breakdown [1]. The entry of lubricant borne solid particles into machine element contacts is important, both for prediction of the body abrasive wear and for an understanding of the behaviour of solid lubricant additives [2]. Mechanical devices do fail due to the wear of the rubbing surfaces of their bearings and journals. Debris is characterized into ferrous and non-ferrous particles in which sand, atmospheric contaminants and eroded particles from the bearing belong [3]. The wear of the surfaces can theoretically be eliminated by introducing a material weak in shear (i.e. lubricant) between them. If the film of lubricant is deep enough, the surfaces will be sufficiently far apart to prevent the formation of any welded junctions directly between them. Lubricant helps to reduce forces necessary to make the surfaces slide thereby reducing the energy loss at the

bearing points and to cool the sliding surfaces.

Related works were thermo-mechanical analysis of dry clutches under different boundary conditions [4], synthesis versus mineral fluids, evaluation of engine parts using nano lubricant in agricultural tractors [5], experimental analysis of lubricant for the prediction of contact surface behaviour of metals [6], experimental evaluation of ball bearings diagnosis by contamination [7], diesel engine lubricant contamination and wear. Estimation of temperature and effects of oxidation in thermal elasto-hydrodynamic lubrication [8], the use of textured surfaces to mitigate sliding friction and wear of lubricated and non-lubricated contacts, the effects of different cooling and lubrication Techniques on material machinability in machining [9], kinetic model and reaction kinetics to analyze the debris in plain bearing [10], and the thermal behaviour of engine oil, they were carried out using experimental methods and modeling.

A bearing is one of the fundamental elements in the machine; even the simplest machine, the lever, must have a bearing or fulcrum [11]. All movements in mechanisms and machines require some sort of bearing to locate and guide the moving parts. A machine designer will try to convert energy put into a machine into useful output work and will, therefore, attempt to reduce the energy losses that arise through friction at the bearings. Mechanical devices stop working after some time due to the failures of mechanical contacts when there are insufficient lube supply and

rapid degradation of the quality of the lubricating oils. Mechanical failures that occur in mechanical contact are fatigue, galling, indentation, erosion and fretting. These failures release debris in the contact. Most of the analysis to determine oil film thickness in machine element assumes a clean lubricant. In this paper, the experimental evaluation of heat released in a Mitsubishi main journal bearing due to different types of debris in it was carried out. Cooling rates of different lubricating oils were evaluated experimentally while considering no debris and when infused with different types of debris in the mechanical contact.

2. Materials and Methods
2.1. Materials
The materials used are Mitsubishi main journal bearing (size: 0.25 from Mitsubishi engine of model number 4G32N24232), copper calorimeter (mass: 200g; specific heat capacity: 400J/kgK), thermometer (mercury-in-glass: 0^0C to 360^0C), stop clock (unicon-1), digital weighing machine (SF-400: 1g to 7000g), electric motor (model no. 5000/99; 0.75kW), lubricating oils (SAE 20W 50), frictional heat and cooling rate evaluation apparatus. The lubricants used are oil A, oil B and oil C. The test rig has adjustable journal bearing fixed at its lower end (see Figure 1).

2.2. Debris Characterization
Two kinds of debris were used in the experiment; Silicon IV oxide debris and Iron filings debris. Silicon IV oxide debris consists of sand of fine particles of diameter 0.012mm. While iron filings debris consists of iron powder of diameter 0.013mm. The method of debris characterization is mechanical characterization (see Table 1).

Table 1: Mechanical characterization of the debris

Properties	Sand	Iron filings
Brittleness	Very brittle	Ductile
Tensile strength (10^9N/m^2)	No value	(180-210)
Chemical constituents	Fragments of coral, limestone, shell and silicon iv oxide.	Iron
Young's modulus ($10^9 pa$)	130-185	210
Thermal conductivity (W/mK)	0.71	79.5
Specific heat capacity (J/gK)	0.73	0.42
Thermal diffusivity (m^2/s)	1.4	2.3

2.3. Methods
An experimental method was used for the evaluation of the amount of heat generated in the mechanical contact like that of rotating journal bearing. The rotating mechanical element releases the frictional heat energy while trying to overcome the friction in the contact. The experiment was performed with three lubricating oils using different types of debris in the contact. Seven experiments were

carried out to evaluate the amount of heat generated in the mechanical contact and the cooling rates of the lubricating oils under different conditions. The first set of experiments was carried out with the lubricants under debris-free condition while the second was done with lubricants containing silicon debris. The third experiment considered the same lubricants containing ferrous materials like Iron filings. To evaluate the amount of heat energy released in the lubricated mechanical contact using a clean lubricant, the following apparatus was used; digital weighing machine, thermometer, stop watch, lubricants (oils 'A', 'B' and 'C'), lagging material (cotton wool) etc. The mass of the bearing (M1) and the mass of the empty calorimeter (M2) were measured and recorded. A known volume (V) of the lubricating oil 'A' was poured into the calorimeter. The mass of the calorimeter and its content (M3) was equally taken. The initial temperature of the calorimeter and its content was recorded. The oil and the calorimeter will have the same initial and final temperatures according to the Zeroth law of thermodynamics [12], [13]. The temperature of the bearing is approximately mid-way between the temperature of the oil film [14]. The calorimeter and its content were placed under the frictional heat evaluation apparatus as shown in the figure 1, so that the rotating journal bearing and its housing were completely immersed in the oil 'A', that is, electro-hydrodynamic lubrication EHL. The motor and the stop watch were started at the same

time and the final temperatures, were read and recorded at an interval of 3minutes respectively. The quality of heat energy released cannot be measured with an instrument directly but can be calculated with the elementary formula [12], [13], were M = mass, C = specific heat capacity of the substance, change in temperature. The components that absorb the heat are the journal bearing, the oil and the copper calorimeter. The same procedures were repeated in the second and third experiments with Silicon IV oxide debris and Iron fillings debris introduced in the mechanical contact respectively. The above procedures were replicated for oil 'B' and oil 'C'. Calculating the quantity of heat, the amount of heat supplied is equal to the amount of heat absorbed by the lubricant, copper calorimeter and the bearing at a particular temperature.

$$Q_T = Q_1 + Q_2 + \cdots + Q_n$$
(1)

Where: Q_1 = quantity of heat absorbed by the bearing.

$$Q_1 = M_1 C_1 (\theta_{i+1} - \theta_i)$$
(2)

Where: M_1 = mass of the bearing (g); C_1 = specific heat capacity of steel (bearing); θ_{i+1} = final temperature at the end of each 3min which will be the same for the three materials mentioned above; θ_i = Initial temperature; Q_2 = quantity of heat absorbed by the calorimeter.

$$Q_2 = M_2 C_2 (\theta_{i+1} - \theta_i)$$ (3)

Where: M_2 = mass of the copper calorimeter (kg); C_2 = Specific heat capacity of copper calorimeter (J/kgK); M_3 = mass of oil +

calorimeter; M_2 = mass of the empty calorimeter; C_3 = specific heat

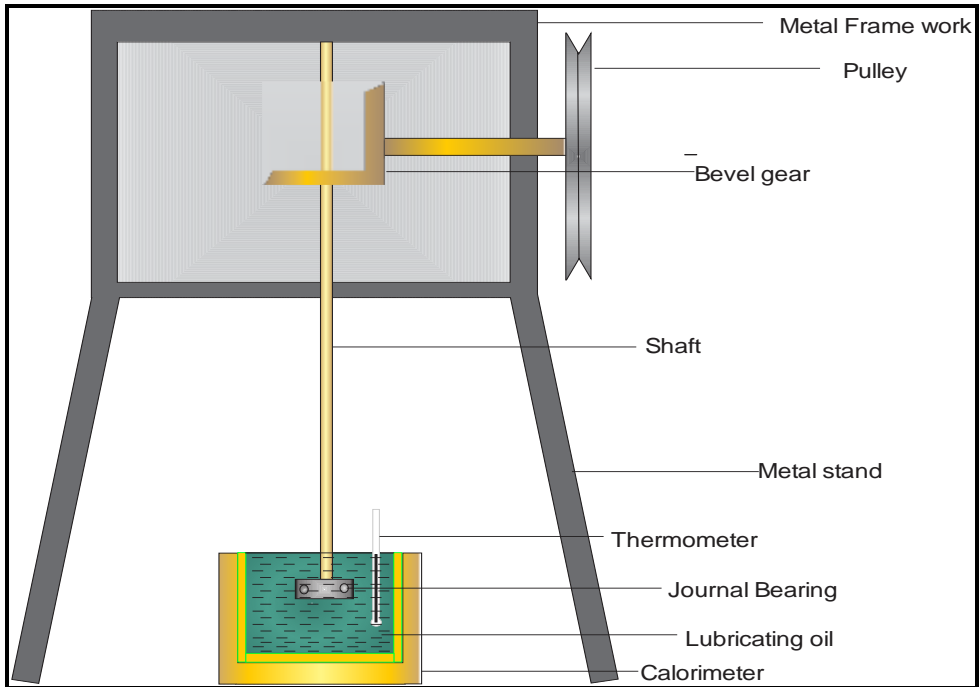capacity of the lubricating oil = 2.09J/kgK.

Figure 1: Schematic of the Frictional Heat and Cooling Rate Evaluation Apparatus

3. Results and Discussion

The results of the change in temperature in a Mitsubishi journal bearing when there was no debris in the contact in the three oils are shown in Figure 2.
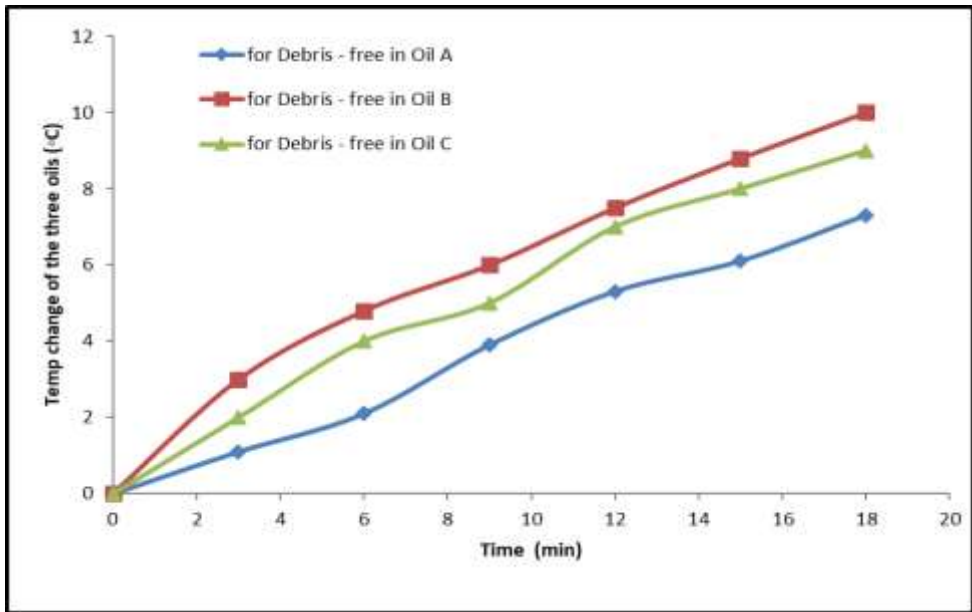
Figure 2: Comparison of change in temperature with time in the three debris-free oils

From Figure 2, oil 'B' showed the highest temperature change than the other oils. This was because the hot molecules of oil 'B' have higher kinetic energy than those of other oils. Since temperature is the measure of the average kinetic energy of the molecules of fluid [15]. The entropy of the hot molecules of oil 'B' was higher than that of oil A and oil C. Entropy is directly proportional to the quantity of heat absorbed [15]. The increased molecular movement helped to maintain a uniform temperature in the mechanical contact. The velocity of the hot molecules of oil 'B' was highest because of its low molecular mass and weak intermolecular bond. The inertia of the molecules of the other oils was too high, so the molecules could not move very fast. The change in the temperature-time curve of oil 'B' was similar to the one proposed by [16]. The temperature-time curves of the oils showed that the molecules of the oils did not absorb frictional heat at the same time. The shear stress of oil 'B' was the least and its molecules move faster than those of oils 'C' and 'A'. This movement helped to transfer the frictional heat and increase the temperature of the oil 'B'.

The results of the change in temperature of a Mitsubishi journal bearing generated in oil 'A' when the three debris conditions were considered are shown in figure 3.

Figure 3: Comparison of temperature change in oil 'A' for the three debris conditions

It could be seen from Figure 3 that the temperature increased when there was debris in the contact. The velocity of the molecules and the average kinetic energy increased gradually. The mobile free electrons on the outermost shell of iron helped to transfer the frictional heat and this affected the temperature change when iron particles were present. The average increase in temperature when there was debris in the contact was $2.5°C$ while it was $1.0°C$ when there was no debris in the contact. The increase in temperature was due to the fact that more kinetic energy was needed to overcome friction caused by the presence of debris in the contact. The change in temperature due to the presence of sand debris was reduced and that of iron filings started to increase above that of sand debris immediately after 4.6minutes. Until after 15minutes, the increase in change in temperature became equal due to the fact that the quantity of iron particles present in the contact has an equivalent effect with the available sand debris in the contact. The iron particles have free mobile electrons in their outermost shell, so it helped to transfer the heat. The charge distribution on the surface of the molecules of oil 'A' was very small thus facilitating heat transfer.

The results of the change in temperature in a Mitsubishi journal bearing generated in oil 'B' for the three debris conditions are shown in Figure 4.

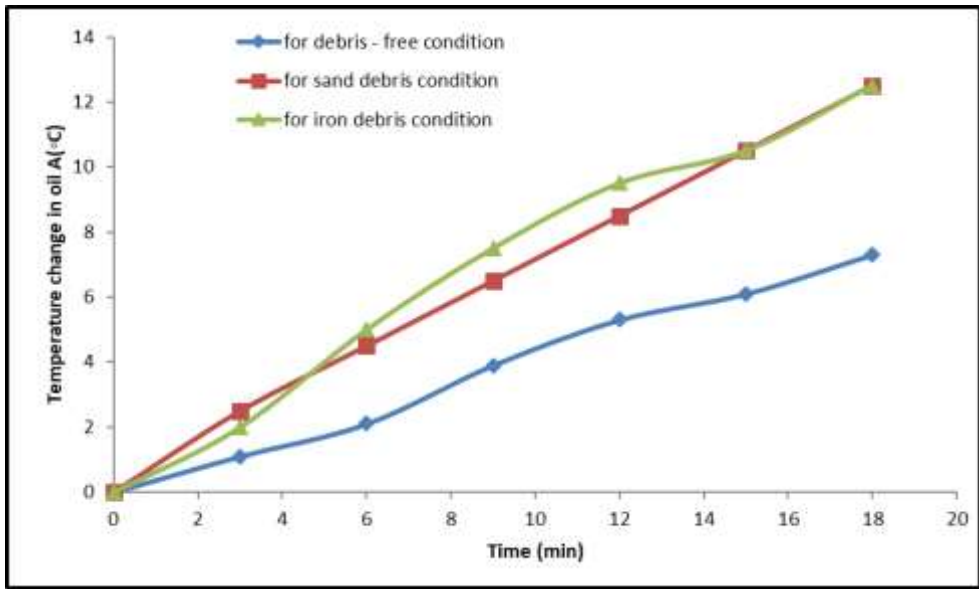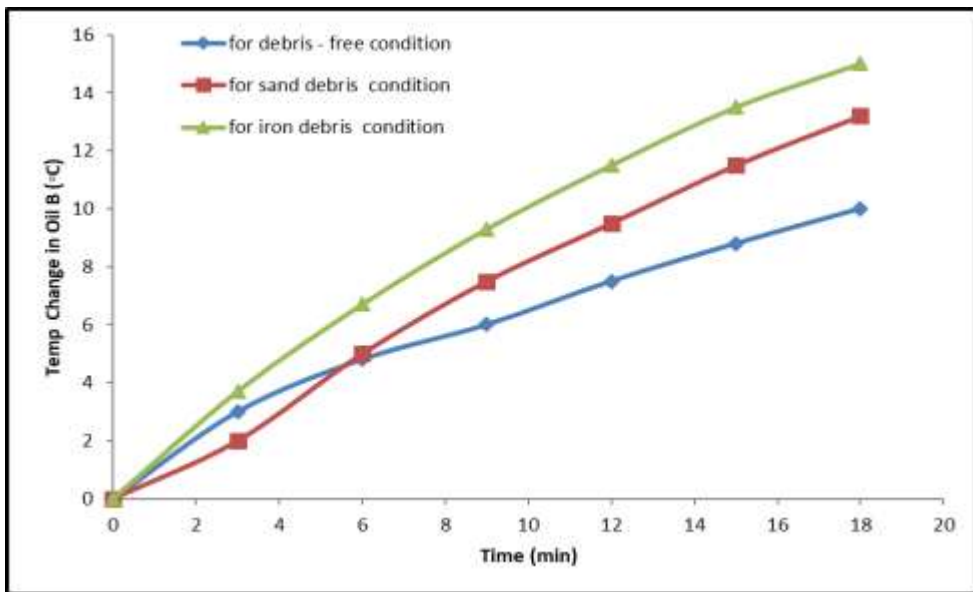Figure 4: Comparison of temperature change in oil 'B' for the three debris conditions

From Figure 4, the change in temperature when Iron debris was present was higher than others. The same explanations that were adduced in the analysis of the frictional heat in oil 'B' are applicable in temperature change and so both have the same temperature-time curves. The degree of disorderliness of the hot molecules of oil 'B' was the highest. The temperature changes when there were iron particles in the mechanical contact was greater than those of sand debris condition and debris-free condition. Hot iron debris moved easily in the oil 'B' because of its low viscosity and shear stress such that the hot iron particles transferred frictional heat uniformly and easily in the oil. This made the temperature-time curve of oil 'B' to be a smooth curve when there were iron particles in the contact. The change in temperature generated in oil 'B' when Iron particles were present in the oil was the highest. The intermolecular bond strength of oil 'B' was the smallest when compared with the other two oils thus, its molecules moved faster than the molecules of the other two oils. The mass of a molecule of oil 'B' was smaller than those of the other two. The mobile free electrons of the iron particles helped to transfer uniform temperature coupled with the charge distribution on the surface of the molecules of the oil 'B'. It could be deduced from this experiment that the hot molecules of the oil 'B' have the highest charge distribution. Also, the heat capacity of the oil 'B' was higher than the other two oils. The viscosity of oil 'B' was the smallest among the three oils and so it allowed the debris to move faster in it such that the hot particles transferred the frictional heat uniformly in the oil.

The results of the change in temperature in a Mitsubishi journal main bearing generated in oil 'C' for the three debris conditions are shown in Table 5. The temperature changes of oil 'C' is presented in Figure 5. The change in temperature increased when there was debris in the oil. It shows that the oxygen in Silicon IV oxide reacted with the oil and so it reduced the molecular movement of the oil while increasing its heat capacity. The presence of oxygen bond and silicon carbide formed helped to increase the heat content, thus increasing the change in temperature of the oil. Oxygen is an electronegative element and it has a high polarizing ability. It made the oil 'C' to become slightly polar and possess more distributed charges on its molecules. This effect was initially great but it was reduced after 6minutes due to the reduction in the concentration of sand particles present in the contact. The presence of debris increased the amount of friction in the contact and it had to be overcome before the rotating shaft maintained its motion.
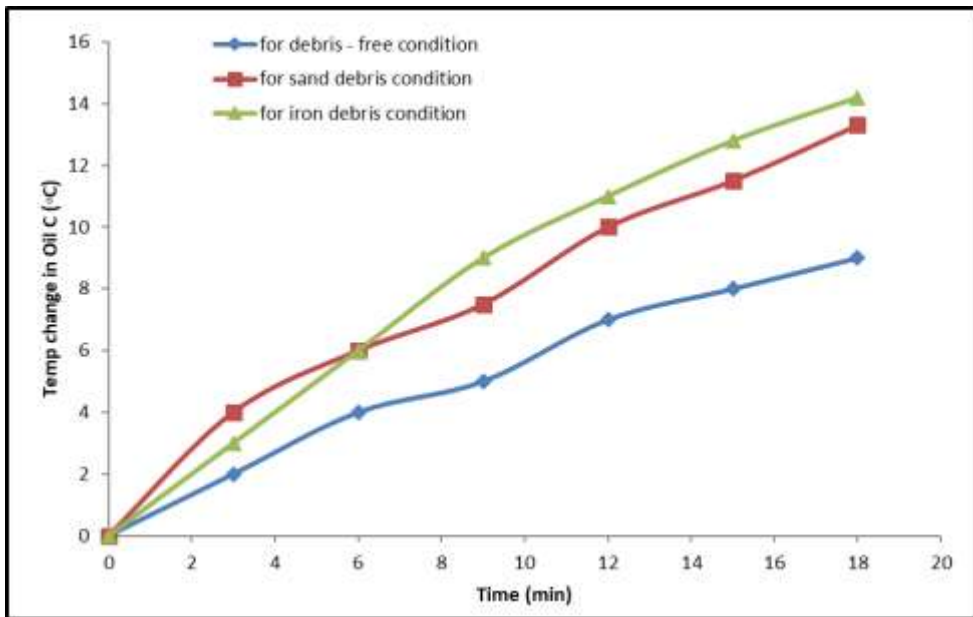
Figure 5: Comparison of the change in temperature of oil 'C' due to the three debris conditions

From Figure 5, the change in temperature when Silicon IV oxide debris was present in the oil is greater than that of the debris-free condition but less than that of iron-particle contaminated oil after 6minutes. The kinetic energy of the rotating shaft was converted into heat. The temperature of the oil was found to increase after the energy transformation. The movement of hot particles in the oil also helped to

transfer the frictional heat in the oil. The mobile free electrons of the Iron particles and the oil's charge distribution helped to increase the

temperature of the oil. This change in temperature was the highest.

The results of variations in viscosity with temperature in the three oils are shown in Tables 2 – 4.

Table 2: Variations of Absolute viscosity of oil 'A' with Temperature

Table 3: Variation of Absolute Viscosity of Oil 'B' with Temperature

Absolute viscosity (kg/m-s)	Temperature (^{0}C)	Absolute viscosity (kg/m-s)	Temperature (^{0}C)
0.422	29.2	0.309	34.0
0.363	31.0	0.274	35.8
0.352	32.0	0.254	37.0
0.321	33.4	0.231	38.5
0.305	34.2	0.211	39.8
0.282	35.4	0.196	41.0

Table 4: Variation of Absolute viscosity of oil 'C' with Temperature

Absolute viscosity (kg/m-s)	Temperature (^{0}C)	Absolute viscosity (kg/m-s)	Temperature (^{0}C)
0.330	33.0	0.238	38.0
0.289	35.0	0.223	39.0
0.271	36.0	0.209	40.0

From Table 2, absolute viscosity of lubricating oil decreased with an increase in temperature. As the temperature of the oil increased, hot molecules of oil 'A' gained kinetic energy and velocity. Their intermolecular bonds were broken as the temperature increased. When the molecules were very far apart from one another, its absolute viscosity decreased. The absolute viscosity of oil 'A' was higher than those of oil 'B' and oil 'C' but its performance was not better than those of oil 'B' and oil 'C'. From table 3, the absolute viscosity of oil 'B' decreased with an increase in temperature. The absolute viscosity of oil 'B' was smaller than that of oil 'A' at a given temperature

when compared with results in table 2. The same explanations proffered above are applicable in the case of oil 'B' and oil 'C'. The table of values of absolute viscosity of oil 'C' with temperature is shown in table 4. The values in the tables 3 & 4 are slightly different because their intermolecular covalent bond and their molecular velocity are slightly different. As the temperature of oil 'C' was increased, the degree of its molecular disorderliness increased also. The covalent bonds of the molecules were broken and so its viscosity reduced as shown in Table 4.

The results of the heat generated in a Mitsubishi journal bearing when there was no debris in the contact in the

three local oils are shown in Figure 6. During the experiment, heat energy was generated as the journal rotated on the surface of the bearing as powered by an electric motor of 0.75kW. This was due to the conversion of mechanical energy of the motor into frictional heat which was absorbed by the lubricants. It made the molecules of the bearing to vibrate about their mean positions. This molecular vibration helped to transfer the frictional heat energy through the bearing to the lubricant, its housing and the calorimeter. The vibrational movement of the molecules increased as the frictional heat increased. This heat was absorbed by the bearing, it's housing, lubricant and the calorimeter.
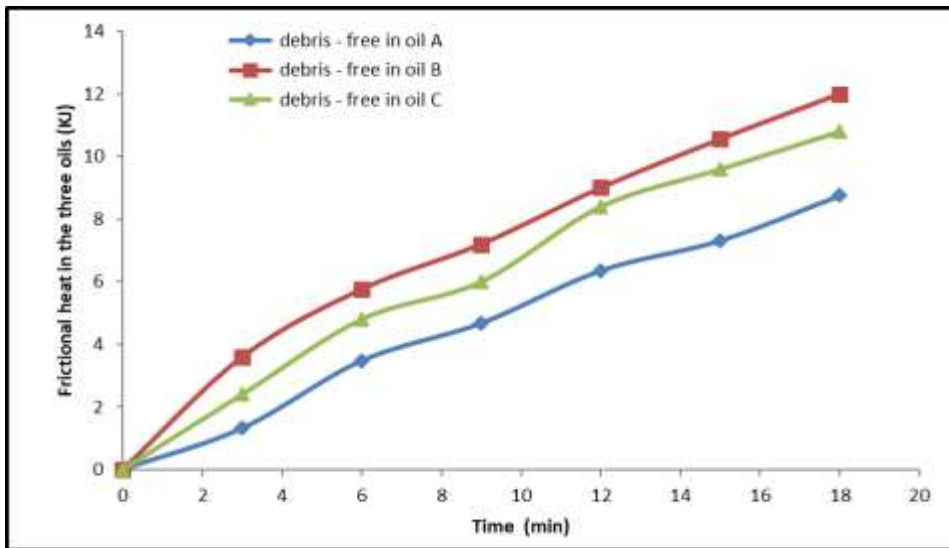
Figure 6: Comparison of the frictional heat generated in the three oils

From Figure 6, oil 'B' absorbed the highest frictional heat because its molecular movement was the highest hence the generated frictional heat was easily transferred uniformly in it. It is noteworthy that the molecules of oil 'B' were not strongly bonded together and so its molecules moved faster than others. The mass of a molecule of oil 'B' and its intermolecular bond was smaller than those of oil 'A' and oil 'C' because the average speed of the hot molecules of oil 'B' was greater than those of oil 'A' and oil 'C'. It is for this reason that the hot molecules of oil 'B' moved faster than those of molecules of oil 'A' and oil 'C'. Also, the specific heat capacity of the oil 'B' was greater than those of oil 'C' and oil 'A'. Figure 6 shows that frictional heat in the three oils ('B', 'A' and 'C') increased as the time of heat generation increased.

The results of the heat generated in a Mitsubishi journal bearing when it was immersed in oil 'A' while considering the three debris conditions are shown in Figure 7. It could be asserted that as the journal

rotated on the bearing, the molecules of oil 'A' gradually gained kinetic energy due to the heat generated in the contact. The viscosity of oil 'A' was the highest among the three oils and so it restricted the movement of the hot debris in it. This was due to the high shear stress of the oil. The frictional heat distribution in it was not uniform. The entropy of the molecules of oil 'A' was the lowest.

The amount of frictional heat generated in oil 'A' when there were sand and Iron debris in the oil was greater than that of debris-free condition. Owing to the high shear stress of the molecules of oil 'A', the hot Iron particles could not move easily in the oil so the amount of frictional heat transferred in the oil was not all that high when compared with that of oil 'B'.
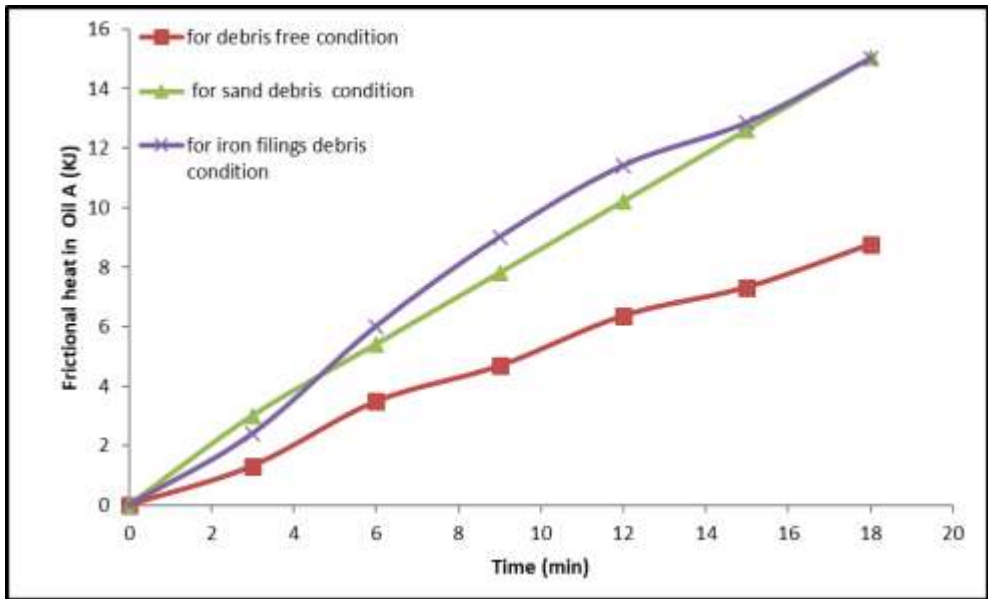
Figure 7: Comparison of frictional heat generated in oil 'A' due to the three debris conditions

From Figure 7, the hot molecules increased translational, rotational and vibrational movements due to the fact that the frictional heat increased gradually. These molecular movements increased when there were debris particles present in the journal bearing. The number of sand particles in the contact with the journal bearing was larger than that of

Iron filings of the same mass since the density of sand is less than that of iron. The initial frictional heat generated in the contact by the Silicon IV oxide debris was slightly higher than that of iron. Surprisingly, the sand debris was crushed into tiny particles by the rotating shaft and some escaped through the clearance of the bearing as such, its frictional

heat was reduced and that of iron filings started to increase above that of sand debris immediately after 4.6minutes. However, after 15minutes, the increase in the generated frictional heat became equal due to the fact that the amount of iron particles present in the contact has equivalent effect with the available sand debris in the contact. The iron particles have free mobile electrons in their outermost shell, so it helped to transfer the heat. The charge distribution on the surface of the molecules of oil 'A' was very small thus helping in heat transfer.

The results of heat evaluation in a Mitsubishi journal bearing generated in oil 'B' for the three debris conditions are shown in Figure 8. The amount of frictional heat generated in

oil 'B' was higher than those of the other two oils. The frictional heat-time curve when iron particles were present was relatively a smooth curve. The entropy of the molecules of oil 'B' was the highest. The degree of disorderliness of the molecules of oil 'B' helped to transfer the frictional heat in the oil. The shear stress of oil 'B' was the least and so it allowed the hot debris (sand and iron particles) to move easily in it, thereby increasing the temperature and the amount of frictional heat absorbed by the oil 'B'. The shear stress of the molecules of oil 'C' was slightly higher than that of oil 'B' and so it slightly reduced the movement of hot debris in it. Owing to this effect, the amount of friction absorbed in oil 'C' was smaller than that of oil 'B'
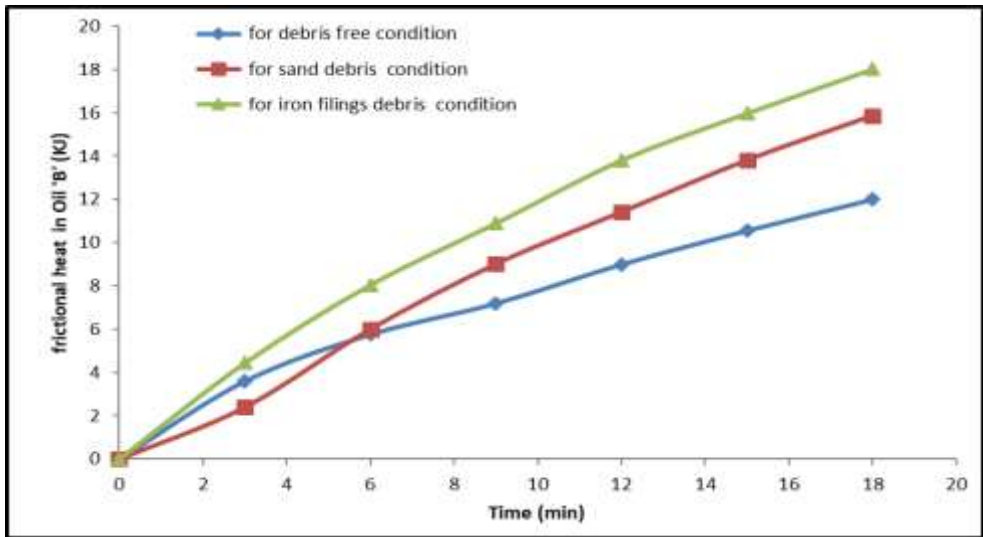

Figure 8: Comparison of frictional heat generated in oil 'B' for the three debris conditions

From Figure 8, the frictional heat generated in oil 'B' when iron particles were present in the oil was the highest. The intermolecular bond

strength of oil 'B' was the smallest when compared with the other two oils thus its hot molecules moved faster than the molecules of the other

two oils. The mass of a molecule of oil 'B' was smaller than those of the other two oils so, it had little inertia to move and transfer the frictional heat. The mobile free electrons of the iron particles helped to transfer heat in conjunction with the charge distribution on the surface of the molecules of oil 'B'. The molecules of oil 'B' have the highest charge distribution also the heat capacity of oil 'B' was higher than those of the other two oils.

The results of heat evaluation in a Mitsubishi journal bearing generated in oil 'C' for the three debris conditions are shown in figure 9. The frictional heat increased when there was debris in the journal bearing. The molecules of oil 'C' gained kinetic energy and moved with high velocity. The velocity and kinetic energy of the hot molecules of oil 'C' was highest when iron debris was present in the oil. This was illustrated in Figure 9. These explanations are based on the charge distribution on the surface of oil 'C' molecules and the mobile free electrons of iron particles were also applicable in this oil. The entropy of the molecules of oil 'C' was higher than that of oil 'A' but it was lower than that of oil 'B'. The shear stress of the oil 'C' was slightly higher than that of oil 'B' but it was less than that of oil 'A' thus hot particles could not move easily in the oil to transfer the frictional heat uniformly.

From Figure 9, the particles of silicon IV oxide was crushed into a fine powder and its concentration was reduced in the bearing. Iron particles are not brittle like the sand particles, so the iron particles were not easily crushed into a fine powder. The iron debris curve intercepted the sand debris curve after 6minutes. This was because the same amount of frictional heat was generated in the journal bearing. The amount of sand particles present in the bearing has an equivalent effect with the iron particles present at that time.

The results of the cooling rates of oil 'A' due to the three debris conditions are shown in Figure 10. The cooling rates decreased non-uniformly with the time taken. This was because the intermolecular force and the covalent bond between the molecules of oil A were very high such that the molecular movement of oil 'A' was reduced. This reduction affected the transfer of frictional heat extracted from the surface of the bearing to the other molecules of the oil. The amount of heat absorbed by the oil 'A' when there was debris in the contact was higher than that of no debris condition. This was because more frictional heat was generated in the contact. In the same vein, more kinetic energy was needed to overcome friction in the contact. The amount of frictional heat absorbed by the oil from the surface of the bearing when there was debris in the contact would increase also.
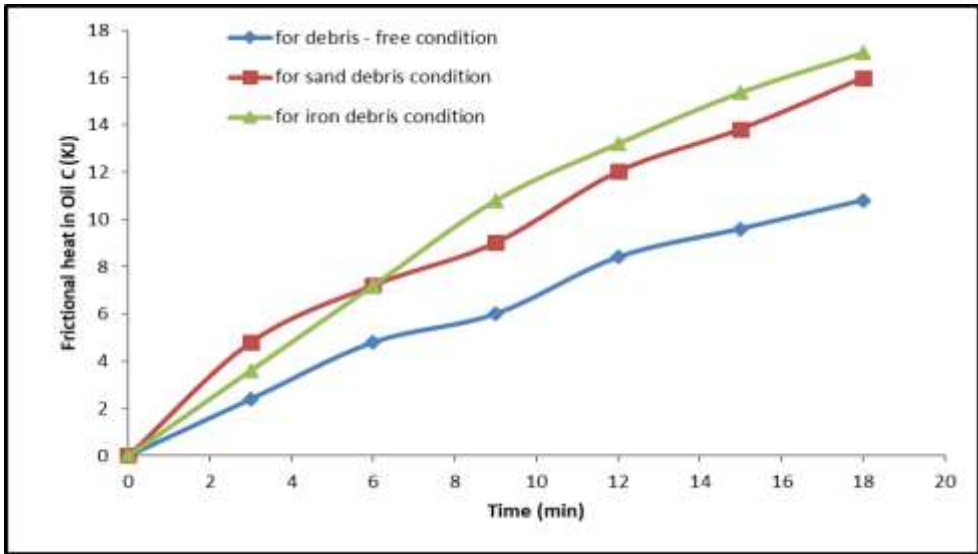
Figure 9: Comparison of frictional heat in oil 'C' for the three debris conditions
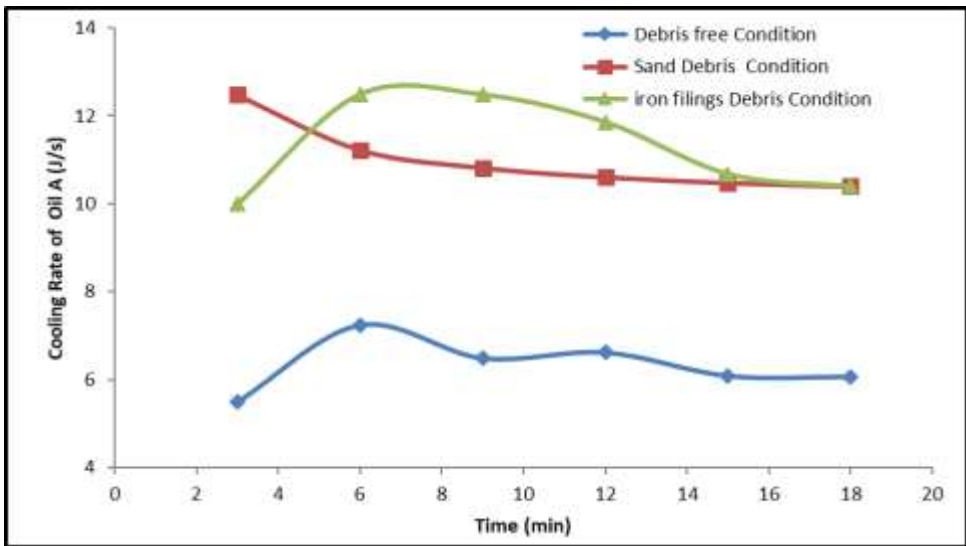
Figure 10: Comparison of cooling rates of oil 'A' due to different debris conditions

It could be derived from Figure 10 that the amount of heat absorbed by the oil when iron particles were present initially decreased and then subsequently increased. This was because iron is a metal and it conducts heat very fast. The cooling rate of oil 'A' decreased non-uniformly as the temperature increased. This was because the heat generated was absorbed into the intermolecular domain which was used to break the covalent bonds of the oil. Also, all the

URL: *http://journals.covenantuniversity.edu.ng/index.php/cjet*

molecules of the oil did not absorb the frictional heat at the same time. This affected the viscosity and heat capacity of the oil. In sand particle contamination, there was an increase in the amount of heat generated and so its cooling rate was higher than that of debris free condition. The amount of sand debris in the contact was higher than that of iron particles of the same mass since the density of iron is greater than the density of sand. But, in each case, the cooling rate decreased with time. The mobile free electrons on the surface of iron particles helped to generate more frictional heat.

The results of the cooling rates of oil 'B' when considering the three debris conditions are shown in Figure 11. The cooling rate of oil 'B' due to the three debris conditions decreased with

time. According to the values, in oil 'B', it showed that the amount of frictional heat absorbed from the surface of the bearing was higher than that of oil 'A' so the heat capacity of oil 'B' is higher than the heat capacity of oil 'A'. The hot iron particles moved freely in oil 'B' while carrying a large amount of frictional heat through the oil owing to its low shear stress. The heat carried by the hot iron particles was absorbed by the oil so the amount of heat absorbed by the oil 'B' when there was iron debris in it was the greatest. The degree of disorderliness of the molecules of oil 'B' was increased when it absorbed more frictional heat. This disorderliness promoted the breaking down of the covalent bonds of its molecules and so it decreased the cooling rate of the oil.
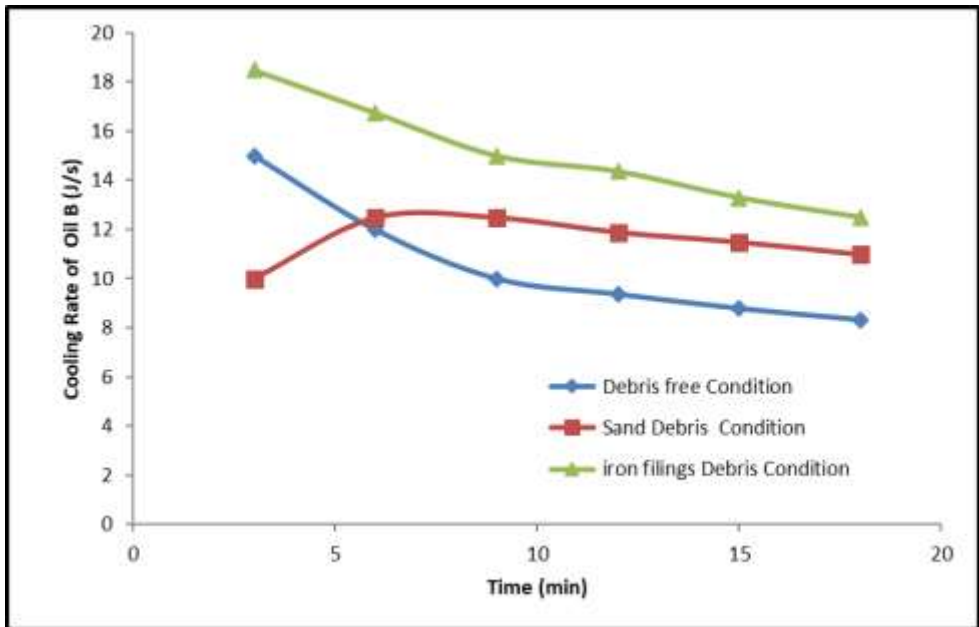

Figure 11: Comparison of cooling rates of oil 'B' due to three debris conditions

In Figure 11, Silicon IV oxide reacted with the oil 'B' and it formed larger molecules which reduced their molecular velocities. This affected the amount of heat transferred by the oil. As the temperature increased, the molecular bond broke down. The breaking apart of the intermolecular bond due to the amount of heat absorbed prompted the reduction of the cooling rate. The molecules became far apart from one another. The amount of heat carried by each molecule was smaller compared with when they clustered together. The charge distributions on the surface of the molecules of oil 'B' were higher than that of oil 'A'. Mechanical failure of the surface of the bearing occurred when the vibrational kinetic energy of its molecules was greater than the binding energy of the bearing lattice. This made the atomic particles to break out from the surface of the bearing. It took a long time to occur when there was no debris in the mechanical contact than when there was debris in the contact. Silicon IV oxide is not a good conductor of heat and so it acted as an insulator. This phenomenon could not allow much heat to be extracted from the surface of the journal bearing.

The results of the cooling rates of oil 'C' when considering the three debris conditions are shown in Figure 12. The cooling rates decreased with time because the intermolecular bonds of oil 'C' molecules were broken. The hot molecules moved away from one another such that the heat absorbed when they clustered together was higher than when they were scattered apart. When there was debris in the contact, the frictional heat absorbed by the oil increased. At some points, the cooling rate remained constant because the frictional heat absorbed was used to break the inter-molecular bond and such could not be detected by the thermometer.
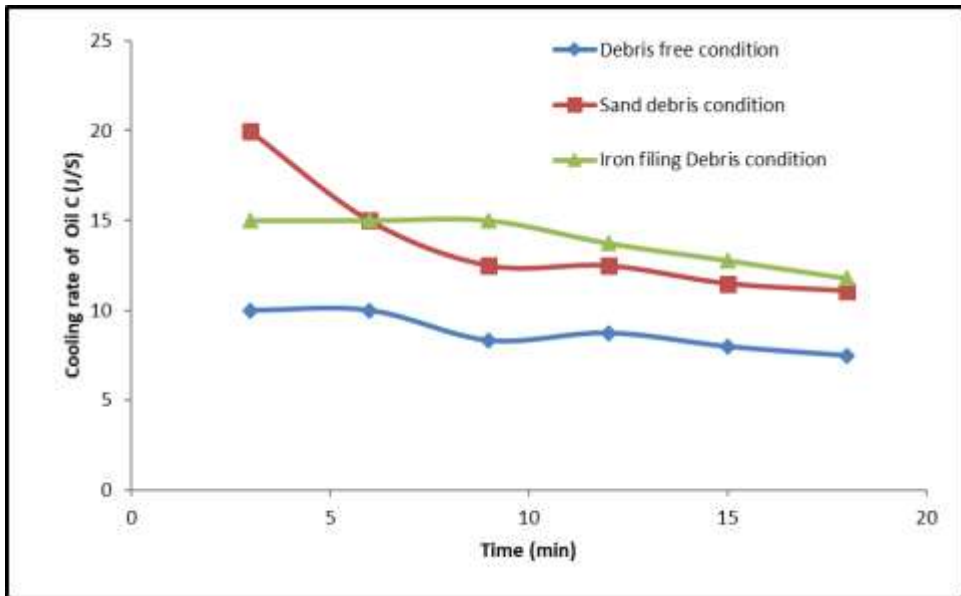

Figure 12: Cooling curves of oil 'C' due to different debris contamination

From Figure 12, when the molecules of oil 'C' were far apart, the molecules could not conduct much heat away from the surface of the bearing. As the hot molecules moved away from one another when their bonds were broken, their cooling rates decreased with time. The cooling rates in debris-free condition were smaller than the other two conditions. There was an increase in frictional heat generated in the journal bearing due to the debris contamination. There were constant cooling rates because the heat absorbed by the oil was used to break some intermolecular bonds, this is in line with Nasiri-khuzani et al., [17]. The shapes of some curves resembled that of Newton's cooling curve.

4. Conclusion

The amount of frictional heat generated in a Mitsubishi journal bearing depends on the nature of the debris in the contact and the amount of frictional heat absorbed depends on the chemical compositions of lubricants. The molecular movement and the heat capacity of the lubricants play a vital role in the cooling ability of the oils. The covalent intermolecular bonds of the three oils investigated differ and this affects conduction and convection of frictional heat in Mitsubishi main journal bearing. The cost of lubricating oil depends on quality and performance of the oils and the performance of lubricating oil does not depend on how viscous the oil appears to be but it depends on how its viscosity decreases over a range of temperature. The presence of debris in a mechanical contact reduces the bearing life cycle and thus causes the failure of the machine element. Apart from frictional heat generated in the bearing, other effects of debris are galling, abrasion, adhesion, erosion and indentation of the mechanical contact. The temperature of the oil film varied linearly with the surface temperature of the bearing. The performance of lubricating oil also depends on the charge distributions on the surface of the molecules of the oils. The frictional heat will be evenly distributed on the surface of the molecules due to the presence of charge distribution. The viscosity of lubricating oils decreases with time due to the fact that the molecules move far apart from one another after bond breaking.

Reference

[1] Moon, M. (2007). Gear solution, Journal of Tribology, (18): 574 – 588.

[2] Dwyer-Joyce R.S., Heymer J. (1996). The entrainment of solid particles into rolling elastohydrodynamic contact, ASME Journal of Tribology, 3(124): 420.

[3] Okokpujie, I. P., Okokpujie, K. O., Ajayi, O. O., Azeta, J., & Obinna, N. N. (2017). Design, construction and evaluation of a cylinder lawn mower. Journal of Engineering and Applied Sciences, 1254-1260.

[4] Abdullah O.I., Schlattmann J., Al-shabibi, A.M. (2014). Thermomechanical Analysis of the Dry Clutches under Different Boundary Conditions. Tribology in Industry, 36(2): 172 – 180.

[5] Madhuri M., Tiwari S., Ganai P. (2014). Analysis of lubricant for Prediction of Contact Surface Behaviour of Metals, International Journal of

Innovative Technology and Research, 2(3): 933 – 939.

[6] Okonkwo, U. C., Okokpujie, I. P., Sinebe, J. E., & Ezugwu, C. A. (2015). Comparative analysis of aluminium surface roughness in end-milling under dry and minimum quantity lubrication (MQL) conditions. Manufacturing Review, 2(30), 1-11.

[7] Ghanbari A., Khanmohamadi S. (2016). Experimental Evaluation of Ball Bearing Diagnostics by Contamination, Proceedings of the 10th WSEAS International Conference on Systems, 10(12): 80 – 85.

[8] Raj S., Jesse K. (2016). Estimation of temperature and Effects of Oxidation in Thermal Elastohydrodynamic Lubrication, Lubrication Fundamental III, 2(11): 1 – 12.

[9] Sredanovic B., Gordana G. L., Cica D. (2013). Effects of Different Cooling and Lubrication Techniques on Material Machinability, Journal of Mechanical Engineering, 59(12): 748 – 754.

[10] Shojace, Maryam (2015). Modelling for the Thermal Behaviour of Engine Oil in Diesel Engine, Journal of Tribology, 14(15):1 – 15.

[11] Carter, G. (1993). Tribology, Published by Macmillan Education, Loughborough University of Technology,

Engineering Science Project, (3): 20–25.

[12] Odume, P.N. (2011). Basic Physics, First Edition, Published by Nukak Publishers, Enugu, Nigeria, 239 – 255.

[13] Achebe C.H., Nwagu A.I. Anosike B.N. (2016). Evaluation of Frictional Heat Generated in a Mechanical Contact due to Debris Formation and the Cooling Rates of some Lubricating Oils. SCIREA Journal of Mechanical Engineering, 1(1): 12 – 32.

[14] Khurmi R.S., Gupta J.K. (2012). Machine Design, Fourteenth Edition, Published by Eurasia Publishing House (p) Ltd, 7361, Ram Nagar, New Delhi (8): 978– 980.

[15] Osei Y.A., Akpanisi L.E.S., Igwe H. (2011), New School Chemistry, Sixth Edition, Published by African First Publishers plc, Africana First Drive, Onitsha, Nigeria, (8): 436 – 439.

[16] Macek J., Emrich M. (2011). A simple physical model of ICT mechanical losses, Journal of Tribology,(12): 1– 25. Nasiri-khuzani Gh., Asooder M.A., Rahnama M. Sharifnasab H. (2012). Evaluation of Engine parts wears Using Nano lubricant Oil in agricultural Tractors Nano lubricant, Global Journal of Science Frontier Research Agricultural and Veterinary Science, 12(8): 1 – 10.

An Open Access Journal Available Online

Mismatch between Anthropometry Characteristics of Nigerian Occupational Bus Drivers and the In-Vehicle Measurement

Fajobi Moses O[1]*, Onawumi Ayodele S.1.[2], Mfon Udoh M. O[2] & Awoyemi Elijah A[3]

[1,2]Department of Mechanical Engineering, Ladoke Akintola University of Technology,
P.M.B. 4000, Ogbomoso. Oyo State. Nigeria.
[2]Department of Mechanical Engineering, Covenant University,
P.M.B. 1023, Ota, Ogun State, Nigeria.
[3]Department of Works and Maintenance, Osun State University,
Osogbo, Osun State, Nigeria.
mofajobi54@lautech.edu.ng

Abstract- The characterization of interfacing elements of in-vehicle and driver's anthropometric variables of a randomly selected operators with sample size of 161 subjects of commercial buses in the study area were considered in this work. Participatory ergonomic intervention approach was employed in data mining, opinion gathering and subsequent analysis. Related variables between the two systems were compared to establish fitness as well as the level to which human operator were accommodated in the vehicle dimension. A few cases of misfit were recorded based on drivers' opinion and the measurements taken. Work related musculoskeletal disorder experienced by the users under study were traceable to inappropriate design variable of the in-vehicle elements.
Keywords: Anthropometry, Workstation, Bus Driver, Ergonomics, Musculoskeletal Disorders

1. Introduction
The movement of goods and services plays significant role in everyday life bustle with varying means of transportation resulting from vivid research and development activities. Common technological systems in use are usually operated by human being whose capabilities and limitation are rarely considered at the development stage of the means of transportation especially in the face of international trading of automobile industry. Work related musculoskeletal disorder reported by drivers of automobile continue to create design challenges

URL: *http://journals.covenantuniversity.edu.ng/index.php/cjet*

receiving attention of ergonomists and automobile in-vehicle developers [1] [2]. Although the risk exposure of both driver and passengers of automobiles are seemingly of the same level, the vigilance level required for save control of the system place higher demand on the driver [3]. Some of the occupational risks experienced by the users includes fatigue, health damages by noise, vibration, toxic and irritable effects by atmospheric pollution, injury or death in case of fatal accidents. Significant mismatch of in-vehicle design variables and the anthropometric characteristics demand of taxi cab drivers in Nigeria was found to be responsible for reported disorder and other uncomfortable conditions [4] [5] [6]. Much of the challenges, trauma, and disorders complained by operator of automobiles in Nigeria were more of absence of effective legislation and absence of enforcement of existing rules and regulations in automotive industry. Ongoing efforts to mitigate persistence musculoskeletal and psychological trauma imposed by imported technological systems are yet to yield reasonable result due to technically missing link [7]. The combined work design and ergonomics approach, especially for the redesign of faulty physical environment do not only increase the production output but also the user's safety and comfort for effective and efficient performance [8].

Anthropometry: is the art and science of measurement the physical geometry, mass properties, and strength capabilities of the human body [9] [10] [11]. It is concerned with the scientific study of human subjects for the development of standards and evolving of specific demands associated particularly with manufactured goods and services to enhance product usability and ergonomics suitability for the user population [12] [13]. Anthropometric data bank for citizen of varying age group have been developed in most developed countries and used in area of product design and manufacture. However, anthropometric dimensions and other various factors such as gender, age, race, nutritional status, physiological build and nature of work were found to vary widely across every region, state and country [14]. This suggests significance differences in anthropometric data of populace/subject from among countries and the misfit of products imported from place with organised database (UK, USA, Japan. Germany. China etc.) into developing countries like Nigeria, Ghana, Cameroon etc. where required body dimensions were not considered in product development [4]. In the case of automobile industry, a number of drivers' workstation were reported to cause discomforts due poor design and inadequate adjustability as well as lack of application of ergonomic principles in the design of some in-vehicle components. Reliable anthropometric data for a targeted population becomes necessary when designing for that population otherwise the product may not be suitable for the users [15].

The challenges associated with the applications ergonomic principles become obvious due to significance of

the variations in human capabilities and the unavailability of updated user's anthropometric database. These have posed enormous task for ergonomists and designers of products and components peculiar [16] [17] [18].

Anthropometric data application in man-machine system and similar facilities design can be stressful due to number of design parameters involved [19] [20], this problem has recently been made much easier giving some developed design principles like design for adjustable range, design for average sizes (50th percentile) and design for extremities (5th/95th percentiles).

This study seeks to identify research and development gaps and areas of mismatch between driver and technological systems characteristics. Driver's posture is also important to vehicle design process, man-machine system as well as the static and dynamic anthropometric demands of the operator [21] [22]. Other variables that could be used to determine ergonomic suitability of driver in the workstation are; seating comfort, postural composition and body flexibility. These can also be used to estimate the driver's resilience and endurance level at work [23] [24].

To have a better understanding of the causal factors of musculoskeletal disorder and discomfort to the driver while at workstation, the relationship between the operator's seat, steering column and wheel and pedals in the workstation must be clearly understood [25].

These have a great influence on posture of the operator. Previous researches have it that sitting position enhances the comfort and effectiveness of bus drivers. The posture is however limited to 30 minutes in constrained location and/or fixed position.

2. Materials and Methods
Sampling Technique

Two commonly used model of passenger vehicles namely Toyota Hiace and Mazda identified through preliminary survey at the study area were considered for further study. With the use of participatory ergonomic intervention approach, opinion of 161 randomly selected bus operators from six prominent motor park units were used for ergonomic evaluation and anthropometric characterization study. Three trained enumerators were involved in the procedure for collection of fifteen relevant anthropometric measurements for each of the subjects who volunteered to the rigour of the procedure adopted by [26].

Bus Operators Anthropometric Characterization Procedures: The procedure for taking subject's anthropometric measurement used by [4] was adopted in this study with the assistance of three trained enumerators. Body variables considered were Shoulder-Height-Sitting, Shoulder-Elbow-Length, Shoulder-Breadth, Sitting-Height-Normal, Sitting-Height-Erect, Buttock-Knee-Length, Buttock-Popliteal-Length, Thigh-Clearance-Height, Popliteal-Height-Sitting, Thumb-Tip-Reach-Sitting, Anterior-Arm-Reach, Stature, Hip-Breadth and Maximum-Body-Breadth.

The instrument employed in the measurement include Stadiometer, Vernier-Callipers, measuring Tape, Anthropometric-Seat, and Bathroom-Weighing-Scale, clipboard, Data collection form pencil with cleaner and digital camera. The average values of the triplicated measurements were calculated and considered for further analysis.

A 2D model of each of the anthropometric dimension of a seated operator were divided into three groups for easy identification as follows:

i. Sagittal Plane (Vertical Dimensions)
ii. Sagittal Plane (Horizontal Dimensions) and
iii. Frontal Plane.

Driver's Seat and Workstation Characteristics: Twenty-three physical characteristics of driver seat and other workstation parameters were considered for the study. The considered physical dimensions of the driver and the workstation were characterised with measurements which include: Seat height, Seat depth, Backrest seat plane height, Backrest height, Distance from edge of seat to application of force point, Lumber support height, Lumber support depth Lumber support extension, Rounded front edge width, Armrest clearance, Backrest width (Lumber level), Backrest width (Thoracic level), Horizontal lumber concavity (Radius), Horizontal Thoracic concavity(Radius), Headrest length, Headrest width, Armrest surface length, Armrest surface breadth, Backrest angle and Seat plane angle. Data collected were processed in Microsoft Excel Spreadsheet 2010 version and imported into SPSS 17.0 for further analysis. Descriptive statistics which included; mean, standard deviation, range and percentiles (5th, 50th and 95th percentiles) were determined. Results obtained from both characterizations were compared with each other and these formed the bases upon which bus design specifications were developed and the anthropometric database created.

Table 1: Anthropometric Description of Seated Vehicle Operator from Vertical View of the Sagittal Plane

Model	Description	In-vehicle applications
Shoulder Height Sitting	**Shoulder Height (Sitting) (SHS):** The vertical distance from the sitting surface to the uppermost point on the lateral edge of the shoulder (acromiale).	Backrest height, Door Height, Headrest adjustable range, Seat belt design

Shoulder Elbow Length	**Shoulder – Elbow Length (SL):** The vertical distance from the uppermost point on the lateral edge of the shoulder (acromiale) to the bottom of the elbow (alecranon).	Armrest height Armrest depth Armrest clearance, Side gear control knob. Door opening lever location Side door armrest buttons
Sitting Height Normal	**Sitting Height Normal:** The vertical distance from the sitting surface to the uppermost point of the head (subject sits relaxed)	Vehicle roof-seat plane distance, Seat plane vatical adjustment range,
Sitting Height Erect	**Sitting Height Erect:** The vertical distance from the sitting surface to the uppermost point of the head (subject sits erect)	Backrest-seat plane height, Headrest height, Vehicle roof-seat plane distance, Seat plane vatical adjustment range,
Popliteal Height Sitting	**Popliteal Height Sitting (PHS):** The vertical distance between the floor and to the thigh immediately behind the knee.	Seat plane height Seat plane vatical adjustment range, Seat depth
Thigh Clearance	**Thigh Clearance Height (TCH):** The vertical distance from the sitting surface to the top of thigh at its intersection with the abdomen.	Seat plane-steering wheel distance Seat depth adjustment range

	Stature/Standing Height: The vertical distance between the centre of the head and the sole of the feet was measured.	Seat stretch and pedal room design

Table 2: Anthropometric Description of Seated Vehicle Operator from Horizontal View of the Sagittal Plane

Model	Description	In-vehicle Applications
	Buttock – Knee Length (BNL): The horizontal distance from the most posterior point on the buttocks to the most anterior point on the knee.	Seat plane depth Backrest-dashboard distance Pedal room design Knee-dashboard clearance
	Buttock – Popliteal Length: The horizontal distance from the most posterior point on the buttocks to the most interior point on the knee (i.e., back of the kneel)	Seat depth Seat plane contour
	Anterior Arm Reach, Sitting (AAR): The horizontal distance from the back of the shoulder (greatest bulge of trapezium) to the tip of the extended middle finger.	Seat Backrest- windscreen distance, In-vehicle work space evilop.
	Thumb – Tip Reach, Sitting (TRS): The horizontal distance from the back of the shoulder (greatest bulge of trapezium) to the tip of the extended thumb.	Dashboard buttons-driver distance, Seat Backrest- windscreen distance, In-vehicle work space evilop. Door opening lever location Side door buttons Armrest surface length

Table 3: Anthropometric Description of Seated Vehicle Operator from Front View of the Sagittal Plane

Model	Description	In-vehicle Application
	Shoulder Breadth (SB): The maximum horizontal distance across the deltoid (triangular muscle on the human shoulder) muscles.	Backrest width (Thoracic level) Backrest contour design
	Hip Breadth (Sitting) (HB): The maximum horizontal distance across the hips.	Backrest width (Lumber level) Pedal room width
	Maximum Body Breadth (MBB): The maximum horizontal distance between the lateral surfaces of the elbows.	

3. Results and Discussion

In-Vehicle's Variable and Anthropometric Characteristics: Age group of the studied subjects ranges between 18 to 60 years. Table 4 shows the summary of the descriptive and percentiles statistics of the anthropometric characteristics. Table 5 shows the results of the in-vehicle geometrical characterization. Table 6 shows individual characteristics of the in-vehicle geometry against the pertinent anthropometric dimension(s).

Driver's door (Height and Width): Data obtained from the design reveals that existing door variables (door height) of the buses (135.7cm by 99.5cm) does not adequately meet the operators' requirements as indicated in the percentile statistics of the drivers. The suggests a redesign using design recommendation dimension of average door height and width of 140.0cm by 99.5cm respectively for the extreme 95th percentile.

Ground-to-driver's door height: Interactions and personal observations revealed that the existing ground-to-driver's door height might not be adequate as it is too high (70.4cm) especially for the short drivers. This makes the drivers uncomfortable while ingress and egress his workstation. Therefore, as suggested by Brooks, 1979, ground-to-driver's door height be lowered to an average of 34.8cm and stair steps would be necessary. The existing handrail should be designed to ergonomically conform to the driver's fingers shape

in order to generally reduce the problems (like sliding of the hand against the handrail) faced by the drivers while entering as well as exiting through the driver's doors.

Seat: As defined by SAE 2013 (Motor Vehicle Seating System), motor vehicle seat system is a structure engineered to seat the driver and/or passengers, including all pads, upholstery, decorative metal trim parts and seat adjusters or supporting components. For better performance of the drivers at workstations, the seat should be designed putting into consideration, the following design specifications for each of the variables;

Seat widths: From Table 3 the seat width is seen to be satisfactory for the 95th percentile of the drivers as compared with the hip breadth as an anthropometric dimension. Since it is suitable for the 5th percentile of the drivers, it is therefore recommended that the average seat width for the bus should be maintained as existing 49.8cm.

Seat length: Over 50% of the studied drivers might find the average seat length in the existing design as measured (55.6cm) uncomfortable. So it is suggested that the average seat length in the existing design should be reduced to about 17.8% of the present dimension i.e., 45.7cm, so as to comfortably accommodate at least 5th percentile range, i.e., 95% of the drivers.

Seat adjustments: Upper, middle and lower; back pains, knee joints pain, elbows pains, chest pain, neck pain amongst others were identified as major musculoskeletal disorders experienced by drivers [4]. Consequently, these forms of disorders can be reduced to the barest minimal if all the necessary adjustments ranges and devices are in place and functional. These adjustments include; seat fore/aft adjustment, seat height adjustment and seat back angle adjustment (tilting).

Seat heights: Although through interview, none of the drivers said the seat height were too high but many agreed that the seat height was too low, therefore, it is suggested that the average seat height should remain as 45.1 and seat adjustment be included to accommodate users in the extreme percentiles. Therefore, the seat height adjustments should be 7.2cm for total upward and downward adjustment. This will enable drivers in the 5th percentile to adjust the seat to their comfort.

Table 4: Anthropometric Data of Ogbomoso Bus Operators (n = 161)

Anthropometric Variables	Mean	Std. Dev	Range	Percentile		
				5th	50th	95th
Shoulder Height Sitting	57.54	2.55	9.7	53.9	57.3	61.5
Shoulder-Elbow Length	37.26	2.26	7.7	34.0	37.0	40.8
Shoulder Breadth	45.42	3.25	10.6	40.4	45.1	50.1
Sitting height normal	79.32	4.31	16.8	72.7	79.3	85.0
Sitting height erect	83.36	6.65	27.4	75.0	83.2	93.6
Buttock-Knee Length	58.89	2.88	13.6	55.0	59.0	63.1
Buttock-Popliteal Length	48.97	2.57	10.5	45.7	48.6	53.2
Thigh Clearance Height	14.06	1.38	4.49	12.1	13.9	16.1
Popliteal Height Sitting	49.39	2.02	6.79	46.3	49.3	52.3

URL: *http://journals.covenantuniversity.edu.ng/index.php/cjet*

Thumb-Tip Reach Sitting	81.44	3.53	12.7	76.7	80.9	87.2
Anterior-Arm Reach	89.19	3.99	15.3	83.7	89.2	95.4
Stature	176.12	6.17	21.8	167.6	175.6	185.9
Hip Breadth	37.95	3.62	15.7	32.8	37.9	42.7
Maximum Body Breadth	46.1	3.2	11.2	41.0	46.2	50.8
Weight	74.05	6.70	31.5	61.7	73.6	85.1

All dimensions were measured in centimetres (cm) except weight which is in kilogram (kg)

Table 5: In- Vehicle Design Data

Design Parameters	Mean Dimension	
	Toyota Hiace	Mazda
Seat height	45.1	45.4
Seat width	49.8	50.2
Seat length	55.6	55.6
Back-rest length	53.3	53.5
Back-rest width	47.7	48.1
Dashboard-backrest length	75.1	75.3
Steering-wheel external diameter	44.7	44.7
Steering-wheel thickness Minimum	38.1	38.1
Steering-wheel thickness Maximum	44.7	44.7
Thigh clearance (steering wheel-seat height)	22.6	22.7
Driver's door height	135.7	135.9
Driver's door width	99.5	99.6
Ground-to-driver's door height	70.4	70.3
Elbow clearance	N/A	N/A
Seat-pedal length	34.4	34.4
Rounded front edge width	8.7	8.7
Headrest length	23.8	23.7
Headrest width	12.7	12.6
Headrest breadth	27.8	27.9
Armrest surface length	N/A	N/A
Armrest surface breadth	N/A	N/A
Seat Adjustment Minimum	87.7	88.3
Seat Adjustment Maximum	101.6	101.6

All variables were measured in centimetres (cm)

Seat fore/aft adjustment: Buses with fixed adjustments give drivers problems as the level of inconvenience and discomfort increases. During the study, it was noted by critical look at the seats that, most of the seats had fore/aft seat adjusters, but just few were functional. In fact most seats were found permanently welded to the

URL: *http://journals.covenantuniversity.edu.ng/index.php/cjet*

driver's workstation thereby not giving room for maneuvering to suit driver's postural comfort. It was also gathered at one of the motor park units visited that over 70% of the buses used by the motorists were brought into the country right handed, possibly due to less cost of procurement. To comply with the use of road act of Nigerian government these buses were converted into a left handed drive. But with this they could only to convert the steering column and dash boards alone and not the seats. Hence they manipulate workstation thereby making the seat not adjustable for the driver but the passenger who sits at the front. It is of paramount importance to note that with these findings, discrepancies in the design variables and that of the anthropometric dimensions of the drivers becomes intensified. Hence it becomes more pronounced that the buses were not pre-designed for Nigerians i.e., anthropometric data of Nigerians were not incorporated into the existing bus design. In general, the seat adjustments of the buses across the studied motor park units were not adequate even those that seem to be functional could not be adjusted in their full length of 13.5cm. Therefore, as it is suggested by [27], that a driver's seat should have a seat adjuster to be maintained at an average of 18.4cm for total fore/aft adjustment for Molue buses, also 13.5cm for Toyota Hiace and Mazda buses.

Backrest adjustments: Observations from the buses measured showed that a very limited number among the buses had adjustable backrest, though by looking closely at the seats, it was revealed that most of the seats had damaged backrest adjusters. It is therefore suggested that the driver's seat backrest should adjust backward (Tilt) to 35 degrees from the vertical to accommodate user to who may lean against the backrest as suggested by [25].

Other design considerations include the inclusion of armrests that is adjustable in height and width, to accommodate various body dimensions on the seats as desired by the drivers, to reduce some musculoskeletal problems, relating to hand and back pains. In addition, introduction of removable seat cushions will go a long way in reducing soiling, odour retention and wear; the seats are subjected to, due to the fact that diverse drivers use the same workstation. Also to increase driver's satisfaction and comfort in his workstation, seats should be designed to have a perfect seat depth and well comfortable seat to fit the user.

Backrest width: To ensure that the backrest width covers the shoulder breadth, the average backrest width should be increased by 5.87% of the present dimension, thereby making it 50.5cm so as to accommodate 95% of the drivers.

Backrest length: For the backrest length at least to be at the shoulder height for comfort of 95% of the drivers, the average backrest length should be increased to about 5.87% of the present dimension (47.7cm) to make it 50.5cm. Seats with air actuated lumbar and back side bolster support backrest will be desirable by

the bus drivers and as suggested by [28] for bus operators, to reduce some musculoskeletal disorders, relating to back pains. Also adjustable headrest (up/down and forward/backward adjustments) will be necessary as suggested [28] and desired by the surveyed drivers. Although there are headrests in the existing design yet most were found to be designed alongside (merged) with the backrest and not separately. Incorporation of this in the future design would help in curtailing some musculoskeletal problems, relating to neck and back pains while it enhances the comfort of the drivers.

Dashboard-backrest length: Driving task is an activity that requires maximum concentration by the driver as various judgments need to be made at every point in time. However, while he does these, there is need for the driver to interact with various in-vehicle components. For ease of reach for various controls on the dashboard, control lever/knobs and side/rear mirrors, it is necessary the design for control reach is within the maximum arm reach so as not to pose discomfort on the driver. On this note, it is suggested that the dashboard-backrest length is increased by 11.45% of the present dimension to become 83.7cm. This will allow the workstation to accommodate 95% of the drivers. The proposed design specification for bus is shown in Table 4.

Anthropometric Comparison of Ogbomoso Bus Drivers with Lagos Molue Bus and Ibadan Taxicab Drivers

The comparison of major anthropometric dimensions of Ogbomoso bus operators with those of Lagos Molue bus drivers and Ibadan taxicab drivers of the same region, south western urban centres of Nigeria, reveals that there are variations in most of the dimensions for; Shoulder Breadth, hip breadth, Thumb-Tip Reach Sitting/Anterior Arm Reach and Stature which stands at (166.8, 173.3, 179.7) for Lagos drivers, (161.3, 172.0, 182.76) for Ibadan drivers and (167.6, 175.6, 185.9) for Ogbomoso drivers for 5th, 50th and 95th percentiles respectively, Table 5. It may be due to nutrition and body build. This shows the distinct nature of the anthropometry of the urban centres and the dynamism. Although the anthropometric data of Ibadan were not obtained from bus operators but it is stipulated that driving is a free for all kind of work in Ibadan, it is possible that majority of these drivers also at one-time drive buses. Therefore, buses to be designed for the Ogbomoso bus drivers at south western Nigeria, need to be modified with suitable adjustment in body dimensions affected.

The mean values of some major anthropometric data (body dimensions) of Ogbomoso in south western Nigeria were also compared with mean values of passengers in buses as indicated in Table 6. Analysis of variance (ANOVA) performed on the mean values revealed at 95% confidence level that there was no significant difference ($p > 0.01$). The comparison reveals that the Ogbomoso bus operators are variably smaller than the passengers

in bus of Ogun south western Nigeria in all structural body dimensions where data were available except in stature where they have 176.12 as against 174.8. The variation may be attributed to the discrepancies in physiological factors and body build up. The lower body dimensions may lead to uncomfortable postures adopted while driving buses posing fatigue on drivers and possibly inefficiency.

Table 7 presents the comparison of sitting height to stature ratio of Ogbomoso (south west) bus operator in Nigeria with different ethnic groups across Nigeria. Result from this comparison shows almost similar ratio of sitting height to stature among different ethnic groups which is in line with survey carried out on anthropometric data of Indian workers [29]. Consequently, this comparison is in accordance with [30-34] who also stipulated that there is a high probability that whatever the mean stature of a sample, any given body dimension of length will be very nearly a constant proportion of the stature. Therefore, if the stature is known, any dimension that is not available in the sample can be obtained by proportion [35].

Table 6: Driver's workstation design variables fitted with related anthropometric variables

Design Variables	Mean Dimension	Anthropometric Variable	Mean	SD	5th	50th	95th
Seat height	45.1	Popliteal height sitting	49.39	2.02	46.3	49.3	52.3
Seat width	49.8	Hip breadth sitting	37.95	3.62	32.8	37.9	42.7
Seat length	55.6	Buttock-popliteal length	48.97	2.57	45.7	48.6	53.2
Back-rest length	53.3	Shoulder height, sitting	57.54	2.55	53.9	57.3	61.5
Back-rest width	47.7	Shoulder breadth	45.42	3.25	40.4	45.1	50.1
Dashboard-backrest length	75.1	a. Anterior arm reach sitting	89.19	3.99	83.7	89.2	95.4
			81.44	3.53	76.7	80.9	87.2
		b. Thumb –tip reach sitting c. Buttock-Knee length	58.89	2.88	55.0	59.0	63.1
Steering-wheel external diameter	44.7	Anterior arm reach sitting	89.19	3.99	83.7	89.2	95.4
Steering-wheel thickness	6.6	Na	na	na	na	na	na
Thigh clearance (steering wheel-seat height)	22.6	Thigh height sitting	14.06	1.38	12.1	13.9	16.1

Driver's door height	135.7	Stature	176.12	6.17	167.6	175.6	185.9
Driver's door width	99.5	Max. body breadth	46.1	3.2	41.0	46.2	50.8
Ground-to-driver's door height	70.4	Stature	176.12	6.17	167.6	175.6	185.9
Elbow clearance	Na	Na	na	na	na	na	na
Seat-pedal length	34.4	Popliteal height sitting	49.39	2.02	46.3	49.3	52.3
Rounded front edge seat width	8.7	Popliteal height sitting	49.39	2.02	46.3	49.3	52.3
Headrest length	23.8	Sitting height Normal	79.32	4.31	72.7	79.3	85.0
		Sitting height Erect	83.36	6.65	75.0	83.2	93.6
Headrest width	12.7	Sitting height Normal	79.32	4.31	72.7	79.3	85.0
		Sitting height Erect	83.36	6.65	75.0	83.2	93.6
Headrest breadth	27.8	Sitting height Normal	79.32	4.31	72.7	79.3	85.0
		Sitting height Erect	83.36	6.65	75.0	83.2	93.6
Armrest surface length	Na	Na	na	na	na	na	na
Armrest surface breadth	Na	Na	na	na	na	na	na
Seat Adjustment	13.1	Buttock-Knee length	58.89	2.88	55.0	59.0	63.1

All variables were measured in centimetres (cm), SD denotes Standard Deviation

Table 7: Proposed In-vehicle design specifications

	Design variable	Proposed design variable (cm)
A.	Seat height	45.1
B.	Seat width	49.8
C.	Seat length	45.7*
D.	Back-rest length	50.5*
E.	Back-rest width	50.5*
F.	Dashboard-backrest length	83.7*
G.	Steering-wheel external radius	44.7
H.	Steering-wheel thickness	6.6 (with padding)
I.	Thigh clearance (steering wheel-seat height)	22.6

J.	Driver's door height	140*
K.	Driver's door width	99.5
L.	Ground-to-driver's door height	34.8*
M.	Elbow clearance	Suggested
N.	Seat-pedal length	34.4
O.	Seat fore/aft adjustment (Forward and Backward)	13.5
P.	Seat adjustment (Upward and Downward)	7.2*

* Not Present

Table 8: Comparison of Mean Sitting Height to Mean Stature Ratio with other studies on anthropometry

Study	Mean Ratio	Source
Ogbomoso (South Western Nigeria)	0.4733	Present study (2015)
Ibadan (South Western Nigeria)	0.4839	Onawumi 2008
Igbo (South Eastern Nigeria)	0.5122	Onuoha 2012
Doko (North Central Nigeria)	0.4661	Jonathan and Shehu 2012
Kutigi (North Central Nigeria)	0.4926	Jonathan and Shehu 2012

All variables were measured in centimetres (cm)

4. Conclusions and Recommendation

Stakeholders in the automotive industry has yet relent in search for a system that meet up with the recent challenges of user's population requirements, established technical standards, and other basic specifications for research uses. The basis for achieving these has been found to be through a comprehensive Participatory Ergonomic Intervention (PEI) approach.

However, in ensuring an ergonomically suitable products and physical equipment, anthropometry becomes an inevitable tool to define the population of the potential users. Mainly because the human body occupies a central position in the design of man machine interface and the system at large. Also, this study has opened up the need to conduct a national anthropometry survey for user population in Nigeria. Such data can be used to configure the vehicle, driver's workstation layout and in-vehicle interface for the purpose of enhancing functional effectiveness, human comfort and ergonomic suitability. Consequently, integrating the limitations of the potential users in

relation to such's demographics and other physical characteristics enhances the driver's comfort. Although as a matter of research and development a number of studies have been carried out on driver fatigue and low back disorders however the needs

for overall assessment of driver's workplace, the extent to which the existing bus design is found to be ergonomically suitable and its user friendliness are inevitable, hence the conception of this work.

References

[1] Deborah A. N. (2010), 'Low Back Pain among Professional Bus Drivers: Ergonomic and Occupational-Psychosocial Risk Factors', Department of Physical Therapy, Tel Aviv University, Ramat Aviv. Israel.

[2] Adel M, Mohammadreza F. and Hedayat T., (2012) 'Ergonomic Evaluation of Interior Design of Shoka Vehicle and Proposing Recommendations for Improvement' Iranian Rehabilitation Journal, Vol. 10, February

[3] Caragliu B., (2006) 'Fitness for Drivers'. G. Ital Med Lav Ergonomics 28 (1), 82-84.

[4] Lucas E. B. and Onawumi, A. S. (2013) 'Ergonomic Evaluation of In-Vehicle Interface Design of Taxicabs in Nigeria' International Journal of Engineering Research and Applications (IJERA) ISSN: 2248-9622 www.ijera.com Vol. 3, Issue 4, Jul-Aug, pp.566-572

[5] Baba M. D., Nor-Hassanil H. H., Dian D. I. D. and Shamsul B. M. T. (2015) 'Incorporating Malaysian's Population Anthropometry Data in the Design of an Ergonomic Driver's Seat' Procedia - Social and

Behavioral Sciences 195 (2015) 2753 – 2760

[6] Safitri D. M., Azmi N., Singh G. and Astuti P. (2016) 'Redesign of Transjakarta Bus Driver's Cabin' IOP Conf. Series: Materials Science and Engineering 114 (2016) 012086 doi:10.1088/1757-899X/114/1/012086

[7] Mozafari, A., Vahedian, M., Mohebi, S., & Najafi, M. (2015) 'Work-Related Musculoskeletal Disorders in Truck Drivers and Official Workers'. Acta Medica Iranica, 53(7), 432-438.

[8] Das B., Shikdar A. A. and Winters T., "Workstation Redesign for a Repetitive Drill Press Operation: A Combined Work Design and Ergonomics Approach," Human Factors and Ergonomics in Manufacturing, vol. 17 no. 4, pp. 395-410. 2007.

[9] Seva R. R., Axalan J. D. M. and Landicho A. R. P. (2011) 'Workplace Efficiency Improvement for Jeepney Drivers in Metro Manila' HFESA 47th Annual Conference. Ergonomics Australia - Special Edition

[10] Maria E. B. and Bianca C. (2015) 'A Proposed Approach for an Efficient Ergonomics Intervention in Organizations',

2nd Global Conference on Business, Economics, Management and Tourism, Procedia Economics and Finance, pp. 54 – 62.

[11] Fadhli M. Z. K., Humairah N. H. R., Khairul N. M. I., Kaswandi M. A and Junaidah Z. (2016) 'Ergonomic Risk Factors and Prevalence of Low Back Pain among Bus Drivers'. Austin J Musculoskelet Disord. 3(1): 1028.

[12] Okuribido, O. O., Shimble, S. J., Magnusson, M. and Pope, M., (2007), 'City Bus driving and Low Back Pain: A Study of the Exposures to Posture Demands Manual Materials Handling and Whole Body Vibration'. Applied Ergonomics, 38: 29-38.

[13] Onawumi A. S., (2008). 'Ergonomic Assessment And Anthropometric Characterization of Taxi Operators Urban Centres of Oyo State, Nigeria', Pg 4 Unpublished Phd Thesis, Ladoke Akintola University of Technology, Ogbomoso, Nigeria.

[14] Agrawal, K. N., Singh, R. K. P. and Satapathy, K. K. (2010). 'Anthropometric considerations of Farm Tools/Machinery Design for Tribal Workers of Northern INDIAN. Agric Eng Int: CIGR Journal,12(1):143-150.

[15] Onawumi, A. S., Adebiyi K. A., Fajobi, M. O. and Oke E. O. (2016) 'Development of Models For Predicting Some Anthropometric Dimensions of Nigerian Occupational Bus Operators' European International Journal of Science

and Technology Vol. 5 No. 5 12 -27 www.eijst.org.uk

[16] Kyung G. (2008) 'Integrated a Human Factors Approach To Design And evaluation of The Driver Workspace And Interface: Driver Perceptions, Behaviors, And Objective Measures', Blacksburg, pp 9, 14-20, 224, 34, 63, 88, 113, 126, 188.

[17] Julitta S. B, Monique H. W., Henk F. M, (2015) "Use of Ergonomic Measures Related to Musculoskeletal Complaints among Construction Workers: A 2-year Follow-up Study", Safety and Health at Work, pp. 90-96.

[18] Asafa T. B., Ajayeoba A. O. and Adekoya L. O., (2010) 'Prediction of some anthropometric data of Bus Passengers using Artificial Neural Network: A case study of Molue bus in Lagos State, Nigeria'. International Journal of Biological and Physical Sciences 15(3): 345-356.

[19] Maheshkumar M. D., Narendra-Babu B. R., Ganesh K. and Chandrashekara K. (2015) 'Ergonomics Study to Improve Workstation Productivity in Manufacturing Sector' International Journal of Scientific Progress and Research (IJSPR) ISSN: 2349-4689 volume-10,pp.31- 36.

[20] Deepak K. K. and Prasad V. K. (2015) "Ergonomic assessment and workstation design of shipping crane cabin in steel industry", International Journal of Industrial Ergonomics, pp. 1-11.

[21] Ebe, K. and Criffin M. J., (2001). 'Factors affecting static seat cushion comfort'. Ergonomics. 44(10): 901-921.

[22] Safitri, D. M., Malinda, A., Azmi, N. & Astuti, P., (2015), 'Warning Display Design For The Transjakarta Bus Cockpit To Minimize The Driver's Error Behavoiur', Proceeding of International Seminar on Industrial Engineering.

[23] Zhang, L., Helander, M. G. and Drury, C.G., (1996) 'Identifying Factors of Comfort and Discomfort in Sitting'. Hum. Factors 38 (3), 377–389.

[24] Azmi N., Safitri, D. M., Puspitasari, L. A. and Astuti, P. (2014), 'Working Conditions Measurement of Transjakarta's Drivers at Corridor 2 and 3 Using Physiological and Biomechanical Approach', Proceeding of APCHII-Ergofuture 2014.

[25] Harry S., (2000) 'Durable Ergonomic Seating for Urban Bus Operators'

[26] Triano I. J. (2008), Reducing back Pain while sitting in Office Chair Available in http://www.spine.health.com

[27] Ajayeoba A.O, (2005). 'Ergonomic Assessment of Molue Transit Buses'. Unpublished Masters Thesis. Obafemi Awolowo University, Ile-Ife, Nigeria.

[28] Gilmore, B. J., Bucciaglia, J., Lowe, B. You, H., and Freivalds, A., (1997) 'Bus Operator Workstation Evaluation and Design Guidelines', TCRP Report F-4, Transportation Cooperative Research Program (TCRP), Transportation Research Board US, (www.tradeshall.org.znz/stagecoach/cabergon.html)

[29] Yadav, Rajvir, Tewari, V. K. and Prasad, N. (2000) 'Anthropometric Data of Indian Farm Workers – A Module Analysis'. Applied Ergonomics, 28(1): 69-71.

[30] Murrel, K. H. F. (1975) 'Ergonomics, Man and His Working Environment', Chapman and Hall, London.

[31] Onuoha S. N., Idike F. I. and Oduma O., (2012) 'Anthropometry of South Eastern Nigeria Agricultural Workers' International Journal of Engineering and

[32] Dunmade, I., Udo, M., Akintayo, T., Oyedepo, S., & Okokpujie, I. P. (2018, September). Lifecycle impact assessment of an engineering project management process–a SLCA approach. In IOP Conference Series: Materials Science and Engineering (Vol. 413, No. 1, p. 012061). IOP Publishing.

[33] Onawumi, A., Udo, M., Awoyemi, E., & Okokpujie, I. P. (2018, September). Alternate Maintainability Evaluation Technique for Steering System of Used Automobiles. In IOP Conference Series: Materials Science and Engineering (Vol. 413, No. 1, p. 012062). IOP Publishing.

[34] Azeta, J., Okokpujie, I. P., Okokpujie, K. O., & Salawu, E. Y. (2018). ANALYTICAL

STUDY OF A ROAD TRAFFIC CONFLICT AT THE T-JUNCTION OF UNIVERSITY OF BENIN MAIN GATE. International Journal of Civil Engineering and Technology (IJCIET), 9(8), 1048-1061.

[35] Omoruyi, O. N., Omoruyi, M. G., Okokpujie, K. O., & Okokpujie, I. P. (2018). Electronic Fare Collection Systems in Public Transits: Issues, Challenges and Way-Forward. Covenant Journal of Engineering Technology, 2(1)

An Open Access Journal Available Online

A Review of Voice-Base Person Identification: State-of-the-Art

Folorunso C. O.[*1], Asaolu O. S.[2] & Popoola O. P.[3]

[1, 2, 3]Department of Systems Engineering, University of Lagos, Akoka, Lagos.
[*1]comfortfolorunso@gmail.com, [2]oasaolu@unilag.edu.ng,
[3]toyin_net@yahoo.com

Abstract - Automated person identification and authentication systems are useful for national security, integrity of electoral processes, prevention of cybercrimes and many access control applications. This is a critical component of information and communication technology which is central to national development. The use of biometrics systems in identification is fast replacing traditional methods such as use of names, personal identification numbers codes, password, etc., since nature bestow individuals with distinct personal imprints and signatures. Different measures have been put in place for person identification, ranging from face, to fingerprint and so on. This paper highlights the key approaches and schemes developed in the last five decades for voice-based person identification systems. Voice-base recognition system has gained interest due to its non-intrusive technique of data acquisition and its increasing method of continually studying and adapting to the person's changes. Information on the benefits and challenges of various biometric systems are also presented in this paper. The present and prominent voice-based recognition methods are discussed. It was observed that these systems application areas have covered intelligent monitoring, surveillance, population management, election forensics, immigration and border control.

Keywords: Person-identification, biometrics, information and communication technology, authentication, voice-base person identification.

1. Introduction
Person identification is the process of recognizing an individual based on specific characteristics. Identification by name is the most common method of distinguishing between persons. Conventional person identification technologies are developed based on "something we know" (password and personal identification number (PIN)),

"something we have" (Token, an Identity Card, an Access Control Card or a Radio Frequency Identity (RFID) card), unlike something we are (i.e. bodily features like fingerprint, finger-vein, voice, gait). These identification schemes have their limitations. For instance, a password or a PIN can easily be forgotten or even guessed by an impersonator while a token or an identity card can be lost, stolen or even cloned. As such, the conventional forms of identification may not really distinguish between an authorized user and an impersonator [1].

The need to verify the identity of an individual before such individual can have access to some restricted places is very important as so many means of breaking into one's privacy is being developed every day by hackers. The use of the state-of-the-art person identification technology which uses biometrics technology cannot be over-emphasized, due to so many advantages this type of recognition system proffers. Biometrics is the science and technology of measuring, analysing and comparing some human physiological and sociological related data [2]. Many biometrics-based identification systems have been employed both for domestic and commercial applications. The use of biometrics has shown increasing significance in our daily life and as such, many books, journals and conference proceedings have enumerated advances in theory and application of this technology. In all, the use of biometrics has emerged as the best way of identifying an individual since no two persons share entirely the same biometric traits [3].

With numerous developments in technology, the security sector has encountered some significant advancement. We can safely say that technology has transformed security. The challenge was how to make computers identify or recognise an individual. Biometric being based on measuring physical characteristics uses features which are common and readily available to all class of people. These features are distinct, easily collected and tested, and have high variability to carter for repetition of data class. Some of the biometric features currently used include: Facial thermogram, hand vein, gait, keystroke, odour, ear, hand geometry, fingerprint, face, retina, iris, palm-print, voice, signature and DNA.

In voice-based recognition system, the features of an individual's voice are based on the physical characteristics of their vocal tract, nasal cavities and the articulators (which include mouth, lips, teeth and so on) which are used in generating sound. These features are unchanging for an individual though the behavioural features may change over time due to age, location, medical conditions and/or emotional state [4]. Voice-based recognition methods are classified into two ways: Automatic Speaker Verification (ASV) and Automatic Speaker Identification (ASI) system [4]. The limitations of the conventional person identification system have always been challenging, hence the need to research into the state-of-the-art biometric technologies novel

biometric features that can be proposed.

2. Review of related works

So much research has been done on person identification using biometrics technology. Biometrics traits or characteristics are divided into two major categories. The first category is physiological characteristics, which are based on how one is, using data (features) that are derived from direct measurements of parts of the human body (fingerprints, face, finger geometry, iris scans, retina scans, hand geometry, finger-vein among others) as shown in Figure 1. The second category, which is the behavioural characteristics are based on what one does (a person's action), it uses data that are derived from indirect measurement of a person's action (voice recognition, keystroke scans, signature, gait and so on as shown in Figure 2 [1], [5].
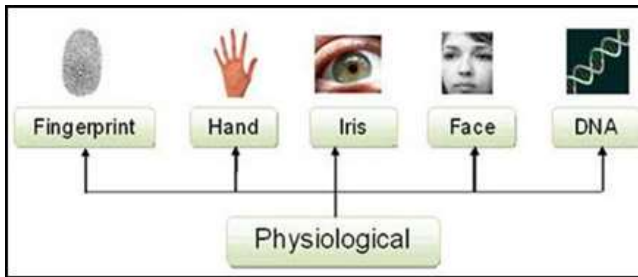
Figure 1: Selected physiological biometrics in use [3]
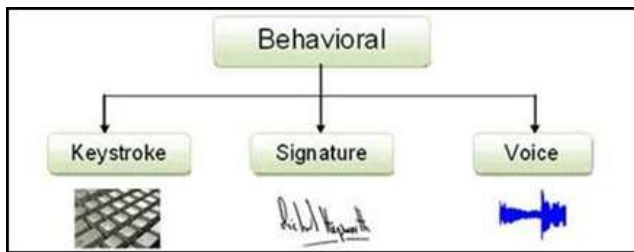
Figure 2: Selected behavioural biometrics in use [3]

A biometric authentication system can be further classified either as identification or a verification system. Identification system is a one-to-many system where biometrics is used to determine a person's identity from a number of some people's data stored in a database. For example, the police may try to identify an individual's fingerprint or face from a Forensic database. Verification on the other hand, is a one-to-one system of identification where biometrics is used to confirm a person's identity for access control [6], [7].

Kaur and Kaur [8], presented a brief survey of different voice biometric for speaker verification in an attendance

system. They proposed the use of voice, having considered different methods that have been employed for automatic attendance for students and as such the use of voice for this purpose is a very important and highly welcome phenomenon. They used Gammatone filter bank instead of Mel filter bank, after which the discrete cosine transform was applied to separate overlaying signals. The use of Gammatone frequency cepstral coefficient (GFCC) with the Gaussian Mixture Model as well as Artificial Neural Networks was incorporated for training and matching task respectively.

Tran et al [9] introduces normalization technique which depends on fuzzy set theory to improve the performance of voice-based verification system. In order to authenticate a claimed personality, a likeliness value was evaluated with a threshold in order to allow or reject the person. The use of noise clustering as well as the c-means clustering membership function was introduced to eradicate the problem of ratio-type scores which affects the false acceptance rate. Result however, showed great reduction in the false acceptance and false rejection rate.

Delac and Grgic [4], and Dugelay et al [10] presented a concise summary of different biometric methods which include single as well as multiple biometric systems. Voice-based biometric system uses some of the features of human-speech that are not changing for a particular individual. Though the behavioural features of the same human speech varies over time due to age medical, emotional as

well as environmental conditions. The voice-based biometric system is classified into automatic speaker verification (ASV) and automatic speaker identifications (ASI). The former uses voice as validation characteristic in a one to one verification scenario. While the latter uses voice to recognise who a person truly is. A particular voice feature of an individual is matched against a stored pattern in a database. A typical voice feature can be formants or any other sound characteristics which are unique to each individual's vocal tract.

Belin et al [11] working from a neuro-cognitive point of view looked at neural association of voice perception. Having considered the ability to evaluate a person's gender and age bracket from listening to their voices was a very strong motivation behind this work. They tried to look at the voice as an auditory face in comparison with the face recognition system. They then proposed the use of Bruce and Young's model of face perception as a structure for understanding the perceptual as well as the cognitive processed contained in voice perception. This purpose model predicts functional detachment similar to those perceived for faces. In future, the use of face archetype to test the prediction of the proposed model was suggested. Similarly, more research is needed in order to ascertain some of the following; -

- Are voices more noticeable than any other sound around irrespective of the fact that such sound contains speech or not.

- To what degree does the voice perception system permit us to excerpt identity and emotional information from the expression of other species such as cats, dog and so on.
- What is the perceptual emergent of voices?

Aronowitz [12] considering the rapid development of smart phones and mobile internet banking, there is no doubt the imperative need of a very strong authentication system. While the current use of password or pattern to unlock phones is not sufficient for the smart phones having considered the high threat of the device getting to the custody of an un-authorized user. Current developments in voice-based biometric system present a huge potential for a robust authentication of a mobile smart phone using voice. This aspect is very crucial for the financial and banking industry, where financial organizations are considering a flexible mobile customer services and easy authentication and at the same time maintaining security and most importantly, reducing fraudulent usage.

They presented the use of the current technology text-independent as well as text-dependent speaker authentication skills for user verification speaker specific digit strings, global digit strings, prompted digit strings as well as text independent were evaluated adapting the Joint Factor Analysis (JFA), Gaussian mixture models with nuisance attribute projection (GMM-NAP) and Hidden Markov Model (HMM) with NAP to improve

security as well as reliability of the system.

Korshunov and Marcel [13] considered the fact that most biometric technology systems are vulnerable to spoofing which reduces their wide use sometimes hence they presented the need to develop anti-spoofing detection methods also referred to as presentation attack detection (PAD) systems. They presented an integration of PAD and Automatic Speaker Verification (ASV) systems using i-vector and local binary pattern histograms based ASV-PAD hybrid system. The AVspoof database which contains practical presentation attack was used to validate this method and result obtained show a significantly enhanced resistance of this hybrid system to attacks at the detriment of trivial degraded implementation for scenarios without spoofing attacks.

The use of cascading scheme for score synthesis and evaluating it with the joint ASV-PAD system was suggested for future research. In addition, the state of the art spoofing database can be employed to explore multi-model system considering ASV and PAD systems of different modalities for instance speech and image may be combined to enhance the performance in both 'licit' and 'spoof' scenarios.

Krawczyk and Jain [14] considering the large evolution from paper-based medical records towards electronic medical records, guaranteeing the security of such private and highly sensitive data cannot be over-emphasized since the health care giver only need to edit and update patient's record on the tablet, personal

computers (PC) or even smart phones, hence the need to protect the patient's privacy as required by all governmental regulations. A safe authentication system must be put in place anytime such records are to be accessed, hence the need for biometric-based access cannot be disputed. Research showed that on-line signature integrated with voice modalities is the most appropriate means for the users in such verification system since tablet PC is built with the associated devices. Evaluation of hybrid system of online signature and voice-based biometrics was carried out in this work. Dynamic programming method of string matching was incorporated for the signature verification while off-the-shelf commercial software development kit was used for voice verification. Fusion of these two methods were carried out at the matching score level after normalization of the data. The prototype of these hybrid systems was tested using a small truly multi-modal database of fifty users and an EER of 0.86% was reported.

Mazaira-Fernandez et al [15] came from the view of looking at the environment which has been so much improved by technology of social media whereby some other people uses these social media as a form of terrorism to transmit their message. In such a situation a typical biometrics recognition method such as face or fingerprints have been substituted by another biometric traits such as voice as this may be readily available in such scenario. They proposed a gender-dependent extended biometry

factors (GDEB). The GDEB factors classify features extracted from voice source and tract factors and other pertinent features such as format data, having in mind that male and female voices show both acoustic-phonetic variations as well as physiological differences. The main idea was to improve classification rate in speaker recognition using few parameters.

Scheffer et al [16] worked on two of the challenges facing voice biometrics technology. These challenges include non-ideal recording conditions (these are often operational situation problems such as noise, echoes, voice channels and so on) and audio compression. Adapting the SRI International's innovations which arise from the Intelligence Advances Research Project Activity (IARPA) Biometric Exploration Science and Technology (BEST) and the Defence Advances Research Projects Agency (DARPA) Robust Automatic Transcription of speech (RATS) projects. The SRI's approach uses various features excerpted from speech which are demonstrated using latest machine learning algorithm. They recommended a general audio classification system that excerpts metadata facts using i-vector. The logistic regression and the cross entropy was used to combine the various features that are automatically extracted from the audio signal at the i-vector level.

Bhogal et al [17] research showed that voice is a more natural means of communication and verbal communication is quicker and more efficient than textual communication. Considering a virtual environment,

URL: *http://journals.covenantuniversity.edu.ng/index.php/cjet*

they evaluated the use of virtual universe (VU) residents also known as Avatars in online service employing audio biometrics. The method for example can include, spurring consumer applications with a demand for an utterance, managing the response to the demand and developing a voiceprint or voice summary of the speaker or participant. This voiceprint can be connected to an avatar and when an utterance is obtained, the avatar can be recognized by evaluating the utterance with the voiceprint. Such evaluation can be used to recognise avatars as they go from one online service to another and as such, voice biometrics can be used to verify an avatar for a particular activity. The main idea of their research was that they used voiceprint to approve an operation limited to an authorized user. In other word, they demonstrated the possibility of using biometric in internet based activities.

Zhang et al [18] came from the view of the inability of a system to recognize an individual from a non-frontal view. They presented the people in photo Albums (PIPA) corpus with very high differences in pose, clothing, image resolution, illumination and camera viewpoint. They proposed the pose-invariant Person Recognition (PIPER) algorithm to tackle the problem identified earlier. PIPER combines the signals of pose-let level individual identifiers trained by Deep Convolution Neural Network (DCNN) to reduce the differences in pose and then combine with a global recognizer and face recognizer. Result obtained showed that this algorithm

out-perform one of the best face recognizer (Deep face)

Khitrov [19] at the speech technology centre reviewed the use of voice-based biometrics for data access and security. He identified some challenges and advantages of the system.

However, voice can be used with any other biometric technology system in order to achieve 100% accurate recognition and verification. Voice-based person identification system can be used in the following areas to safeguard security and expedient user verification. These areas include:-

1. Call centres and interactive voice response systems (IVRs) such as to get account balance, medical result etc. which are private and highly sensitive information in order to save time while delivering these services to the rightful owners once the system can recognize their voices.

2. Mobile voiced based verification system helps in securing our sensitive and private information stored on the smart devices.

3. For cloud computing and Bring Your Own devices (BYOD) applications, employees prefer the use of their personal smart devices to access organization resources. There is a dire need to secure the organizational information of these smart devices. Hence the use of voice signature presents a natural, appropriate and legally binding option to hand-written signatures.

4. Voice-based authentication system can be employed to secure and enhance security of our social

networking platforms such as Facebooks, LinkedIn and so on.

Vatsa et al [20] having researched into various biometric technology, they identified some serious problems affecting this technology and they categorise them into accuracy, computational speed, security, cost, real-time attacks and scalability. They also identified the various possible attacks on biometric technology and these include impersonation, coercive, replay attack, as well as the attack on feature extractor, template database, matcher and matching results to mention a few. In improving the performance of biometric technology they identified two major ways one can protect the biometric information from such attack. These include encryption as well as watermarking. They introduced a three level Redundant Discrete Wavelet Transform (RDWT) biometric watermarking algorithm to implant the voice biometric MFCC in a colour face image of the same person for enhanced robustness, security and accuracy. In biometric watermarking, a particular quantity of information also known as watermark is implanted into the initial cover image using a private key such that the constituents of the cover image are not altered. The result obtained was over 90% verification accuracy.

2.1 Biometric system architecture

Biometrics system for identification encompasses different stages as shown in Figure 3.

In recognition mode, the system executes a one-to-many comparison against a biometric database in an attempt to establish the identity of an unknown individual. The system will be successful in identifying the individual if the comparison of a biometric sample to a template in the database falls within a previously set threshold. This mode can be used for positive recognition (so that the user does not have to provide any information about the template to be used) or for negative recognition of the person "where the system establishes whether the person is who he or she (implicitly or explicitly) denies to be". The latter function can only be achieved through biometrics since other methods of personal recognition such as passwords, PINs or cards are ineffective [6].

When an individual uses a biometric system for the first time, it is referred to as enrolment. During this process, biometric data from the individual is captured and saved. In subsequent uses, biometric data is sensed and matched up to data saved at the time of enrolment. The storing and recovery of such systems must be critically protected if the biometric system is to be robust. In Figure 3, the data acquisition phase is made up of some sensors, which act as link between the real world and the system; it has to obtain the entire required data e.g. image or fingerprint. All necessary pre-processing of the raw audio signal in order to remove sensor noise and unwanted sections are carried out in this phase using some kind of standardization. The second stage is the feature extraction phase, where highly descriptive and discriminative features are extracted and represented. This stage is a very important stage of

a biometric system architecture. At the third stage, a vector of numbers or an image with specific characteristic is used to build a template. A template is a representation of most descriptive features. It is often created and then stored in a database for future use. During the enrolment phase, the template is either stored on a card, within a database or both. At the matching stage, the obtained input features are passed to a matcher that evaluates it with other current templates and estimate the distance between them using a metric (e.g.

Hamming distance). Decision is based on the outcome of their evaluation such as granting access or denial from a restricted area [6].

The use of biometrics as a verification system consists of three phases. In the first phase, a sample of a biometric feature is captured, processed and stored in the database as a reference model for future use. In the second phase, some samples are compared with a reference model in order to see if the newly presented biometrics matches or
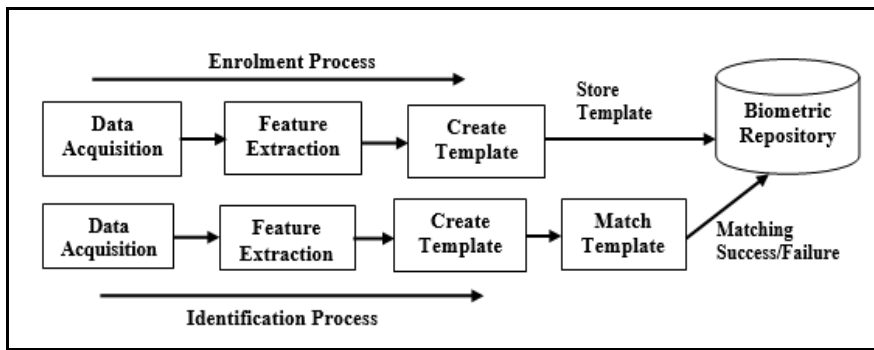

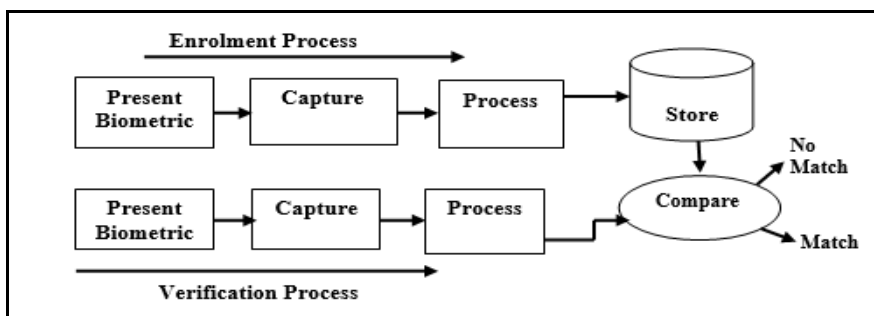Figure 3: Biometrics system architecture, for identification process

Figure 4: Biometrics System Architecture, for Verification Process

not, after which a threshold is computed. During the third phase, access is given if the feature matches

or access is denied if the features do not match. Positive recognition is a common use of the verification mode,

"where the aim is to stop many people from registering into the system by using similar identity but separate biometric data each time they enrol" [21].

Figure 5: Word cloud of popular biometric signatures

Figure 5 shows the popularity of various biometrics used to develop person identification technologies. The popularity is determined by these key factors: universality, permanence, collectability, uniqueness, acceptability, reducibility, circumvention, privacy, performance and inimitability. Brief explanations of these factors are presented as follows:

   i. Universality implies that every person must possess this characteristic,
   ii. Permanence implies that the attributes should not change with time,
   iii. Collectability requires that the properties must be suitable for capture and measured quantitatively without delay,
   iv. Uniqueness means no two people should have the same characteristics,
   v. Acceptability implies that the system must be accepted by the majority,
   vi. Reducibility means the extracted data should be reduce-able to a file,
   vii. Circumvention requires that the property should not be masked or manipulated or even fooled,
   viii. Privacy, demands that capturing process should not defy the privacy of the individual,
   ix. Performance requires that the identification accuracy should be very high, and
   x. Inimitability means the attribute should be irreproducible by other means.

2.2 Commonly used algorithm in biometrics technology

   i. Artificial Neural Networks (ANN): ANN are computational tools used for analysing many complex real world problems by using the biological neuronal networks based on the structure and functions of neurons. It is made up of layers of computing

neurons that are interconnected by some weighted lines that are capable of performing very large parallel computations for data processing. ANN has been used in various areas ranging from speech recognition to prediction as well as in medicine [22]–[24].

ii. Gaussian Mixture Model (GMM): The GMM is a parameter based probability density function, which is represented as a weighted sum of Gaussian element densities. It is majorly used for measuring continuous distribution features in biometrics as well as vocal tract associated spectral features in speaker recognition system. It can also be used in automatic laughter recognition system as well as hand geometry detection [25], [26].

iii. Support Vector Machine (SVM): SVM is an algorithm for solving a binary classification and regression analysis problem. This algorithm maximize margin by defining an optimal hyper-plane. It is used for non-linearly separable problems. It also maps data to higher component area where it easily classifies linear decision surfaces. Its uses ranges from handwritten digit recognition to face recognition to medicine [25], [27].

iv. Hidden Markov Model (HMM): HMM is a statistical tool used for demonstrating generative sequences described by a set of observable sequences. HMM is made up of two stochastic processes which include the invisible process of hidden states and a visible process of observable symbols. The hidden state makes up the Markov chain and the probability distribution of the observed symbol depend on the fundamental state. It is used for modelling time-varying spectral vector sequences [28]–[30].

v. Deep Neural Network (DNN): Deep learning is a machine learning algorithm that is being introduced to the area of large vocabulary speech recognition system. It has many hidden layers as compared to the artificial neural network (ANN) and it incorporates new method for training its data [30], [31].

The discussion on these algorithms pros and cons are presented in Table 1.

Table 1: Selected person identification algorithms pros and cons

Algorithm	Pros	Cons
i. ANN	It has been used to train very complex models. It is easy to conceptualize. It has lots of libraries for easy implementations. It can be used extensively	It requires more data for training Choosing the right parameters may be very complex. Final model may use up a lot of memory. Multi-layered neural networks are

		usually harder to train and require tuning of lots of parameter [32].
ii. GMM	It is a lot more flexible with regards to cluster covariance. GMM allows mixed membership of points to cluster.	Learning may be a little difficult Few libraries for implementation [33].
iii. SVM	It reduces overfitting in the course of training. It manages high dimensional problems. It is used for linearly and non-linearly separable data. Its optimality is guaranteed due to its convex optimization. It can be implemented in various programming languages (Python, Matlab), and its libraries are easily accessible.	It can be time consuming to train. It may not be explanatory enough as it does not return a probabilistic confidence value. It does not support structured representations of text which gives high performance in Natural Language Processing (NLP) [34].
iv. HMM	It is highly flexible. It is suitable for better data fitting. It is highly statistical in nature. It can learn from raw data.	It has a huge numbers of unstructured parameters. It can only represent a small fraction of the entire distributions. Dependencies between layers may not be explicitly represented [35], [36].
v. DNN	It continuously grows data to improve its training. It creates its new features.	It requires very large amount of unlabeled data for training. It requires very high performance hardware for its implementation. It requires more time to train [37].

3. Timeline of Biometrics technology

The advancement of biometric recognition is still in progress, hence the need for continuous improvements in performance and usability.
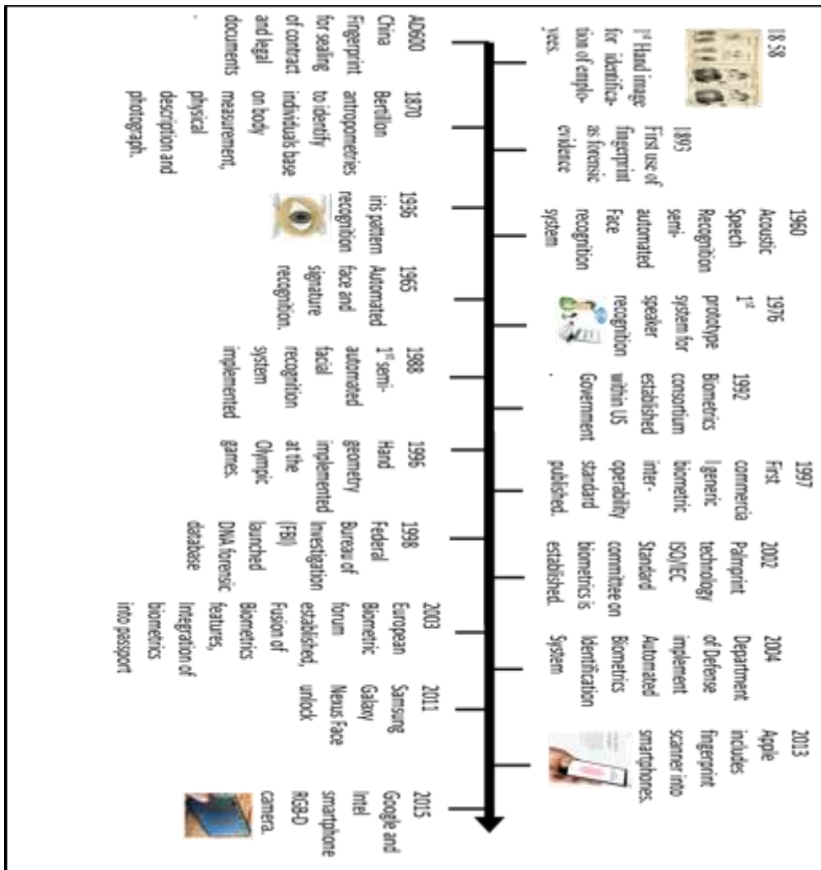
Figure 6: Biometrics timeline over the past one and a half centuries

3.1 Importance and application of biometrics technology timeline

The importance of biometrics technology cannot be over emphasized. There are various areas of applications of this technology around the world. Among the various applications are:

- As far back as 1792-1750BC, the kings of Babylon used the imprint of their right hand for authenticating the written codes of law printed on clay and also for business transactions [38], [39].
- 618-907 Chinese use both fingerprint and handprint on clay as authentication. They also employed palm and footprints to differentiate one child from another [39], [40].
- 1800, Thomas Bewick, an English naturalist, used the printing of his fingerprint to identify his published books [41].
- 1856, Sir William Herschel, a British officer who worked for the Indian civil service, commenced the use of thumbprint on documents as alternative for written signature mostly for illiterate and other people [39].

- 1892, Juan Vucetich, an Argentinean police researcher used fingerprint to identify a mother in the murder of her children, hence, Argentina was the first Country to substitute anthropometry with fingerprint [42], [43] .
- 1920s, fingerprint identification was employed by the law enforcement all over the world including the US military and the Federal Bureau of Investigation (FBI) as a form of identification [39].
- 1974, first commercial hand geometry system for access control, time, attendance and personal identification became available [40].
- 1975, FBI sponsors the development of devices and minutiae extracting expertise [44].
- 1996, Iris scanning was implemented in prison in USA [45]. More so, the hand geometry recognition system was implemented at the Olympic games where over 65,000 people were successfully enrolled [46].
- 1998, Nationwide Building Society in Britain introduced iris recognition within its cash dispensing machine in substitute of the Personal Identity Number (PIN)[45].
- 1999, National Bank United in USA introduces the iris recognition technology to three ATM outlets in Houston, Dallas and Ft Worth [45].
- Late 1990s and early 2000s biometrics was introduced for verification of electorates during election. As research in this area

intensifies, different biometric traits were used to verify electorates during election. Somaliland was the first to use the iris biometrics voting system in the world [47]. Also some other countries throughout the world also implement biometrics technology for election purpose, among them are Kenya, Nigeria, Ghana, Angola which implements the fingerprint biometrics system to identify registered voters. So many other biometric technology have been used over the years all over the world[48].
- 2001, Face Recognition was used at the Super Bowl in Tampa Florida [49]. Also, Malaysia was one of the first countries to implement thumbprint on her national Identity card. Australia included chips for biometric identification on the international passports. In addition, Canada used biometric for anti-terrorism measure [39].
- 2002, the enhanced Border security and Visa Reform Act was put into law. This act include biometric data in the passports of VISA waiver program travelers like Belgium and other Union Member States [39].
- 2003, US Government National Science and Technology Council, inaugurated a subcommittee on biometrics to coordinate biometrics research and development, policy, outreach and international collaboration [50]. Also, in December 2003, the United Linkers Company was born in India. This company offers

biometric solutions in car security implementing various biometrics system ranges from voice to fingerprint [51].

- 2004, US implemented biometrics into immigration services and it was tagged- US-Visit. Also, US government called for compulsory government-wide personal identification card for all federal workers and contractors [50]. In addition, Europe adopted the use of biometric system for passports and travel documents using both facial images and fingerprints [39].

- 2005, OMRON Corporation show case the world's first face recognition technology at the security show tagged Japan 2005. This technology can be deployed on Personal Digital Assistants (PDAs), mobile phones and other mobile devices with camera function [52]. Moreso, seven countries in Europe consisting of Austria, Belgium, The Netherlands, France, Germany, Luxembourg and Spain signed an agreement on the improvement of cross border information exchange and data comparison using DNA profiles, fingerprints and vehicle registration data [39].

- 2008, US Government commenced the organization of the use of biometric database [40]. Also [53] presented an experimental result on fusion of iris and palm print for multi-biometric system. The result obtained showed a very great improvement on a single biometric system. In addition, FBI set up a 1-billion dollar database which

consist of fingerprint, iris, facial images and DNA samples [39].

- 2010, US national security apparatus employs biometrics for terrorist identification [40]. In addition, SBTel and devices commenced the selling of biometrics devices for attendance and access control solutions in Nigeria [50].

- 2011, Biometrics identification was employed in the identification of Osama Bin Laden. Also. SBTel, a biometric device vendor, launched web based biometrics attendance for a cloud-based attendance system [50].

- 2013, Apple included fingerprint scanner into smartphones [40].

- In January 2017, Australia's Department of Immigration and Border Protection announced strategy to execute a novel system at the country's international airport by 2020. This biometric system makes use of face, iris and/or fingerprint recognition system. The biometric system is intended to replace the existing paper identity card passports [54]. In addition, in January of the same year, President Donald Trump ordered that all non-citizens be subjected to biometric checks while entering or leaving the United States [54]. Moreover, in August 2017, First-Biometrics announces the use of next biometrics flexible fingerprint sensor for smart payment and identity card [54].

3.2 Evolution of voice-based recognition system

The initial objective of speech recognition was to develop a system which imitate a person's speech communication ability.

- 1773 – The Russian scientist Christian Kratzenstein, a professor of physiology in Copenhagen created vowel sound with the use of resonance tubes which was attached to the organ pipes [55].
- 1791 – Wolfgang Von Kempelen in Vienna developed the acoustic mechanical speech machine [55].
- Mid 1800s – Charles Wheatstone constructed Von Kempelen's speaking machine employing resonators from leather such that different speech-like sounds could be produced by using hand to change the configurations [55].
- 1879 – Thomas Edison discovered the first dictation machine [56].
- 1930s – Homer Dudley developed a speech synthesizer called Voice Operating Demonstrator (VODER) which was an electrical prototype of Wheatstone's work [55].
- 1952 – Davis, Biddulph and Balashek of Bell laboratories developed Audrey a system for segregated digit recognition for a particular talker [55].
- 1950s – Oslon and Belar of RCA laboratories constructed a ten (10) syllable recognizer for a particular talker[55].
- 1959 – Fry and Denes of University College in England constructed a phoneme recognizer which identifies four (4) vowels and nine (9) consonants [55].
- 1960s – Atal and Itakura invented the basic theory of Linear Predictive Coding (LPD) which abridged the approximation of the vocal tract reponse from speech waveform [55].
- 1962 – IBM shoebox was developed and it can understand 16 English words [56].
- 1971 – Alexander Waibel, developed the Harpy machine at Carnegie Mellon University. This machine can understand 1,011 words with some phrases [56].
- 1970s – Tom Martins started the leading speech recognition company named Threshold Technology incorporation building the first Automatic Speech Recognition (ASR) product known as VIP-100 system. Also, Lenny Baum of Princeton University discovered a mathematical speech recognizer called the Hidden Markov Model (HMM). In addition, the use of pattern recognition technology to speech identification system using LPC was introduced [55].
- 1980s – The use of Artificial Neural Network was introduced for speech hence; speech recognition tends towards prediction.
- 1986 – IBM Targora was developed employing the HMM to predict the next phonemes in

speech. This system was the world's fastest typist at the time as it was able to recognize up to 20,000 English words and a number of sentences [56].

- 1990s – The emergence of Automatic Speech Recognition (ASR) [55].
- 1997 – The world's leading uninterrupted speech recognizer was announced as a Dragon's naturally speaking software. This software was able to understand 100 words per minute without any break in between the words [55].
- 2006 – The National Security Agency (NSA) commenced the use of speech recognition to identify key terms in recorded speech [56].
- 2008 – Google introduces a voice exploration app on mobile devices [56].
- 2011 – Apple launches Siri, for voice based digital assistant [56].

3.3 Benefits and challenges of biometrics systems

Despite this progress, a number of challenges continue to restrain the full potential of biometrics to automatically recognize humans. Some specific challenges, in terms of biometrics groups, are presented in Table 2 [6].

The need for a reliable system for person identification cannot be over-emphasized, while the state-of-the-art biometric identification systems are taking over access control and many security establishments. These systems have been in existence for over five decades, though it started gaining attention in recent time.

Although, there are many challenges that are needed to be addressed in order for these systems to be robust and more accurate (Table 2). A major challenge of these systems is spoofing attack. It is a condition whereby a person effectively impersonates another person. This is often done in order to gain an illegal access to a facility or system.

3.4 Areas of implementation of Voice-based recognition system

1. For attendance system
2. In mobile phone for auto texting
3. Forensic
4. Banking and financial institutions
5. Using one's indigenous language for recognition purpose.
6. In medicine.
7. Assisting the aged in text composition, bank transaction and many more
8. According to Boyd [56], "cloud-based computers have entered millions of homes and can be controlled by voice, even offering conversational responses to a wide range of queries".
9. Voice activated home speakers.
10. Purchases can be made over the internet using voice enabled machines.

According to Akhtar et al [57], the US National Institute of Standards and Technology enumerate the susceptibility of biometrics to spoofing in their national vulnerability database. Most of the existing biometrics systems are susceptible to this attack. For instance, the iris, finger print and face images taken from impersonators were identical with that of the real users. In order to

cub this attack, there is a need to introduce a liveness detection into biometrics systems. This is an area of future research. In addition, the use of different biometric systems combination that is a multi-modal biometric technology has the potential to reduce this attack [58-60]. Thus, more studies are required in this direction. Finally, biometric trait and databases are needed in order to validate new biometric systems such as the use of tongue, ear, sneeze, cough, laughter and so on.

Table 2: Benefits and challenges of Biometrics systems

Biometrics systems	Benefits	Challenges
Hand based: Fingerprint or finger scan Hand geometry Palm print	Easy to use and non-intrusive. High accuracy and long term stability. Ability to enrol various fingers. Mature technology	Fingerprint of those working in chemical production companies, or farming is frequently affected. Affected by skin condition. Affected by a few cuts, blister or wound either short term or permanent.
Face/Eye based: Facial recognition Retina scan Iris scan Facial thermograph	Ability to operate secretly. Non-intrusive. Not affected by environmental condition.	. Twins may have similar face features The eyes of people with diabetes may get affected hence resulting in differences. It may change as the person gets older
Behavioural characteristics. Voice recognition Signature recognition Key stroke scan Speaker recognition, Gait recognition	It uses current telephony setup. It is easy to use and non-intrusive. The voice-based biometrics further enjoys the following benefits: - It does not need to be in contact with the individual in order to be captured, hence it can be taken remotely. It can be used while driving, from another room, through mobile device, while a person is busy with some other activity and so on. It is simple and easy to use Recorded voices cannot be used to spoof this system.	Signature is affected by inconsistency in signing which makes it difficult to use. The voice is affected by cold. Environmental noise. It may change as the person gets older. Channel effects such as inference and distortion, frequency response, channel encoding. Presentation effects such as speech sample duration, psycho physiological state of the speaker (such as illness, emotions), effects of vocal strain and so on.

4. Conclusions

Even though there are some challenges facing biometrics technology, it has tremendous usage in this information technology age. Choice of biometric type depends on characteristics measurement and user requirement. Other factors which affect the choice of a biometric based are sensor and device availability, computational time and reliability, cost, sensor size and power consumption. In addition, cultural disposition is also a factor that affects biometric technology selection.

Currently, due to divers' nature of biometric applications, no single biometric trait is likely to be ideal and satisfy all the requirements of all applications, hence the need to use multiple biometric features in order to ensure very high reliability is essential. Investigating new biometric features for identification is an area where more research is needed to be carried out.

Having considered the advancement in technology, moving from the use of paper to electronics and online base medical records to banking and financial industry as well as social media. The huge and sensitive data involved must be adequately protected from being hacked into. Voice-based recognition system has however, been considered as a very appropriate biometrics for this task having considered the speed, efficiency and customer relation characteristics it possesses.

URL: *http://journals.covenantuniversity.edu.ng/index.php/cjet*

According to [56], "Voice is the future. The world's technology giants are clamouring for vital market share, with ComScore agitating that 50% of all searches will be voice searches come 2020."

References

[1] A. K. Jain, K. Nandakumar, and A. Ross, "50 years of biometric research: Accomplishments , challenges , and opportunities," vol. 79, pp. 80–105, 2016.

[2] T. Reuters, "Global directory," 2017. [Online]. Available: https://blogs.thomsonreuters.com /answerson/biometrics-technology-convenience-data-privacy/. [Accessed: 03-Oct-2018].

[3] D. Carlson, "Biometrics - Your Body as a Key," 2014. [Online]. Available: http://www.dynotech.com/article s/biometrics.shtml. [Accessed: 04-May-2017].

[4] K. Delac and M. Grgic, "A survey of biometric recognition methods," 46th Int. Symp. Electron. Mar., 2004.

[5] A. M. Bojamma, B. Nithya, and C. N. Prasad, "An Overview of Biometric System," Int. J. Comput. Sci. Eng. Inf. Technol. Res. ISSN 2249-6831, vol. 3, no. 2, pp. 153–160, 2013.

[6] R. B. Jadhao and A. Bakshi, "An Overview of Biometric System," Int. J. Sci. Res. Educ., vol. 3, no. 7, 2015.

[7] B. P. Salil and W. L. Damon, "Biometric authentication and identification using keystroke dynamics: A survey," J. Pattern Recognit. Res., vol. 7, no. 1, pp. 116–139, 2012.

[8] J. Kaur and S. Kaur, "A Brief Review: Voice Biometric For Speaker Verification in Attendance Systems," Imp. J. Interdiscip. Res., vol. 2, no. 10, 2016.

[9] D. Tran, M. Wagner, Y. W. Lau, and M. Gen, "Fuzzy methods for voice-based person authentication," IEEJ Trans. Electron. Inf. Syst., vol. 124, no. 10, pp. 1958–1963, 2004.

[10] J.-L. Dugelay, J.-C. Junqua, C. Kotropoulos, R. Kuhn, F. Perronnin, and I. Pitas, "Recent advances in biometric person authentication," in International Conference on Acoustics, Speech, and Signal Processing (ICASSP), IEEE, 2002, vol. 4, p. 4060-4063.

[11] P. Belin, S. Fecteau, and C. Bedard, "Thinking the voice: neural correlates of voice perception," Trends Cogn. Sci., vol. 8, no. 3, pp. 129–135, 2004.

[12] H. Aronowitz, R. Hoory, J. Pelecanos, and D. Nahamoo, "New developments in voice biometrics for user authentication," in Twelfth Annual Conference of the

International Speech Communication Association, 2011.

[13] P. Korshunov and S. Marcel, "Joint operation of voice biometrics and presentation attack detection," 8th Int. Conf. Biometrics Theory, Appl. Syst. (BTAS), ieeexplore.ieee.org, 2016.

[14] S. Krawczyk and A. K. Jain, "Securing electronic medical records using biometric authentication," in International Conference on Audio-and Video-Based Biometric Person Authentication, 2005, pp. 1110–1119.

[15] L. M. Mazaira-Fernandez, A. Álvarez-Marquina, and P. Gómez-Vilda, "Improving Speaker Recognition by Biometric Voice Deconstruction," Front. Bioeng. Biotechnol., vol. 3, Sep. 2015.

[16] N. Scheffer, L. Ferrer, A. Lawson, Y. Lei, and M. McLaren, "Recent developments in voice biometrics: Robustness and high accuracy," in International Conference onTechnologies for Homeland Security (HST), IEEE, 2013, pp. 447–452.

[17] K. S. Bhogal, A. Rick, D. Kanevsky, and Pickover C A, "Using voice biometrics across virtual environments in association with an avatar's movements," US Patent, Google Patents, 2012.

[18] N. Zhang, M. Paluri, Y. Taigman, R. Fergus, and L. Bourdev, "Beyond frontal faces: Improving person recognition using multiple cues," in Proceedings of the IEEE Conference on Computer Vision and Pattern Recognition, 2015, pp. 4804–4813.

[19] M. Khitrov, "Talking passwords: voice biometrics for data access and security," Biometric Technol. Today, vol. 2, pp. 9–11, 2013.

[20] M. Vatsa, R. Singh, and A. Noore, "Feature based RDWT watermarking for multimodal biometric system," Image Vis. Comput., vol. 27, no. 3, pp. 293–304, 2009.

[21] P. Ghosh and R. Dutta, "A new approach towards biometric authentication system in palm vein domain," Int. J. Adv. Innov. IJAITI, vol. 1, no. 2, pp. 1–10, 2012.

[22] O. N. A. Al-Allaf, "Review of face detection systems based artificial neural networks algorithms," arXiv Prepr. arXiv1404.1292, pp. 1404–1292, 2014.

[23] F. Amato et al., "Artificial neural networks in medical diagnosis," J. Appl. Biomed., vol. 11, pp. 47–58, 2013.

[24] A. S. George, E. Roy, A. Antony, and M. Job, "An Efficient Gait Recognition System for Human Identification using Neural Networks," Int. J. Innov. Adv. Comput. Sci., vol. 6, no. 5, 2017.

[25] J. R. Pinto, J. S. Cardoso, A. Lourenço, and C. Carreiras, "Towards a Continuous Biometric System Based on ECG Signals Acquired on the Steering

Wheel," Sensors, vol. 17, p. 2228, 2017.

[26] J. S. Edwards, "Using Gaussian Mixture Model and Partial Least Squares regression classifiers for robust speaker verification with various enhancement methods," Rowan University, Rowan Digital Works, 2017.

[27] C. D. Smyser et al., "Prediction of brain maturity in infants using machine-learning algorithms," Neuroimage, vol. 136, pp. 1–9, 2016.

[28] U. Jerome, "Acoustic Laughter Processing," TCTS Lab. Publ. Univ. Mons., 2014.

[29] Ç. Hüseyin, U. Jérôme, and D. Thierry, "Synchronization rules for HMM-based audio-visual laughter synthesis," in IEEE International Conference on Acoustics Speech and Signal Processing ICASSP, 2015.

[30] A. Hannun et al., "Deep speech: Scaling up end-to-end speech recognition," arXiv Prepr. arXiv1412.5567, 2014.

[31] F. Lingenfelser, J. Wagner, J. Deng, R. Bruckner, B. Schuller, and E. Andre, "Asynchronous and Event-based Fusion Systems for Affect Recognition on Naturalistic Data in Comparison to Conventional Approaches," IEEE Trans. Affect. Comput., 2016.

[32] L. Matthew, "Deep Learning," 2014. [Online]. Available: https://www.quora.com/What-are-the-pros-and-cons-of-neural-networks-from-a-practical-perspective-Personal-comments-

from-heavy-users-welcome. [Accessed: 03-Jul-2018].

[33] O. Wibisono, "Deep Learning," 2016. [Online]. Available: https://www.quora.com/What-are-the-advantages-to-using-a-Gaussian-Mixture-Model-clustering-algorithm. [Accessed: 03-Jul-2018].

[34] A. Ng, "Deep Learning," 2016. [Online]. Available: https://www.quora.com/What-are-some-pros-and-cons-of-Support-Vector-Machines. [Accessed: 03-Jul-2018].

[35] P. J. Rani, "Advantages and disadvantages of hidden markov model.," 2016. [Online]. Available: https://www.slideshare.net/joshiblog/advantages-and-disadvantages-of-hidden-markov-model. [Accessed: 04-Jul-2018].

[36] K. Tuzcuoglu, "Deep Learning," 2018. [Online]. Available: https://www.quora.com/What-are-the-advantages-and-disadvantages-of-Hidden-Markov-Models-in-forecasting-values-of-a-time-series-compared-to-other-methods-e-g-ARIMA-Can-we-say-that-HMM-is-a-Non-Statistical-learning-methods. [Accessed: 03-Jul-2018].

[37] O. Maslovska, "Deep Learning: Definition, Benefits, and Challenges," 2017. [Online]. Available: https://stfalcon.com/en/blog/post/deep-learning-benefits-and-challenges. [Accessed: 03-Jul-2018].

[38] J. Ashbourn, "The social implications of the wide scale implementation of biometric and related technologies," Backgr. Pap. Inst. Prospect. Technol. Stud. DG Jt. Res. Centre, Eur. Comm., 2005.

[39] E. J. Kindt, "Privacy and data protection issues of biometric applications," Springer, 2016.

[40] S. Mayhew, "History of Biometrics," 2016. [Online]. Available: http://www.biometricupdate.com /201501/history-of-biometrics. [Accessed: 09-May-2017].

[41] K. Fauci, "Prezi Presentations," 2014. [Online]. Available: https://prezi.com/5nzrgdiroqzn/1 800s-thomas-bewick-an-english-naturalist-used-engraving/.

[42] USA-Govt, "Visible Proofs, U.S. National Library of Medicine," vol. 2017. U.S. National Library of Medicine, 8600 Rockville Pike, Bethesda, MD 20894, 2014.

[43] D. A. Glaeser, "The Fingerprint, in the Service of the SWISS Confederation." Federal Office of Police fedpol, 2013.

[44] S. M. Martinez, "THe FBI-Federal Bureau of Investigation," 2013. [Online]. Available: https://archives.fbi.gov/archives/ news/testimony/overview-of-fbi-biometrics-efforts.

[45] K. Chadwick, J. Good, G. Kerr, F. McGee, and F. O'Mahony, "Biometric Authentication For Network Access And Network Applications," 2001. [Online]. Available:

http://ntrg.cs.tcd.ie/undergrad/4b a2.02/biometrics/now.html.

[46] N. Duta, "A survey of biometric technology based on hand shape," Pattern Recognit., vol. 42, no. 11, pp. 2797–2806, 2009.

[47] TeleSur, "Somaliland: 1st in World to Use Iris Scanner Technology to Stem Voter Fraud," 2017. [Online]. Available: https://www.telesurtv.net/english /news/Somaliland-1st-in-World-to-Use-Iris-Scanner-Technology-to-Stem-Voter-Fraud-20171114-0006.html.

[48] P. Wolf, A. Alim, B. Kasaro, P. Namugera, M. Saneem, and T. Zorig, "Introducing Biometric Technology in Elections," Voter Information, Commun. Educ. Netw. Glob. Knowl. Netw. Voter Educ., 2017.

[49] L. K. Nadeau, "Tracing the History of Biometrics," 2012. [Online]. Available: http://www.govtech.com/Tracing -the-History-of-Biometrics.html.

[50] Solutions-Broadway-Digest, "History of Biometrcs," 2017. [Online]. Available: https://www.sbtelecoms.com/hist ory-of-biometrics-conclusion/.

[51] United-Linkers-Biometric-and-Robotic-Solutions, "World's First Face Recognition Biometric for Mobile Phones," 2017. [Online]. Available: http://automobile-security.com.

[52] World's-First-Face-Recognition-Biometric-for-Mobile-Phones, "World's First Face Recognition Biometric for Mobile Phones," 2005. [Online]. Available:

https://phys.org/news/2005-03-world-recognition-biometric-mobile.html.

[53] V. C. Subbarayudu and M. V. N. K. Prasad, "Multimodal biometric system," in Emerging Trends in Engineering and Technology, 2008. ICETET'08. First International Conference on, 2008, pp. 635–640.

[54] J. Lee, "Biometric Update.com," 2016. [Online]. Available: http://www.biometricupdate.com /201701/biometrics-to-replace-passports-at-australian-airports.

[55] B.-H. Juang and L. R. Rabiner, "Automatic speech recognition–a brief history of the technology development," Georg. Inst. Technol. Atlanta Rutgers Univ. Univ. California. St. Barbar., vol. 1, p. 67, 2005.

[56] C. Boyd, "The startup," 2018. [Online]. Available: https://medium.com/swlh/the-past-present-and-future-of-speech-recognition-technology-cf13c179aaf. [Accessed: 03-Oct-2018].

[57] Z. Akhtar, C. Micheloni, and G. L. Foresti, "Biometric liveness detection: Challenges and research opportunities," IEEE Secur. Priv., vol. 13, no. 5, pp. 63–72, 2015.

[58] K. O. Okokpujie, S. N. John, E. Noma-Osaghae, C. Ndujiuba, I. P. Okokpujie. AN ENHANCED VOTERS REGISTRATION AND AUTHENTICATION APPLICATION USING IRIS RECOGNITION TECHNOLOGY. International Journal of Civil Engineering and Technology (IJCIET). 2019 Feb 28;10(2):57-68.

[59] K. Okokpujie, E. Noma-Osaghae, O. Okesola, O. Omoruyi, C. Okereke, S. John, I. P. Okokpujie. Fingerprint Biometric Authentication Based Point of Sale Terminal. In International Conference on Information Science and Applications 2018 Jun 25 (pp. 229-237). Springer, Singapore.

[60] K. Okokpujie, E. Noma-Osaghae, O. Okesola, O. Omoruyi, C. Okereke, S. John, I. P. Okokpujie. Integration of Iris Biometrics in Automated Teller Machines for Enhanced User Authentication. In International Conference on Information Science and Applications 2018 Jun 25 (pp. 219-228). Springer, Singapore.

An Open Access Journal Available Online

Community-Based LDPE Wastes Recycling Machine

I. D. Okeke [1], T. M. Ibezim [1], O. T. Ndusorouwa [1], U. C. Okonkwo[1] & I. P. Okokpujie [2]

[1]Mechanical Engineering Department, Nnamdi Azikiwe University, Awka
[2]Department of Mechanical Engineering, Covenant University, Ota, Ogun state, Nigeria

Abstract: Several efforts have been made to proffer solution to the burden placed by plastic wastes on man's environment. However, the conspicuous presence of these solid waste pollutants in the communities suggests that the efforts made so far only yielded little result. In this study, a small scale hot extrusion process machine which recycles low density polyethylene was designed and constructed. The machine is powered by a 2 Horse power, 3-phase electric motor which transmits a torque of 200N.m at a speed of 37 rpm through a gearbox with the velocity ratio of 20:1 to a 34 diameter single screw. Low density polyethylene materials were fed in through the hopper. The heat from the heater bands and friction and pressure generated along the transition zone of the screw provided the energy needed for the transformation of the materials conveyed to a well-blended molten state. The extradites were channelled to the cooling tank for heat extraction and then collected as raw materials for the plastic industries. It is recommended that providing this machine in our communities will contribute greatly to achieving a greener environment and creating entrepreneurial opportunities in the society, thus contributing to the achievement of the sustainable development goals.
Keywords: Low density polyethylene, recycling, sustainable development, entrepreneurship

1. Introduction
The setting of the sustainable development goals by the United Nations stirred up global concerns about the impact of man's activities on the environment and the future generation. The indiscriminate disposal of plastic wastes has attracted serious attention globally. The united nation's world environmental day 2018 had the theme "beating plastic pollution" [1-2], capturing the concern of the international community to bring to an end the

URL: *http://journals.covenantuniversity.edu.ng/index.php/cjet*

menace of plastic pollution, knowing that it is fundamental to achieving a green, sustainable environment. It is estimated that about eight metric tonnes of plastic are thrown into the ocean annually [3].

The non-degradable polythene plastics used as commodity goods storage and packaging purposes accounts for over 60 million tons of annual wastes generation worldwide [4]. It was also reported that 30 % of the domestic waste in a typical Nigerian city comprises of the polythene and plastic products in very large quantities; whose disposal has continued to constitute the great environmental pollution challenge and concern in big and small cities [5].

Since the majority of these wastes are generated at the grass root, it is logically sound to think of a solution that would engage and empower individuals at this level to competently manage these pollutants, hence the need for a locally made machine which can be easily operated with little skill.

2. Review of Locally Made Polyethylene Recycling Machine

Gbasouzor [6] designed a model polyethylene recycling machine with economic development and pollution control in view for the Country, Nigeria. The machine was designed to operate at a temperature of 200 – 2200C and requires 1hr 45mins for heating up before melting the polyethylene. This machine makes use of thermostat, a heating element, electric motor, gears, screw conveyor, coupling and keys. Polyethylene that has been cut and dried is feed into the

chopper from where it moves to the barrel. A screw inside the barrel is rotated by the geared electric motor. As the screw rotates, it conveys the polyethylene material to the heated zone of the barrel. From there it moves form the orifices provided at the end of the barrel. The machine takes time to heat up and after melting of the polyethylene there is always a remnant molten polyethylene that gets stuck inside the barrel and this prevents the screw from rotating. This is a major challenge that is facing this model of polyethylene recycling machine.

Odior [7] developed a polyethylene recycling machine from locally sourced materials that uses rotary and forced blades for slitting the loaded wastes. Knife penetration first causes compaction accompanied by frictional heat. It produces a cutting and heating action which partially melts the compacted waste producing thick shreds. The machine uses rotary blades which are rotated by a single phase, high speed electric motor. The rotary blades helped to improve the machine performance. The machine produces an average of 35kg of small flakes of recycled wastes per hour at a machine speed of 2880 rpm.

Ugoamadi [8] optimized the development of a plastic recycling machine that minimizes the limitations of the already existing ones to a great extent and at the same time ensuring effective waste management. The machine is powered by a 3Hp and 900rpm electric motor, while the conveyor shaft runs at 268rpm. It has a capacity of 265kg/hr waste recycling rate and an efficiency

of 97 percent. The results presented show that for every plastic fed into the hopper, at 2000C the plastic was converted into a molten state. The machine employs the principle of conveying and heating to effect shredding and melting of the materials fed through the hopper, and requires only two persons to operate. The use of chain drive in this model from the electric motor could lead to high levels of noise and friction, which are undesirable.

3. Materials and methods

3.1 Extruder Screw

3.1.1 Screw diameter selection

The choice of 34 mm screw was primarily arrived at considering the overall size of the extruder desired since other parts of the machine directly or indirectly relates to it as shown in Fig. 1.
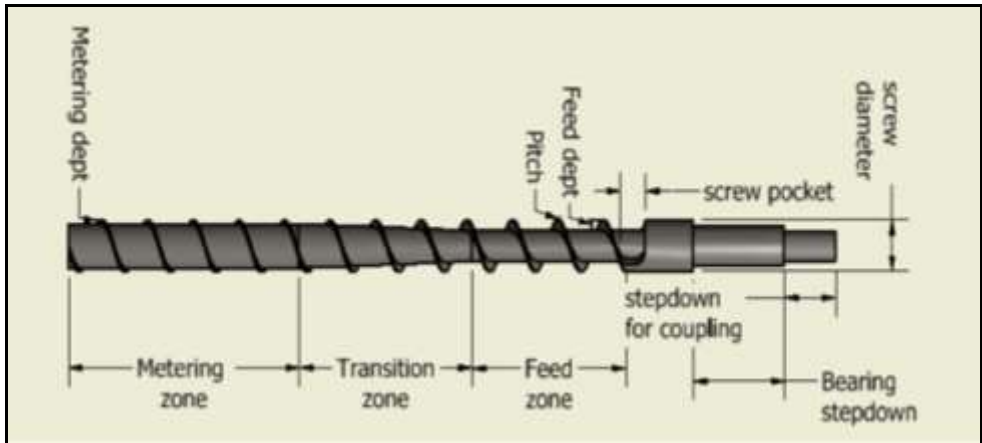
Fig. 1: CAD design of the extruder screw

3.1.2 Length of screw;

This is determined from the length to diameter (L/D) ratio of the screw. This is the ratio of the flight length of the screw to the original diameter of the screw.

A ratio of 10:1 was selected for portability.

This also implies that the flight length of the screw is equal to 10D or 340mm.

The feed section, transition section and metering sections of the screw are in the ratios of 3D:3D:4D respectively.

3.1.3 Design Calculations

Feed section length

$$(FL) = 3 \times 34 = 129\text{mm} \qquad (1)$$

Feed section depth $(Fd) = 0.2D = 6.8\text{mm}$ (2)

Transition section length

$$(TL) = 3 \times 34 = 129\text{mm} \qquad (3)$$

Metering section length

$$(ML) = 4 \times 34 = 172\text{mm} \qquad (4)$$

Metering section depth

$$(Md) = 0.33Fd = 2.267\text{mm} \qquad (5)$$

For standard screw profiles, the angle that the flight makes with a line

perpendicular to the shaft (flight angle) is 17.6568o [9]

Pitch of the screw (Lead)

$$S = \pi \times D \times \tan\varphi \quad (6)$$
$$= 3.142 \times 34 \times 17.6568 = 34mm$$

Where φ = the flight angle

Flight width (screw thickness)

$$WFLT = 0.1D = 3.4mm$$

Screw channel width

$$(W) = \frac{pitch - flight\ thickness}{\cos\varphi} \quad (7) \quad = 32.127mm$$

Screw (in a smooth barrel) standard conveying efficiency

$$\eta F = 0.44 \ [10]$$

Screw-barrel clearance (δ_{FLT}) = 0.0017D= 0.17 ×34 = 0.0578 mm

Distance between screw root and barrel internal wall (H) = S+ δ_{FLT}
$$(8)$$
$$= 34 + 0.0578 = 34.0578\ mm$$

Internal diameter of barrel

$$Db = screw\ diameter + 2\ \delta FLT \quad (9)$$
$$= 34.01156\ mm$$

3.1.4 Screw throughput rate and speed

The speed and through put rate of the recycling machine are interdependent. Therefore, either of the two has to be fixed so as to allow the calculation of the other. Speed or throughput of the machine is a factor that the designer has to choose based on what work the machine is expected to do. An overview of speed specifications for standard screws in their manufacturers' datasheet reveals that similar screws run on speeds between 20rpm and 130rpm. This depends on the material to be extruded and the extrusion process to be adopted.

Selected speed= 38rpm

Bulk density of LPDE ((ρ_0) =590kg/m3 [11]

Throughput rate

$$(\dot{m}) = 60.\rho0.N.\eta F.\pi2.H.Db.(Db-H).\frac{W}{W+Wflt}.\sin\varphi.\cos\varphi \quad (10)$$

Substituting values for this gives

$$26.771kg/hr\ or\ \mathbf{7.436 \times 10 - 3kg/s}$$

3.1.5 Screw Power Requirement

To achieve this, the total power required for the entire extrusion process would first be calculated.

The energy required to raise a kilogram of the material by 10C is referred to as the specific heat capacity (CP). Its value for LDPE is 2300 J/kg.k [12]

Initial temperature LDPE T1=250C or 298k

Final temperature of LDPE (melting point) T2= 115^{0}C or 388k

The power required to just melt the screw

$$(Pactual) = \dot{m}.CP.\Delta T \quad (11)$$
$$Pactual = 7.463 \times 10 - 3 \times 2300 \times (388 - 298) = 1539.33 Watts\ or\ 1.5393kW$$

Allowance for energy losses

Power is lost the cooling section, gear reducers and the surrounding environment. This accounts for about 30% of P$_{actual}$ [13]

$$Ploss = 30\%\ of\ 1539.99 = 461.799W$$

Therefore, the total power required for the extrusion process,

$$(Ptotal) = Ploss + Pactual \quad (12)$$
$$1539.33 + 461.799 = 2001.129\ W$$

This power would be enough to drive the screw at full load neglecting the weight of the screw and frictional losses. To prevent hitting this limit during operation,

some additional 15% of the actual power requirement would need to be added to serve as reserve power and reduce the load of the screw.

$$Preserve = 15\% \times 1539.3 = 230.899W$$

The rotation of the screw contributes the greatest percentage of the total power requirement of the extrusion process [14].

Therefore, screw power requirement

$$= 60\% \text{ of } Ptotal + Preserve \quad (13) = 1431.5764W \text{ or } 1.431576 \text{ Kw}$$

$$1 \text{ kW} = 1.341022 \text{ Horsepower}$$

Screw power requirement

$$= 1.4315764(1.341022) = 1.9198 \text{ Hp}$$

3.2 Barrel design

The barrel is a thick walled cylinder that houses the screw and part of the material housing. Its primary function is to provide a chamber for pressure build up. It has flanges at both ends to provide coupling surfaces for the die head and the bearing housing.

Theoretical Volume of the Material in the barrel (Vm)

This is the difference between the volume of the barrel and the volume of the screw.

Volume of barrel (Vm)

The volume of the barrel,

$$Vb = \pi r2L \qquad (14)$$

Where r = internal radius of barrel

L = total length of the barrel occupied by the material

L = 473.645mm + 30mm = 503.645mm

Therefore,

$$Vb = \pi \times 172 \times 503.645 =$$

$$451,269.5079mm3$$

Volume of Screw

The screw has an irregular geometry; therefore, the volume was evaluated using the CAD model of the screw with Inventor software presented in Fig. 2. It is noteworthy that only the flight length of the screw was used, as that was the only portion of the screw immersed in the material in the barrel.
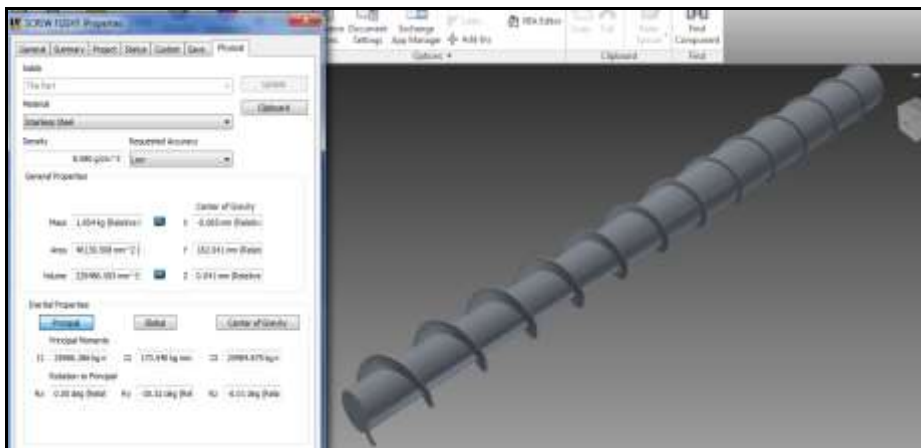

Fig. 2: Analysis of the flight length of the screw

3.3 The Heater bands

From the CAD analysis: Mass of the screw flight length = 1.854 kg, Area of the screw flight length = 46139.508mm2

Volume of the screw flight length= 229,486.505mm^3

Total Volume of material in the barrel, Vm = Volume of barrel – Volume of screw

$$Vm = Vb - Vs \qquad (15)$$

$$= 4,511,269.5079 - 229,486.505$$

$$= 227,783.0029mm$$

62

3.3 The Heater bands

There are three band heaters on the extruder made up of aluminum and nichrome alloys, the energy contribution of one of the heater was computed and multiplied by three to get the total contribution of the heating system.

Heater type: aluminum band heater heating element nickel chrome: (nickel and chromium alloys) heater band diameter is 76.67mm, heater width is 96.67mm (for the die head heater band).

maximum lead amperes are approximately 13.5A, voltage supply was 220V.

The watt density for this heater type is rated at (50W/ in^2) which are approximately (7W/cm^2)

Surface area of each heater is given by equation (16) - (18):

$$\text{Length (circumference)} = 2\,\pi\,r$$

$$= 2 \times 3.14151 \times 0.3833 = 2.408m$$

$$\text{Area} = \pi \times D \times W \qquad (17)$$

$$= 3.1412 \times 0.7667 \times 0.9667 = 2.328\,m^2$$

Resistance of each heater is given by:

$$R = \frac{Pr}{L} \qquad (18)$$

Where:

P_r= resistivity of the heating element at 20°C which is equal to 1.1 x 104 cm

L = average length (circumference) of the heating element = 2.408m

$$A = \text{Area} = \pi \times D \times W = 2.328\,m^2$$

$$R = \frac{1.10 \times 10^{-4} \times 2.408}{2.328} = 1.137 \times 10^{-4}\,\Omega$$

Quantity of heat required to melt the mass of the material:

From earlier calculations, total power required to drive the system is given as 2001, the shear force from the screw rotation contributes 70 to 80% of the total power requirement to melt the material, while the rest is supplied by the heater bands, taking a ratio of 60% to 40%, the energy requirement from the heater band (quantity of heat required to melt the material) is given as shown in equation (19);

40% of 2001.125W = 0.4 x 2001.125 = 800.45 watts (joules/sec)

3.4 Temperature at which to set the controller

From Fourier's law

$$Q = K \frac{A}{B} T_1 - T_2 \qquad (19)$$

T_1 = set temperature for the controller

T_2 = temperature at which the low density polythene melts which is 115^0 C

K = thermal conductivity for high carbon steel = 43 W/m ^{0} C

A = area normal to the direction of heat flow, equivalent to the surface area the heater

Heater bands 1 & 2 = 2 (70 x 100) = 14000mm^2

Heater band 3 = 70 X 150 = 10,500mm^2

Heater band 4 = 150 X 30 = 4,500mm^2

Total Area = 29,000mm^2 = 0.0029m^2

$$T_1 = \frac{Qb}{KA} + T_2 \qquad (20)$$

$$= \frac{800.45 \times 0.041}{43 \times 0.029} + 115 = 141.318 \, oC$$

3.5 Electric Motor Selection

The power of the electric motor usually expressed in horsepower (Hp) as presented in equation (21) [15].

Hp (3-phase motor)

$$= \frac{1.732 \times V \times I \times P.F \times Efficiency}{746} \qquad (21)$$

Where V = voltage of the required electric motor, I = current required by the electric motor

P.F = power factor of the electric motor

V= 220v   I= 4A, P. F= 1.1 (gotten from chart for a light medium screw) Efficiency = 95%.

Substituting the above gives Hp = 1.94hp.

. A 2 horse power electric motor was selected. The selected electric motor has a speed of 1440rpm (from the name plate).

Angular velocity of the electric motor,

$$\omega = \frac{2\pi N}{60} \qquad (22)$$

$$\omega = \frac{2 \times \pi \times 1440}{60} = 150.8 \, rad/s$$

Power of the electric motor = torque × angular velocity

$$= tm \times \omega r = \omega 2r \qquad (23)$$

Where r = radius of the small pulley = 80/2 mm   = 0.04m

Therefore, power transmitted by the electric motor pulley to the gearbox,

$= 150.8^2 \times .04 = 0.90kW$

Torque of the electric motor,

$$T = \frac{60P}{2\pi N}$$

Where P = Power of the electric motor in Watts

N = Number of revolutions of the electric motor shaft

The electric motor selected has the following parameters,

P = 1.5 kW, N = 1440 rpm

Therefore, the torque of the electric motor,

$$T = \frac{60 \times 1500}{2\pi \times 1440} = 9.95 \, Nm$$

3.6 Gear Box Selection

With a speed of 37 rpm of the shaft, the selected motor has a speed of 1440rpm

Note: Input speed of the gear box is approximately half the electric motor's velocity ratio

$$= \frac{Input \, speed}{Output \, speed} \qquad (24)$$

$$= \frac{720}{37} = 1 : 19.5 \, rpm$$

The closest velocity reduction gear in the market was 20, thus a 1:20 gear box was selected.

The torque of the gearbox is a product of the electric motor torque and the gearbox velocity ratio [25].

$$T = Te \times V.R \qquad (25)$$

Therefore, the torque of the gearbox,

$$T = 9.95 \times 20 = 200 \text{ Nm}$$

3.1 Belt Selection

From Fenner catalogue for belt drives 1997 the equation (26) is applied [16] Belt length,

$$L = 2C + \frac{(D-d)^2}{4C} + \frac{\pi(D+d)}{2}$$

Where L = required length of the belt in mm   C = approximate centre distance in mm

D = diameter of the gear box pulley in mm

d = diameter of the electric motor pulley in mm

$$C = 2 \times \sqrt{(D+d) \times d} \qquad (27)$$

Where, D = 150mm   d = 80mm

$$C = 2 \times \sqrt{(150+80) \times 80} =$$

271.3mm

From equation (26)

$$L = 2 \times 271.3 + \frac{(150-80)^2}{4 \times 271.8} + \frac{\pi(150+80)}{2}$$

$$= 908.4mm$$

From the above calculation the maximum length of the belt will be 908.4mm but because of slipping a lower standard belt will be selected. The standard v-belt available within this range is A32 (850mm) according to belt catalogue available [17].

For accurate Centre distance (C_A)

$$CA = A + \sqrt{A^2 + B} \qquad (28)$$

Where $A = \frac{L}{4} - \pi\frac{(D+d)}{8}$

Length of the chosen belt, L = 850mm, D = 150mm, d = 80mm

$$A = \frac{850}{4} - \pi\frac{(150+80)}{8} = 122.18 \text{ mm}$$

$$B = \frac{(D-d)^2}{8} \qquad (29)$$

$$B = \frac{(150-80)^2}{8} = 612.5 \text{ mm}$$

Therefore,

$$CA = 122.18 + \sqrt{122.18^2 + 612.5} = 246$$

3. Results and Discussions
3.1 Throughput Efficiency

Evaluation of the actual throughput of the machine:

This was calculated by obtaining the mass of materials extruded in five different intervals, finding their average and converting to mass per second.

The Table 1, shows the results of the findings

Table 1: Mass of Extruder and Time

S/N	Time (mins.)	Mass of extruder (kg)
1	1	400.54 x 10-3
2	2	400.30x10-3
3	3	400.12x10-3
4	4	400.0 x 10-3
5	5	399.92 x10-3

From the Table 1,

Mass of the extrude per minute

$$M/m =$$

$$\frac{(400.54+400.30+400.12+400.0+399.9) \times 10^{-3}}{5}$$

Mass of extrudate per minute = 400.176 x 10^{-3}kg

Actual Mass flow rate $(mactual)$

$$= \frac{400.176 \ x \ 10-3}{60} = 6.69 \times 10^{-3} \ kg/s$$

Throughput efficiency

$$= \frac{Actual \ mass \ flow \ rate}{theoretical \ mass \ flow \ rate} \ x \ \frac{100}{1}$$

$$\eta_e = \frac{6.669 \ x \ 10-3}{7.436 \ x \ 10-3} \ x \ \frac{100}{1} = 9.63\% 3.2$$

Thermal efficiency
The heat energy in the extradite is calculated using

$$M \ actual \ Cp \ (T2 - T1)$$

where

m_{actual}= actual mass flow rate

T_2 = measured temperature of the extrudate = 100^{0}C = 373K

T_1 = ambient temperature = 25^{0}C =298K

Heat energy possessed by the extrudate
= 6.669 x 10-3 x 2300 x (373 – 298)
= 1150.40W

Heat input = 1500W (obtained earlier)

Thermal efficiency = $\frac{1150.40}{1500}$ x 100

= 76.69%

4.3 Volumetric Efficiency

The volumetric efficiency is the ratio of the actual volume of material the machine can process to the total volume of material contained in the barrel.

From our design calculation the theoretical volume of material the machine can process has been calculated as

4.3.1 Actual Capacity of Barrel

The feed section of the screw only conveys materials to the transition zone where the actual melting and pressurization operation begins, thus is an idle part of the screw in respect to useful work done on the material.

Feed section length = 129

Barrel feed section volume

$$(Bfsv) = \pi \times r2 \times 129$$

$$= \pi \times 172 \times 129$$

$$= 117121.716 mm^2$$

Therefore, the actual volumetric capacity of the barrel is the volume occupied from the transition zone to the die head [18].

4.3.2 Screw feed section volume (Sfsv)

This was easily evaluated using the physical properties of the feed section from the CAD design as shown in Fig. 3

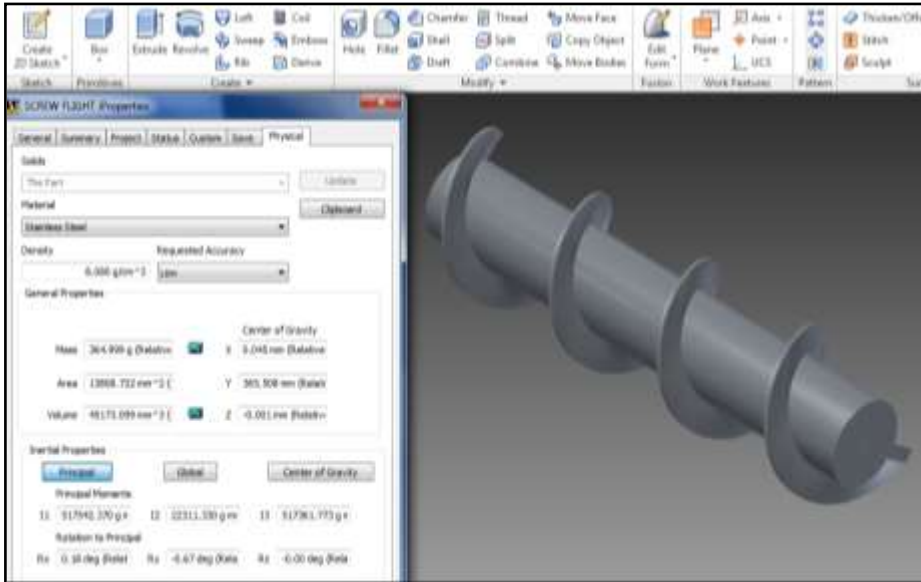Fig. 3: Analysis of the Screw Volume

Fig. 3: Analysis of the Screw Volume

S_{fsv} = 45,173.099mm^3
Feed section material volume,
$$Vfsv = Bfsv - Sfsv$$
$$= 71948.617mm^3$$
Volumetric efficiency,

$$\eta v = \frac{Vmtotal - Vmfs}{Vmtotal} \times 100$$

= 68.414 %
From the calculations above, the efficiency of the machine is obtained to be about 83.16%

4.4 Evaluation of the relationship between machine variables
4.4.1 Die swell variation with temperature procedure is presented in Table 2.

Table 2: Die swell variation with temperature Procedures

Machine set temperature	141	156	171	186	201	216	231
Length of die swell (mm)	2.7	2.5	2.3	2.2	2.1	1.5	0.9

The machine was operated at a constant speed of 37rpm and a feed rate of extrudate were obtained at varied temperature ranges and the

maximum die swell effect length obtained for each of the temperatures. The plot obtained is shown Fig. 4
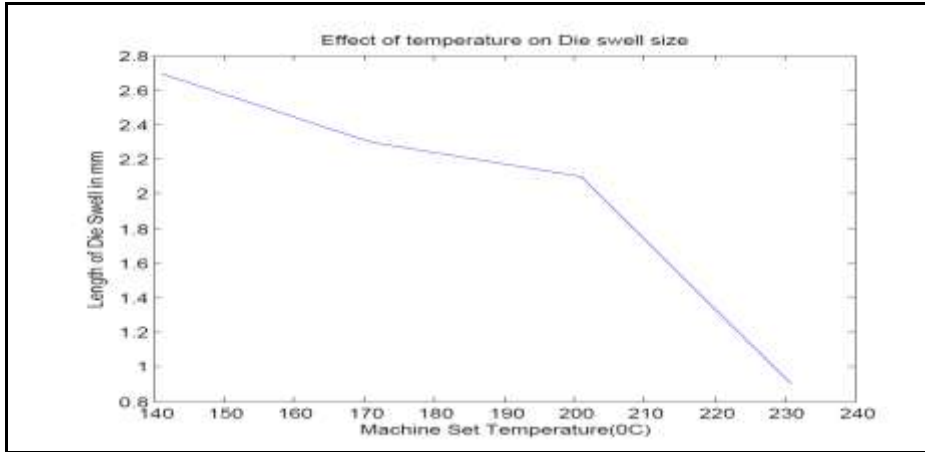
Fig 4: Effect of Temperature on Die Swell size graph

4.4.2 Feed rate/Throughput versus screw speed relationship

The aim of this is to investigate the effect of increasing feed rate on screw speed and throughput and obtain the feed rate at which optimum throughput is obtained.

Procedure of LDPE materials were divided into sets of varying weights each set contained feed batches of equivalent weights the machine was fed continuously with each batch for a duration of two minutes before moving over to the next set of batches. The machine was set at a fixed temperature of 150oc. The result so obtained is shown in Table 3 and from Fig. 5 to 9:

Table 3: Feed Rate and Time

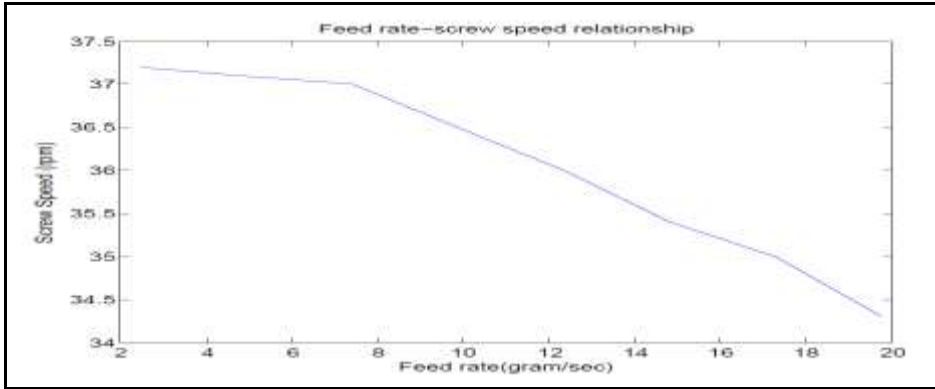| Time (mins)	0-2	2-4	4-6	6-8	8-10	10-12	12-14	14-16
Feed rate (g/s)	2.47	4.94	7.41	9.88	12.35	14.82	17.29	19.76
Screw speed(rpm)	37.0	36.8	36.6	36.5	36.0	35.4	35.4	34.3
Throughput (g/s)	2.30	4.0	7.40	9.33	11.0	10.40	10.05	9.30

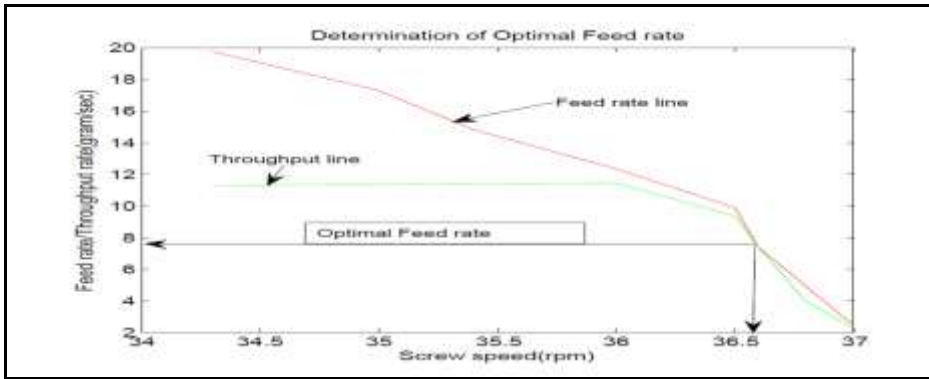Fig 5: Feed rate versus screw speed relationship graph

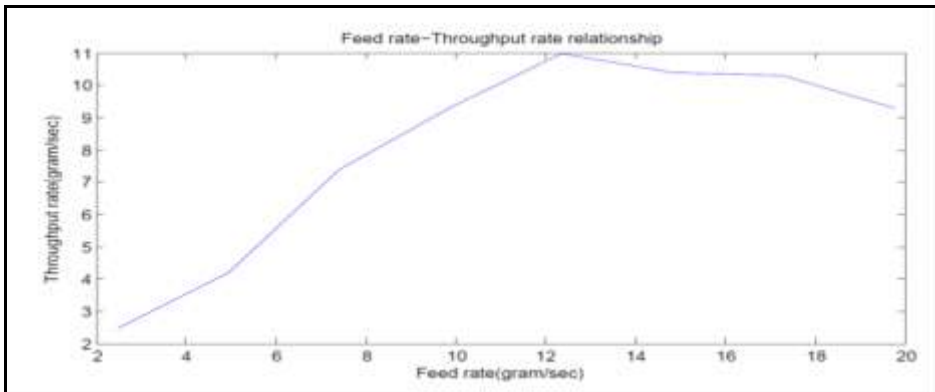
Fig 6: Feed rate versus throughput rate relationship graph

Fig 7: Determination of optimal feed rate graph

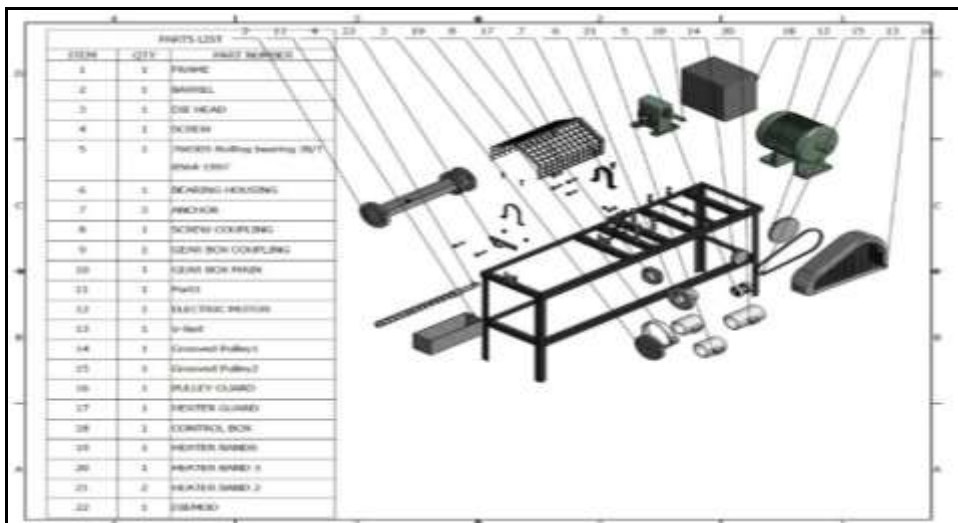Fig 8: Exploded view of the LDPE recycling machine LDPE recycling machine

Fig. 9: Isometric of the LDPE recycling machine

5. Discussion of results

From Fig. 4, the length of die swell decreased with increase in temperature. At a set temperature of 200oc which translates to an internal barrel temperature of 175oc, the die swell length decreased sharply. This was not as a result of elimination of the die swell but rather a significant transition of the material from molten to almost liquid state. The effect of increase in temperature on die swell could not be evaluated as the material could no longer be handled

It was also observed that the feed rate-throughput graph (Fig. 6) reveals a linear increment at the initial phase of feeding, but a point is reached at which the increase in feed rate does not increase output. The feed rate above12g/s would be detrimental to the machine's effective operation.

URL: *http://journals.covenantuniversity.edu.ng/index.php/cjet*

The effect of screw speed on both the feed rate and throughput rate was examined by plotting them on the same graph in Fig. 7. It was observed that at a speed of 36.6rpm, the throughput and feed rate coincided. A further increase in feed rate slightly increased throughput and then yielded no further increase in throughput, rather it decreased the speed and efficiency of the machine. Therefore, feed rates of 7g/s should be the optimal feed rate to run the machine at optimal efficiency.

6. Conclusion

Community-based LDPE wastes recycling machine had been design and tested. The result shows that the efficiency of the machine is 83.16%, Thermal efficiency 76.69% and Volumetric efficiency 68.414 % during operation. Therefore, the machine performed better at the optimized parameters of feed rate of 7 g/s, temperature between 150oC and at screw speed of 36.6 rpm. However,

from the result analysis, increase of the feed rate will affect the performance of the die swell of the LDPE waste recycling machine.

7. Recommendations

- Although the machine does not need much technical knowhow, it is important to give the operators an introductory training to enhance efficiency and safety.
- Low density polyethylene wastes should be properly sorted and processed to avoid introducing impurities that would make the resulting pellets unfit for use as raw material in plastic industries.
- Members of the community should device lucrative means of gathering waste LDPE materials so as to ensure effectiveness of materials collection
- Community policy makers should enact regulations that discourage collective disposal of plastic wastes with biodegradables.

References

[1] UN environment; world environment day 2018. https://www.unenvironment.org/ events/un-environment-event/world-environment-day-2018. Accessed 03 June 2018

[2] Dunmade, I., Udo, M., Akintayo, T., Oyedepo, S., & Okokpujie, I. P. (2018, September). Lifecycle impact assessment of an engineering project management process–a SLCA approach. In IOP Conference Series: Materials Science and Engineering (Vol.

413, No. 1, p. 012061). IOP Publishing.

[3] Jambeck, J. R., et al. "Plastic Waste Inputs from Land into the Ocean." Science, vol. 347, no. 6223, 13 Feb. 2015, pp. 768–771., doi:10.1126/science.1260352.

[4] Babajide Komolafe, 2004: "Polythene Products and our Environment", Vanguard Newspaper, 15th July, P. 20.

[5] Aremu, S. A. 2009. Estimation of parameters for effective collection of municipal waste

bins, University of Ilorin, June, Ph. D (Civil) seminar, Faculty of Engineering &Technology, Unpublished, 21pp.

[6] Gbasouzor A. I., Ekwuozor S.C. and Owuama K.C.(2013). Design and Characterization of a Model Polythene Recycling Machine for Economic Development and Pollution Control in Nigeria.Proceedings of the World Congress On Engineering, July 3-5, 2013 London U.K.

[7] Odior A. O., Oyawale Festus A. and Odusote Joe K (2012). Development of a Polythene Recycling Machine from Locally Sourced Materials Vol 2, No.6, 2012.

[8] Ugoamadi C. C., Ihesiulor O. K. (2011) Optimization of the development of a plastic recycling machine. Nigerian Journal of Technology Vol. 30, No. 3.

[9] Flight angle. www.slideshare.net Retrieved on May, 2018.

[10] Understanding plastic engineering calculation, screw profile, screw zone of a single screw extruder.

[11] Polyethylene Bulk density www.sabie.com/enrope/a/product s/polymer retrieved on 21/09/2015. Specific heat of LPDE www.makeitfrom.com/compare/ highdensitypolyethylene. Retrieved on22 June 2018

[12] Screw Power requirement www.ptonline.com/volume/what- output-should-you-expect. Retrieved on September, 2015.

[13] Nana L. Njobet. Energy Analysis in the Extrusion of plastics.Degree thesis on Plastics Technology Engineering 2012.

[14] Electric motor www.engineeringtoolbox.com. Retrieved on May2018

[15] Igbinigie, O., Okokpujie, I. P., Dirisu, J. O., Igbinowmahia, D. I., & Okokpujie, K. O. (2018). Development and Performance Analysis of Horizontal Waste Paper Baling Machine. International Journal of Mechanical Engineering and Technology (IJMET), 9(10), 84-101.

[16] Okokpujie, I. P., Okokpujie, K. O., Ajayi, O. O., Azeta, J., & Obinna, N. N. (2017). Design, construction and evaluation of a cylinder lawn mower. Journal of Engineering and Applied Sciences, 1254-1260.

[17] Okokpujie, I. P., Okokpujie, K. O., Nwoke, O. N., & Azeta, J. (2018). Design and Implementation of 0.5 kw Horizontal Axis Wind Turbine for Domestic Use. In Proceedings of the World Congress on Engineering (Vol. 2).

[18] Okokpujie, I. P., Okokpujie, K. O., Salawu, E. Y., & Ismail, A. O. (2017). Design, Production and Testing of a Single Stage Centrifugal Pump. International Journal of Applied En

An Open Access Journal Available Online

Ship Propeller Performance Prediction under Cavitation

Thaddeus C. Nwaoha[1*] & Sidum Adumene[2]

[1]Marine Engineering Department, Federal University of Petroleum Resources,
Delta State, Nigeria
[2]Marine Engineering Department, River State University of Science and Technology,
Rivers State, Nigeria

Abstract: In this study, numerically prediction of the screw propeller design that can overcome cavitation is conducted. The research presents a simplified regression model for the analysis of the geometric area ratio, pitch ratio and open water efficiency of propeller, with the aim of revealing quantitatively the effect of cavitation on propeller open water efficiency. The case study takes into consideration factors that can enhance the performance of a propeller. Area of the propeller disc, propeller pitch ratio, diameter of the propeller, delivered power, thrust coefficient, torque is used as inputs into the model, in prediction of performance for cavitated and non-cavitated propellers. Sensitive analysis is carried out by percentage increase and reduction of the blade area ratio, so as to know the effects on the propeller performance. It is revealed that for every 1% increase in the expanded blade areas, the open water efficiency decreases at 0.12% and 0.15% for the non-cavitated and cavitated propellers respectively. This indicates a performance reduction by a cavitation factor of 0.03. The study further shows that at 7.5% reduction in the expanded blade area ratio, the propeller performance in terms of open water efficiency, increases by 1.85%. The analysis exposed an appropriate and accurate operating envelope for optimal screw propeller performance, thus revealing a way of minimizing cavitation effect.
Keywords: Propeller; Cavitation; Regression model; Efficiency; Ship

1. Introduction
Screw propeller of a ship is regarded as a helical surface which on rotation screws its way through the water. It consists of a hub and blades that are space at equal angle about the axis. As the propeller rotates, the face of the blade increases pressure on the water with the aim of propulsion of a ship. The design and analysis of modern,

URL: *http://journals.covenantuniversity.edu.ng/index.php/cjet*

loaded and highly screw propeller is important in the marine field [1]. The growing demand of heavily loaded, highly efficient propeller that is associated with low level noise and vibration onboard, makes the design of marine propeller more complicated. The propeller converts precious power into forward motion, and if it is mismatched or damaged, optimal ship performance is hindered [2]. Therefore, it is mandatory to choose the correct propeller type and size to prevent cavitation from occurring, which can pose threat to ship propeller optimal operations. However, design of propeller and its efficiency also depends on other several factors [3].

The choice of the number of blades plays a significant role in marine propeller performance. Marine screw propeller usually has two, three, four or five blades. Four blades are the most common, but [4] revealed that most efficient number of blades is the one blade type. This is because the single blade can handle effectively the water flow ahead of it. However, there has been doubt in this conception, because a single blade would be impossible to provide balance loading in operation. The next most efficient is two blades, but this can be impracticable because a propeller with a very large diameter that can accommodate large blade area will be needed for generation of large amount of thrust. In view of this, most propellers have three, four or five blades [2]. Propeller blade normally experience problems such as vibration, noise, cavitation etc. According to [5], noise is experienced when there is displacement of the water by the propeller blade profile; pressure difference between the suction and pressure surfaces of the propeller during rotation; and the periodic fluctuation of the cavity volumes caused by the operation of the vessel behind. Three-bladed propellers have generally proven to be the best compromise between blade area and efficiency [5]. Four or five bladed propellers are useful for two reasons. First their extra blades create more total blade area with the same or less diameter and vibration is reduced to great extent as compared to three blades [6].

1.1. Screw Propeller Performance

A propeller blade shape will affect its performance [7]. Some propellers are progressively pitched. Cavitation does not really affect progressive pitched propeller because the leading edge is a lower pitch, thus water is moved under less pressure differential. The water then flows along the blade surface, increasing the pitch toward the trailing edge and this gives higher efficiency. Performance of a propeller depends on speed of rotation, pitch of the blades, diameters and surface of blades [7]. A combination of these factors creates a thrust which is transmitted to the thrust bearing by the transmission shaft and propels the hull through the water. Before the propulsion system moves the hull, it is mandatory to match the engine and propeller. This entails matching unto the engine on a diagram known as engine/propeller matching curve [8].

1.2. Cavitation Phenomenon

The advancement in the development of high-speed hydraulic machinery

and marine propellers has been accompanied by appearance of cavitation [9]. It is a phenomenon that occurs in highly loaded propellers in which beyond certain revolutions results to a progressive breakdown in the flow and consequent loss of thrust [10]. It was first thought to be an oxidation of the metal by free oxygen, liberated from the water at points of low pressure, but investigation has shown it to be a mechanical action. Cavitation do not only cause noise and vibration but pitting in the regions where cavitation bubbles collapse takes place, forming the sponge-lie surface that is characteristics of cavitation erosion [10, 11].

These pits are thought to be caused by the repetition of mechanical stress from the impact wave or the micro-jet produced in the liquid as the cavitation bubbles collapses. The erosive effects of these collapsing bubbles mostly affect the propeller blades, struts and rudders [9]. Cavitation damage can also be dominated by the corrosive action of the liquid. Essentially, when cavitation is severe, the cavitation erosion which occurs is due to the surface fatigue created by the alternative mechanical stresses rather than the corrosive action of the liquid [12]. Similarly, when the cavitation intensity is minor, the damage from the cavitation becomes considerably augmented by the corrosive action of the liquid called the "corrosion erosion" effect [10]. At lower levels of cavitation intensity, the damage can be characterized as "flow-corrosion. Experiments at the Massachusetts institute of technology indicate that no

metal can long withstand this erosive effect and after a period as short as a hundred hours, steel plate that was previously smooth was found to visibly roughen [13].

The avoidance of cavitation and erosion has therefore become an important requirement in the design of nearly all propellers [12]. Detailed predictions of cavitation performance are now possible using high level mathematical models, but such methods are hardly appropriate at the early design stage. Normally, the blade surface area is selected using empirically derived cavitation criteria, which is a function of the propeller dimensions, the operating conditions and of the immersion of the propeller [13].

The problems related to propeller performance in most cases be traced to a lack of knowledge during the design process of the wake field in which the propeller is operating [13]. When a ship had the benefit of model testing prior to construction, a model nominal wake field is very likely to have been measured. This then allows the designer to understand in a qualitative sense the characteristics of the wake field in which the propeller is to operate. The designer needs to transform the model nominal wake field into a ship effective velocity distribution before it can be used for quantitative design purposes [14]. Although computational fluid dynamics is beginning to address this problem, this transformation is far from clearly defined within the current state of knowledge, and so errors may develop in the definition of the effective wake field [15,16].

In the case where the ship has not been model tested, the designer has less information to work with, and must rely on knowledge of experts from similar ships. In this way, predictions are made empirically based on estimation. Clearly, not all performance problems are traceable to lack of knowledge about the wake field. Other causes, such as poor tolerance specification, poor specification of design criteria and incorrect design and manufacture are common causes of poor performance of ship propeller [12, 14]. Modeling the common causes and effects on the propeller performance using Computational Fluid Dynamics (CFD) presents computational complexity, time and cost. Therefore, this work seeks to present a simplified regression model analysis for propeller performance prediction under cavitation to overcome the challenges of computational time and cost associated with propeller hydrodynamic characteristics CFD models and the unavailability of Model Test facilities. The models were developed from previous predicted test model and analysis, and it show capacity for accurate predictive analysis.

1.3 Methods of Propeller Performance Prediction and Analysis

Propeller performance prediction and analysis can be conducted using any of the four basic methods. The methods are momentum theory, blade element theory, numerical methods and regression model. These theoretical methods are used to predict the action of propellers. The development of these methods started in late nineteenth century. Perhaps, the most notable of these early works was that of Rankine, with his momentum theory, which was closely followed by the blade element theories of Froude [5]. The modern theories of propeller action, however, had to wait for more fundamental works in aerodynamics behavior analysis of propeller [2]. A simple performance analysis flow chart of screw propeller under cavitation is illustrated in Figure 1. The momentum theory, blade element theory, regression method and numerical methods are described as follows:

1.3.1 Momentum Theory

The momentum theory of propeller action is based on the axial motion of the water passing through the propeller disc. Hence, this theory did not concern itself with the geometry of the propeller, which was producing the thrust, and consequently, this method is not very useful for blade design purposes. It does, however, lead to some general conclusions about propeller action which have subsequently been validated by more recent propeller theoretical methods [11].

1.3.2 Blade Element Theory

The blade element theory is quite different model of propeller action, which took account of the geometry of the propeller blade. In its original form, the theory did not take account of the acceleration of the inflowing water from its far upstream value relative to the propeller disc. This is somewhat surprising, since this could have been deduced from the earlier

work of Rankine. Nevertheless, this omission was rectified in subsequent developments of the [15]. Blade element theory is based on dividing the blade up into many elementary strips, as seen in Figure 2 & 3. Each of these elementary strips can then be regarded as an aero foil subject to a resultant incident Velocity w. The resultant incident velocity was considered to comprise an axial velocity V together with a rotational velocity r, which clearly varies linearly up the blade. In the normal working condition, the advance angle β is less than the blade pitch angle θ at the section, and hence gives rise to the section having an angle of incidence α [15, 1].

1.3.3 Regression Method

Regression methodology is a form of predictive modeling techniques which investigate the inter and intra relationship between variables in form of target and predictor. It is applicable in forecasting, time series modeling and used for the causal effect relationship between parameters 17]. This method has demonstrated strength for impact analysis in multiple independency system performance. This technique provides a simplified model that can be used for ship propeller performance prediction. The models can be expressed in the form of linear regression, logistic regression, polynomial regression, stepwise regression, ridge regression, lasso regression and Elastic Net regression.

1.3.4 Numerical Method

Numerical methods are used to predict the performance of ship propeller under cavitation effect. The simulation is based on the viscid-flow theory such as the Reynolds-Averaged Navier-Strokes (RANS) solver [14]. It was used in the performance evaluation of a podded propulsion system to model the unsteady thrust and torque of the pod. The blade boundary parameter and zero pressure conditions are applied for the blade profile modeling using CFD [11, 14]. The performance of a propeller hydrodynamic characteristic can be enhanced using numerical models [14], to improve the live cycle of the propeller for sustainable development [18-20]. However, [14] observed that in most cases, the numerical prediction of propeller under sheet cavitation are not consistent with the generic experimental results. They further used the turbulence model to examine a 3-D cavitation flow propeller to validate the measured observations. This method also presents high computational time and cost in performance based analysis.

2 Research Methodology

In this research, the regression model listed as one of the methods for propeller performance prediction and analysis in sub-section 1.3 is used. The regression model is developed for the modeling of the area ratios and open water efficiencies of propeller at different conditions. The developed regression models were modified from the work of [9, 11] as follows:
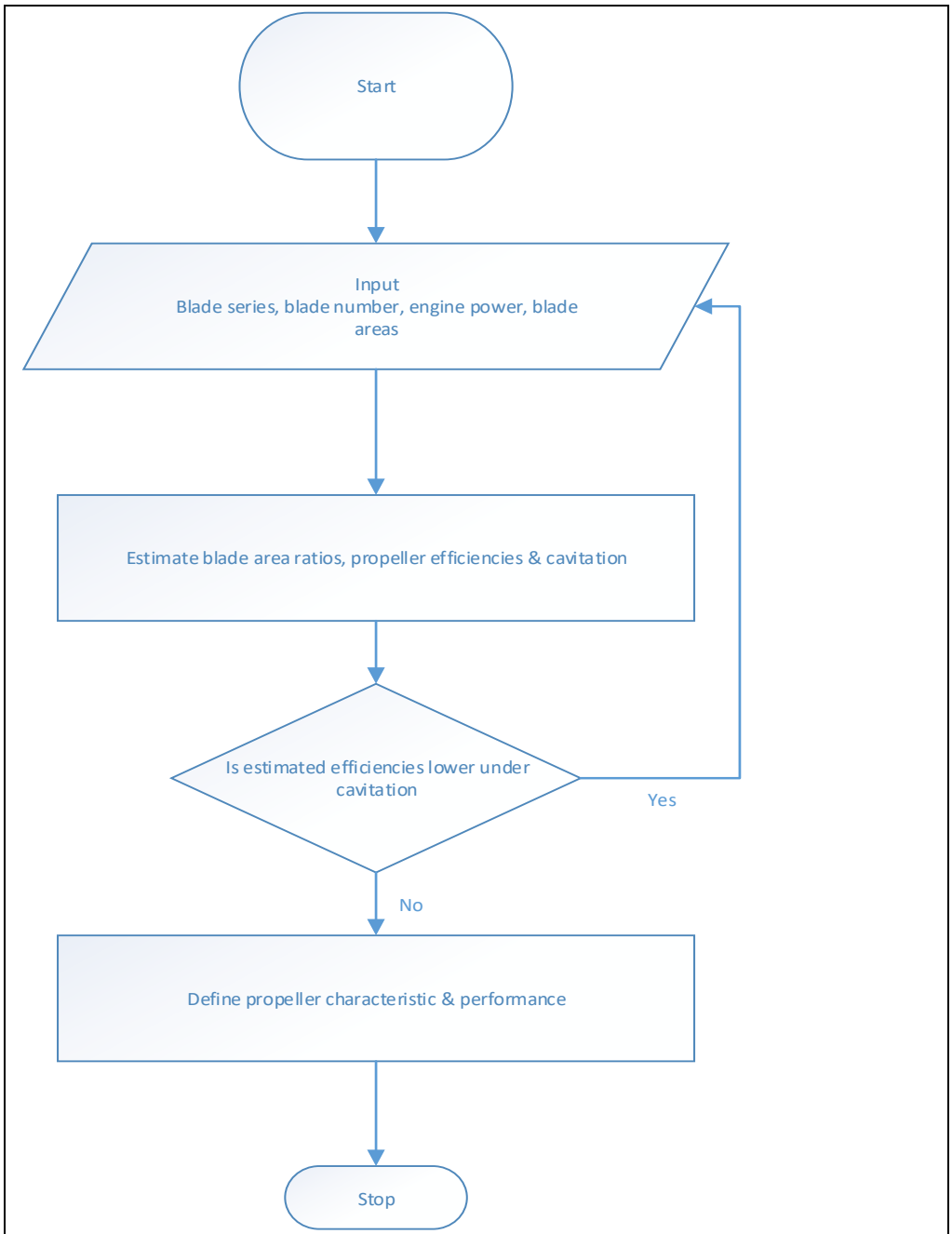
Figure 1: Performance analysis flow chart of screw propeller under cavitation
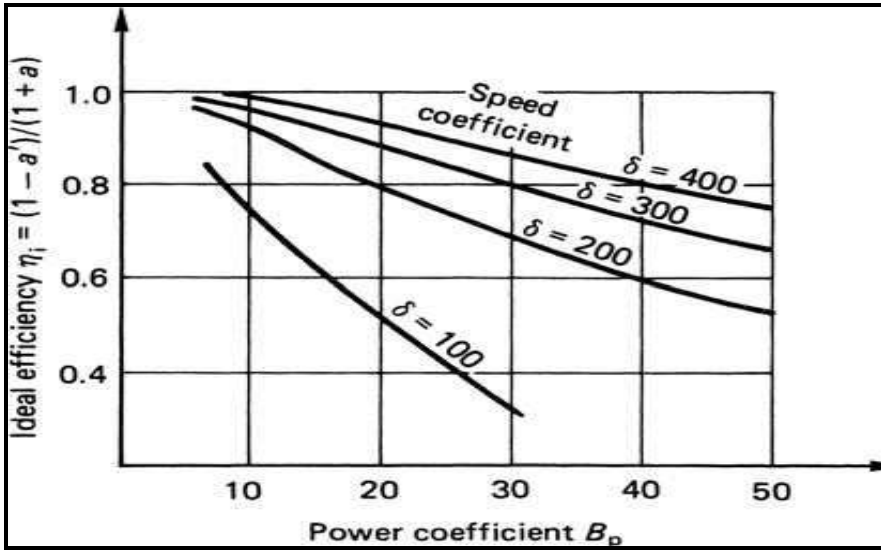
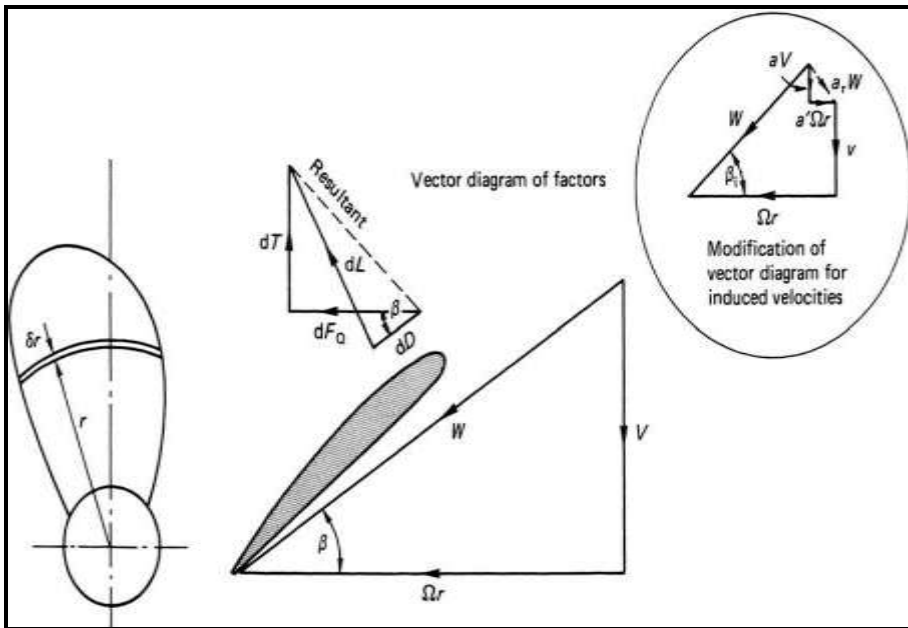Figure 2: Ideal propeller efficiency from general momentum theory [5]

Figure 3: Blade element theory [1]

$$\text{Developed Blade Area Ratio} = \frac{A_D}{A_O} = 0.0876D^2 - 1.1657D + 4.4272 \qquad (1)$$

$$\text{Expanded Blade Area Ratio} = \frac{A_E}{A_O}$$
$$= 0.012812D^2 - 0.3306D + 2.1871 \qquad (2)$$

$$\text{Projected Blade Area Ratio} = \frac{A_p}{A_O}$$
$$= 0.0658D^2 - 0.8924D + 3.4852 \qquad (3)$$

$$\text{Pitch Ratio} = 0.0521D^2 - 0.57883D + 2.5521 \qquad (4)$$

$$\text{Cavitation Number } \sigma_O = \frac{P_O - P_S}{1/2V_A^2} \qquad (5)$$

$$\eta_{0=} -0.133\left(\frac{A_E}{A_O}\right)^2 + 0.133\left(\frac{A_E}{A_O}\right) + 0.61 \qquad (6)$$

$$\frac{d\eta_0}{d\left(\frac{A_E}{A_O}\right)} = -0.266\left(\frac{A_E}{A_O}\right) + 0.133 \qquad (7)$$

where,

A_D is the developed blade area

A_O is the propeller disc area

A_E is the expanded area

D is the blade diameter

V_A is the advance velocity

$P_O - P_s$ is the pressure differential on the blade surface.

A_p is the projected blade area

η_O is the open water efficiency

3. Application of Regression Model in Propeller Performance Prediction and Analysis

The study uses regression model to analyse and predict the performance of a screw propeller for a marine vessel under various assumptions. The prediction is hypothetically evaluated at different blade diameters and geometric blade areas ratio. The results of the analysis at the given

URL: *http://journals.covenantuniversity.edu.ng/index.php/cjet*

range of blade profile and blade area ratios are shown in Figures 4-9.

The result of the analysis in Figure 4 &5 show the trend of the open water efficiency for the selected blade area ratio. As the ratio increases, the open water efficiency decreases at a steep rate with blade diameter of 7.00m. This further revealed that for every 1% increase in the expanded blade areas, the open water efficiency decreases at 0.12% and 0.15% for the non-cavitated and cavitated propellers respectively. This indicate a performance reduction factor of 0.03. This factor, though minimal, over time can results to performance deterioration, especially when the propeller is fully loaded. The consequences may result to catastrophic failures.
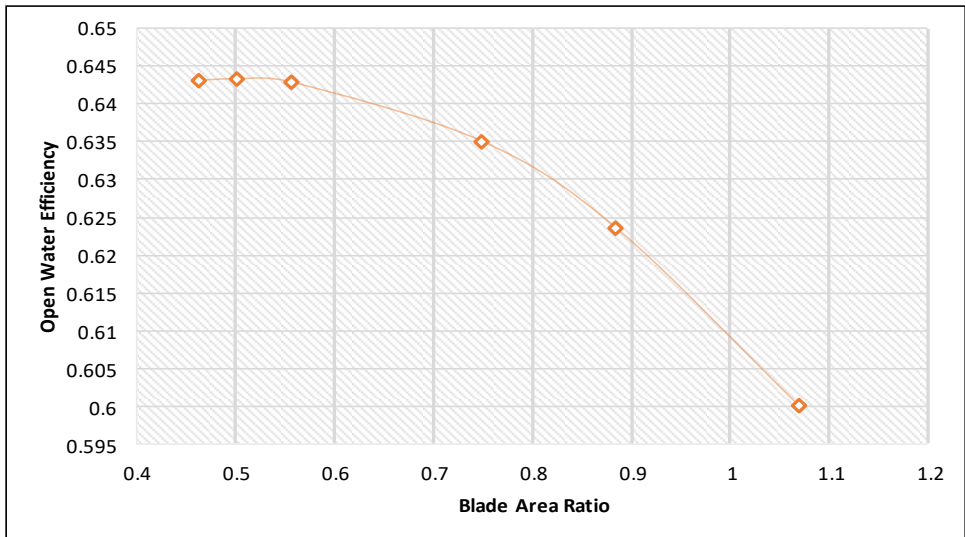
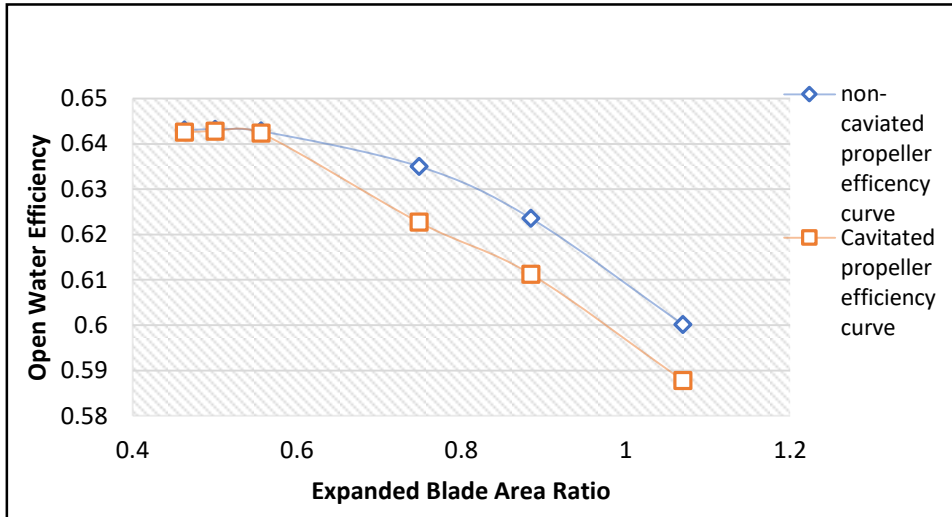Figure 4: Effect of blade area ratio on open water efficiency

Figure 5: Comparative prediction of open water efficiency for non-cavitated and cavitated propeller

Figure 6 describes the effect of expanded area ratio reduction on the performance of the propeller. Selected percentage reduction ranges from 2% to 10%, where used to evaluate the optimal percentage incremental effect on the open water efficiency. The result show that at 7.5% reduction in the expanded blade area, the open water efficiency has the optimal percentage increment. That is at 7.5% increase in the expanded blade area, the propeller performance increase by 1.85%. This is an indication that the blade area ratio is a factor to be considered in propeller choices and performance criteria. Although, the cavitation effects decrease as blade area ratio increases. Beyond certain allowable pressure fluctuation, this increment may result to the overall propeller performance deterioration over time. It is therefore of concern that selection and prediction should be done within the optimum performance envelope for safer operation in fully loaded propeller. From the result analysis of this study, the predicted propeller performance optimizing range is $0.46 \leq {A_E}/{A_o} \geq 0.70$ and $0.62 \leq \eta_o \geq 0.65$.
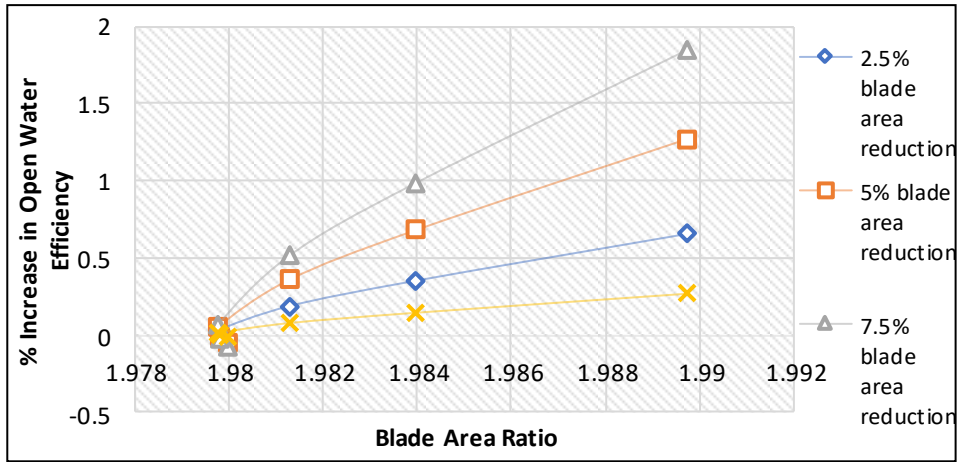
Figure 6: Effect of percentage reduction in blade area ratio on the open water efficiency
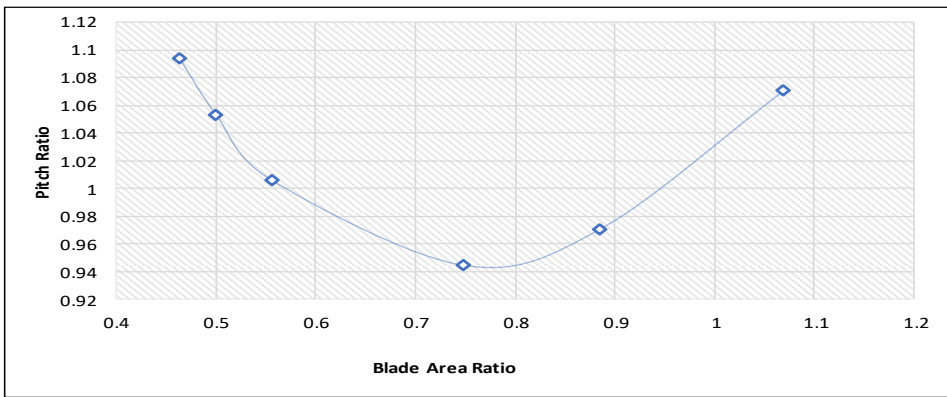

Figure 7: Effect of blade area ratio on pitch ratio of a screw propeller
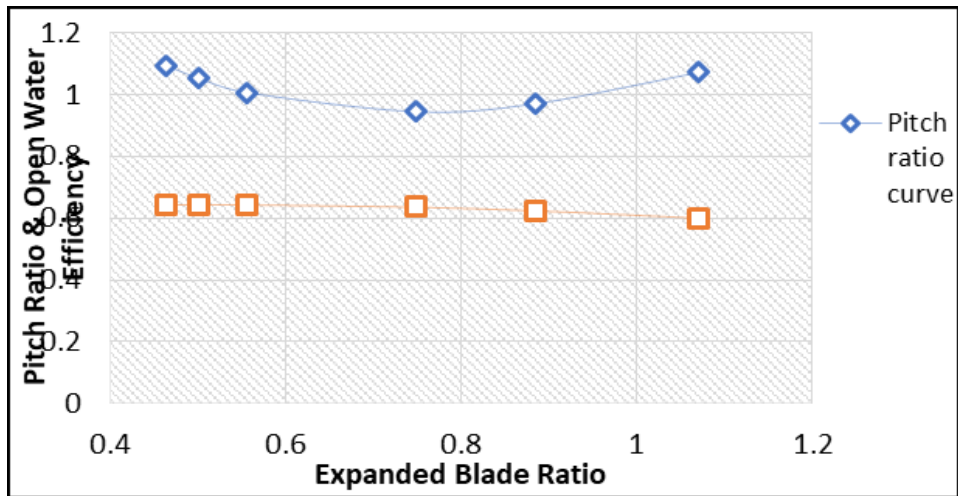
Figure 8: Comparative effects of blade area ratio on pitch ratio and open water efficiency

The result of the study as shown in Figures 7 and 8, show the effect of blade area ratio on the propeller pitch ratio. This described theoretically the advances during the complete cycle and how pitch ratio may lead to an increase in the propulsive efficiency. It also shows that the propeller propulsive efficiency is dependent on propeller pitch ratio. It is therefore important for propeller performance analysis to predict the pitch ratio during propeller design. For the proper performance of a screw propeller, the propeller pitch ratio prediction should be holistic for an optimum output.

Cavitation also affect the propeller pitch ratio as shown in this analysis. It revealed that as there is an increase in the cavitation number, the propeller pitch ratio decreases. Also, the result shows that for a nominal pitch ratio of 0.944 at the blade area ratio of 0.748, the corresponding open water efficiency is 0.635. This further explain the mean performance of the propeller at the given normal pitch. There is an even distribution of the pitch at the right and left sides of the nominal value as shown in Figure 8. So critical decision making is needed to operate within the acceptable criteria considering the decline in the open water efficiency.

Figure 9 indicate that the open water efficiency increases as the blade diameter reduction ratio decrease towards the zero axis. The result show that between the ratio of 0.55 and 0.40, the efficiency has a peak value, which gradually decline as we move toward the zero axis. It also means that the propeller disc area will also affect the propeller efficiency in operation. The propeller disc area is also a major factor of consideration in screw propeller performance due to its significant on propeller efficiency prediction. So, to enhance propeller efficiency during propeller design, the area of the disc should be accurate predicted to avoid errors that can limit performance. Furthermore, a

predictive profile for operational decision making and proactive planning can be deduced from the curves shown in Figure 9. It was observed that operating within the

acceptable limit under cavitation can prolong the life of the propeller and minimize the maintenance downtime in operation.
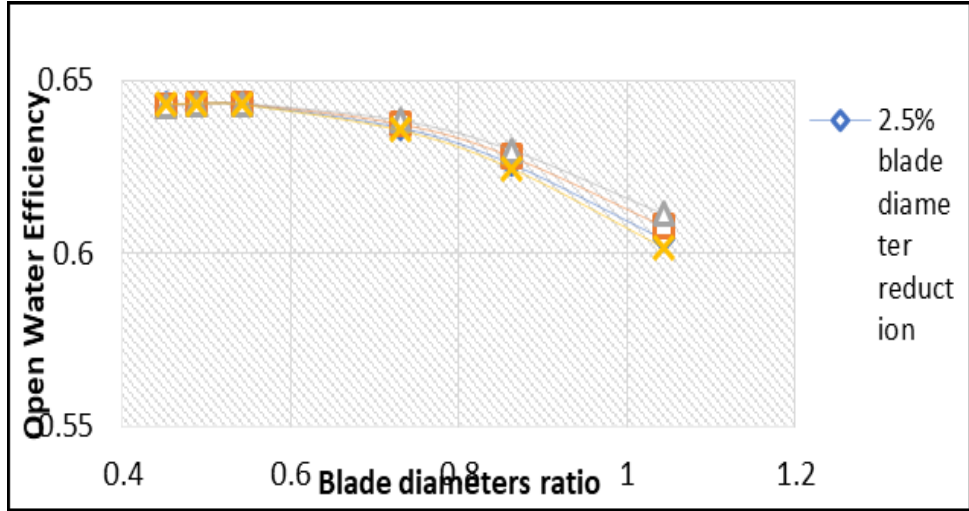

Figure 9: Effect of percentage reduction in blade diameter on open water efficiency

4. Conclusion

In this research, the regression model was utilized in propeller performance prediction, when cavitation is experienced. The model shows accurate predictive result with minimum associated error. It was identified that the cavitation reduces the performance by a factor of 0.03 in the open water efficiency. This factor overtime enhances reduction in the propeller effective power and causes performance deterioration and frequent breakdown. Therefore, an effective operating envelope of

$(0.46 \leq A_E/A_o \geq 0.70$ and

$0.62 \leq \eta_o \geq 0.65)$ was proposed for the operation, considering the

consequences of the effect of cavitation when the propeller is fully loaded.

Furthermore, for operational safety and design consideration, cavitation reduction or monitoring should be integrated into the design for safety of ships. Increasing propeller immersion, introduction of ventilation, increase of clearances from the hull and application of skewed bladed propeller can serves as cavitation reduction measures that can minimize propeller failure in operation and optimize the performance.

Reference

[1] Burger, C (2007). Propeller performance analysis and multidisciplinary optimization using a genetic algorithm, PhD Thesis, Auburn University, USA.

[2] Karlse. M, & Daniel. L, (2001) Introduction to propeller. Available online www.wikipedia.com . Accessed 20th October 2018.

[3] Kerwin, J. E (1986) Marine propeller. Annual review of fluid mechanics, 18:367-403.

[4] Van, G. L. A & Pronk C. (1973). Propeller design concepts. International Shipbuilding Progress, 20(227): 252-275.

[5] Carlton, J (2007). Marine propellers and propulsion. 2nd Edition, Butterworth-Heinemann.

[6] Asimakopoulos, O. A. A (2016). Effects of propeller geometry on cavitation. Master Thesis, University of Strathclyde, UK.

[7] Euler, D. (2010) Third international symposium on marine propulsors and cavitation analysis 2010 May, 10-24.

[8] Pivano R. K. (2004). Screw propeller analysis. Journal of Ship Research, 20:16-22.

[9] Adumene, S & Ombor, P. G (2016). Modeling screw propeller characteristics for optimal performance. Universal Journal of Computers and Technology, 2(2): 101-109.

[10] Basumatory, J. (2017). Cavitation erosion-corrosion in marine propeller materials. PhD Thesis, University of Southampton, UK.

[11] Lee, C.S., Choi, Y. D., Ahn, B.K., Shin, M. S & Jang, H. G (2010) Performance optimization of marine propeller. International Journal of Naval Architecture and Ocean Engineering, 2:211-216.

[12] Nwaoha, T.C., Adumene, S. & Boye, T. E (2017). Modeling prevention and reduction methods of ship propeller cavitation under uncertainty. Journal of Ship and Offshore Structures, 12(4):452-460.

[13] Dang, J. (2004). Improving cavitation performance with new blade section for marine propellers. International shipbuilding progress, 51 (4): 353-376.

[14] Zhu, Z. & Fang, S. (2012). Numerical investigation of cavitation performance of ship propellers. Journal of Hydrodynamics, 24(3): 347-353.

[15] Salvatore, F., Streckwall, H & van Terwisga, T (2009). Propeller cavitation modelling by CFD- Results from VIRTUAL 2008 Rome workshop. First International Symposium on Marine Propulsors Smp'09.

[16] Robert, K., James, W & Dally, K. (1981). Hydro-acoustics of cavitating propeller, far field approximations, Journal of Ship Research, 25(2): 90-94.

[17] Hocking, R. R. (2003). Methods and application of linear models: regression and the analysis of variance. 2nd Edition. John Wiley & Son Inc.

[18] Okokpujie, I. P., Fayomi, O. S. I., Ogbonnaya, S. K., & Fayomi, G. U. (2019). The Wide Margin Between the Academic and Researcher in a New Age University for Sustainable

Development. Energy Procedia, 157, 862-870.

[19] Dunmade, I., Udo, M., Akintayo, T., Oyedepo, S., & Okokpujie, I. P. (2018). Lifecycle impact assessment of an engineering project management process–a SLCA approach. In IOP Conference Series: Materials Science and Engineering (Vol.

413, No. 1, p. 012061). IOP Publishing.

[20] Onawumi, A., Udo, M., Awoyemi, E., & Okokpujie, I. P. (2018). Alternate Maintainability Evaluation Technique for Steering System of Used Automobiles. In IOP Conference Series: Materials Science and Engineering (Vol. 413, No. 1, p. 012062). IOP Publishing.

.